

U.S. Department of Transportation
Federal Highway Administration

Steel Bridge Design Handbook

Design Example 5: Three-Span Continuous Horizontally Curved Composite Steel Tub-Girder Bridge

Publication No. FHWA-HIF-16-002 - Vol. 25

December 2015



FOREWORD

This handbook covers a full range of topics and design examples intended to provide bridge engineers with the information needed to make knowledgeable decisions regarding the selection, design, fabrication, and construction of steel bridges. Upon completion of the latest update, the handbook is based on the Seventh Edition of the AASHTO LRFD Bridge Design Specifications. The hard and competent work of the National Steel Bridge Alliance (NSBA) and prime consultant, HDR, Inc., and their sub-consultants, in producing and maintaining this handbook is gratefully acknowledged.

The topics and design examples of the handbook are published separately for ease of use, and available for free download at the NSBA and FHWA websites: <http://www.steelbridges.org>, and <http://www.fhwa.dot.gov/bridge>, respectively.

The contributions and constructive review comments received during the preparation of the handbook from many bridge engineering professionals across the country are very much appreciated. In particular, I would like to recognize the contributions of Bryan Kulesza with ArcelorMittal, Jeff Carlson with NSBA, Shane Beabes with AECOM, Rob Connor with Purdue University, Ryan Wisch with DeLong's, Inc., Bob Cisneros with High Steel Structures, Inc., Mike Culmo with CME Associates, Inc., Mike Grubb with M.A. Grubb & Associates, LLC, Don White with Georgia Institute of Technology, Jamie Farris with Texas Department of Transportation, and Bill McEleney with NSBA.



Joseph L. Hartmann, PhD, P.E.
Director, Office of Bridges and Structures

Notice

This document is disseminated under the sponsorship of the U.S. Department of Transportation in the interest of information exchange. The U.S. Government assumes no liability for use of the information contained in this document. This report does not constitute a standard, specification, or regulation.

Quality Assurance Statement

The Federal Highway Administration provides high-quality information to serve Government, industry, and the public in a manner that promotes public understanding. Standards and policies are used to ensure and maximize the quality, objectivity, utility, and integrity of its information. FHWA periodically reviews quality issues and adjusts its programs and processes to ensure continuous quality improvement.

Technical Report Documentation Page

1. Report No. FHWA-HIF-16-002 – Vol. 25	2. Government Accession No.	3. Recipient's Catalog No.	
4. Title and Subtitle Steel Bridge Design Handbook Design Example 5: Three-Span Continuous Horizontally Curved Composite Steel Tub-Girder Bridge		5. Report Date December 2015	
		6. Performing Organization Code	
7. Author(s) Brandon Chavel, Ph.D., P.E. and Julie Rivera, P.E.		8. Performing Organization Report No.	
9. Performing Organization Name and Address HDR, Inc. 11 Stanwix Street Suite 800 Pittsburgh, PA 15222		10. Work Unit No.	
		11. Contract or Grant No. DTFH6114D00049	
12. Sponsoring Agency Name and Address Office of Bridges and Structures Federal Highway Administration 1200 New Jersey Avenue, SE Washington, D.C. 20590		13. Type of Report and Period Covered Technical Report Final Report December 2014 – November 2015	
		14. Sponsoring Agency Code	
15. Supplementary Notes The previous version of this Handbook was published as FHWA-IF-12-052 and was developed to be current with the AASHTO LRFD Bridge Design Specifications, 5th Edition with the 2010 Interims. FHWA-HIF-16-002 was updated in 2015 by HDR, Inc., to be current with the AASHTO LRFD Bridge Design Specifications, 7th Edition.			
16. Abstract Tub girders, as closed-section structures, provide a more efficient cross section for resisting torsion than I-girders, which is especially important in horizontally curved highway bridges. The increased torsional resistance of a closed composite steel tub girder also results in an improved lateral distribution of live loads. For curved bridges, warping, or flange lateral bending, stresses are lower in tub girders, when compared to I-girders, since tub girder carry torsion primarily by means of St. Venant torsional shear flow around the perimeter of their closed sections, whereas I-girders have very low St. Venant torsional stiffness and carry torsion primarily by means of warping. This design example illustrates the design calculations for a curved steel tub girder bridge, considering the Strength, Service, fatigue and Constructibility Limits States in accordance with the AASHTO LRFD Bridge Designs specifications. Calculations are provided for design checks at particular girder locations, a bolted field splice design, an internal pier diaphragm design, and a top flange lateral bracing member design.			
17. Key Words Steel Tub Girder Bridge, Steel Box Girder Bridge, LRFD, Bolted Field Splice, Top Flange Lateral Bracing, Box Girder Distortional Stresses		18. Distribution Statement No restrictions. This document is available to the public through the National Technical Information Service, Springfield, VA 22161.	
19. Security Classif. (of this report) Unclassified	20. Security Classif. (of this page) Unclassified	21. No of Pages	22. Price

Steel Bridge Design Handbook: Design Example of a Three-Span Continuous Curved Composite Tub-Girder Bridge

TABLE OF CONTENTS

TABLE OF CONTENTS.....	i
LIST OF FIGURES	vi
LIST OF TABLES	vii
1.0 INTRODUCTION	1
2.0 OVERVIEW OF LRFD ARTICLE 6.11	3
3.0 DESIGN PARAMETERS	5
4.0 GENERAL STEEL FRAMING CONSIDERATIONS.....	7
4.1 Span Arrangement	7
4.2 Field Section Sizes.....	9
4.3 Bridge Cross Section and Girder Spacing	9
4.4 Intermediate Internal and External Cross-Frames	10
4.5 Diaphragms at the Supports.....	12
4.6 Top Flange Lateral Bracing.....	12
5.0 FINAL DESIGN	15
5.1 AASHTO LRFD Limit States.....	15
5.1.1 Strength Limit State	15
5.1.2 Service Limit State.....	15
5.1.3 Fatigue and Fracture Limit State.....	15
5.1.4 Extreme Event Limit State.....	16
5.1.5 Constructibility	16
5.2 Loads.....	16
5.2.1 Dead Load.....	16
5.2.2 Deck Placement Sequence	17
5.2.3 Live Load	19

5.3	Centrifugal Force Computation	19
5.4	Load Combinations	23
6.0	ANALYSIS.....	25
6.1	Three-Dimensional Finite Element Analysis.....	25
6.1.1	Bearing Orientation and Arrangement.....	26
6.1.2	Live Load Analysis.....	27
6.2	Analysis Results.....	28
7.0	DESIGN.....	36
7.1	Girder Section Proportioning.....	36
7.1.1	Girder Web Depth.....	38
7.1.2	Cross-section Proportions	39
7.2	Section Properties	40
7.2.1	Section G2-1: Span 1 Positive Moment Section Properties.....	41
7.2.1.1	Effective Width of Concrete Deck.....	42
7.2.1.2	Elastic Section Properties: Section G2-1	42
7.2.1.3	Plastic Moment Neutral Axis: Section G2-1.....	45
7.2.2	Section G2-2: Support 2 Negative Moment Section Properties	45
7.2.2.1	Elastic Section Properties: Section G2-2	46
7.2.3	Check of Minimum Negative Flexure Concrete Deck Reinforcement (Article 6.10.1.7)	49
7.3	Girder Check: Section G2-1, Constructibility (Article 6.11.3).....	50
7.3.1	Deck Overhang Bracket Load.....	51
7.3.2	Flange Lateral Bending Due to Horizontal Component of Web Shear	53
7.3.3	Flange Lateral Bending Due to Curvature	53
7.3.4	Top Flange Lateral Bending Amplification.....	54
7.3.5	Flexure (Article 6.11.3.2).....	56
7.3.5.1	Top Flange.....	57
7.3.5.2	Bottom Flange	61
7.3.6	Shear (Article 6.10.3.3).....	62
7.3.7	Concrete Deck (Article 6.10.3.2.4).....	62
7.4	Girder Check: Section G2-1, Service Limit State (Article 6.11.4).....	62

7.4.1	Permanent Deformations (Article 6.10.4.2).....	62
7.4.2	Web Bend-Buckling.....	63
7.5	Girder Check: Section G2-1, Fatigue Limit State (Article 6.11.5).....	63
7.5.1	Special Fatigue Requirements for Webs.....	66
7.6	Girder Check: Section G2-1, Strength Limit State (Article 6.11.6)	66
7.6.1	Flexure (Article 6.11.6.2).....	66
7.6.1.1	Top Flange Flexural Resistance in Compression.....	70
7.6.1.2	Bottom Flange Flexural Resistance in Tension	70
7.6.1.3	Concrete Deck Stresses	71
7.7	Girder Check: Section G2-2, Constructibility (Article 6.11.3).....	72
7.7.1	Flexure (Article 6.11.3.2).....	72
7.7.1.1	Top Flange.....	74
7.7.1.2	Bottom Flange	74
7.7.1.3	Shear (Article 6.11.3.3).....	79
7.8	Girder Check: Section G2-2, Service Limit State (Article 6.11.4).....	80
7.8.1	Permanent Deformations (Article 6.10.4.2).....	80
7.8.2	Web Bend-Buckling.....	81
7.8.3	Concrete Deck (Article 6.10.1.7).....	84
7.9	Girder Check: Section G2-2, Fatigue Limit State (Article 6.11.5).....	84
7.9.1	Cross-section Distortion Stresses.....	86
7.10	Girder Check: Section G2-2, Strength Limit State (Article 6.11.6)	95
7.10.1	Flexure (Article 6.11.6.2).....	95
7.10.2	Top Flange	98
7.10.3	Bottom Flange.....	98
7.10.3.1	Cross-section Distortion Stresses.....	105
7.10.4	Shear (Article 6.11.6.3).....	105
7.10.4.1	Interior Panel (Article 6.10.9.3.2)	106
7.11	Bottom Flange Longitudinal Stiffener	108
7.12	Internal Pier Diaphragm Design	110
7.12.1	Web Shear Check.....	111
7.12.1.1	Noncomposite Shear Force	111

7.12.1.2	Composite Shear Force	113
7.12.1.3	Total Factored Shear Force	113
7.12.1.4	Check of Internal Diaphragm Web	114
7.12.2	Bearing Stiffeners	115
7.12.2.1	Bearing Resistance	117
7.12.2.2	Axial Resistance.....	117
7.13	Top Flange Lateral Bracing Design.....	119
7.14	Bolted Field Splice Design	126
7.14.1	Bolt Resistance for the Service Limit State and Constructibility	129
7.14.2	Bolt Resistance for the Strength Limit State.....	130
7.14.2.1	Bolt Shear Resistance.....	130
7.14.2.2	Bearing Resistance on Connected Material	131
7.14.3	Constructibility Checks.....	132
7.14.3.1	Constructibility Check of Top Flange Splice Bolts	133
7.14.3.2	Constructibility Check of Bottom Flange Splice Bolts.....	134
7.14.3.3	Constructibility Check of Web Splice Bolts	136
7.14.4	Service Limit State.....	140
7.14.4.1	Service Limit State Check of Top Flange Splice Bolts.....	141
7.14.4.2	Service Limit State Check of Bottom Flange Splice Bolts	141
7.14.4.3	Service Limit State Check of Web Splice Bolts	143
7.14.5	Strength Limit State	143
7.14.5.1	Positive Flexure Strength Limit State Design Forces	146
7.14.5.2	Negative Flexure Strength Limit State Design Forces.....	148
7.14.5.3	Summary of Flexure Strength Limit State Design Forces	150
7.14.5.4	Strength Limit State Check of Top Flange Splice Bolts	150
7.14.5.5	Strength Limit State Check of Bottom Flange Splice Bolts.....	150
7.14.5.6	Strength Limit State Check of Web Splice Bolts.....	152
7.14.5.7	Strength Limit State Check of Top Flange Splice Plates.....	157
7.14.5.8	Strength Limit State Check of Top Flange Splice Plates - Bearing...	160
7.14.5.9	Strength Limit State Check of Bottom Flange Splice Plates	161

7.14.5.10	Strength Limit State Check of Bottom Flange Splice Plates - Bearing	164
7.14.5.11	Strength Limit State Check of Web Splice Plates.....	166
7.14.5.12	Strength Limit State Check of Web Splice – Bearing on Girder Web	169
7.14.5.13	Strength Limit State Check of Web Splice Plates – Block Shear Rupture	169
8.0	SUMMARY OF DESIGN CHECKS AND PERFORMANCE RATIOS.....	171
9.0	REFERENCES	173

LIST OF FIGURES

Figure 1 Framing Plan of the Tub Girder Bridge (all lengths shown are taken along the centerline of the bridge)	8
Figure 2 Cross Section of the Tub Girder Bridge [2]	10
Figure 3 Plan View of a Warren-type truss lateral bracing system [1].....	13
Figure 4 Plan View of a Pratt-type truss lateral bracing system [1]	14
Figure 5 Diagram showing deck placement sequence	18
Figure 6 Vehicular Centrifugal Force Wheel-Load Reactions	20
Figure 7 Effects of Superelevation of the Wheel-Load Reactions	22
Figure 8 Unit Wheel Load Factors due to Combined Effects of Centrifugal Force and Superelevation.....	23
Figure 9 Girder G2 elevation	37
Figure 10 Sketch of Tub-Girder Cross-Section at Section G2-1	42
Figure 11 Moment of Inertia of an Inclined Web	43
Figure 12 Sketch of Tub-Girder Cross-Section at Section G2-2	46
Figure 13 Deck Overhang Bracket Loading	52
Figure 14 Effective Width of Web Plate, d_o , Acting with the Transverse Stiffener	88
Figure 15 Concentrated Torque at Mid-panel on Continuous Beam - Distortional Bending Stress at Load (DGBGB Figure A6 [11]).....	93
Figure 16 Concentrated Torque at Mid-panel on Continuous Beam – Normal Distortional Warping Stress at Mid-panel (DGBGB Table A9 [11])	94
Figure 17 Sketch of the Internal Diaphragm and Bearing Locations	110
Figure 18 Illustration for the computation of the shear in the internal diaphragms due to St. Venant torsion and tub girder flexure	113
Figure 19 Bolt Pattern for the Top Flange Field Splice.....	127
Figure 20 Bolt Pattern for the Bottom Flange Field Splice, shown inside the tub girder looking down at the bottom flange.....	127
Figure 21 Bolt Pattern for the Web Field Splice, shown along the web slope	128

LIST OF TABLES

Table 1 Girder G1 Unfactored Shears by Tenth Point.....	29
Table 2 Girder G2 Unfactored Shears by Tenth Point.....	30
Table 3 Girder G1 Unfactored Major-Axis Bending Moments by Tenth Point	31
Table 4 Girder G2 Unfactored Major-Axis Bending Moments by Tenth Point	32
Table 5 Girder G1 Unfactored Torques by Tenth Point	33
Table 6 Girder G2 Unfactored Torques by Tenth Point	34
Table 7 Section G2-1 Unfactored Major-Axis Bending Moments and Torques	35
Table 8 Section G2-1: Steel Only Section Properties	44
Table 9 Section G2-1: $3n=22.68$ Composite Section Properties	44
Table 10 Section G2-1: $n=7.56$ Composite Section Properties	45
Table 11 Section G2-2: Steel Only Section Properties	47
Table 12 Section G2-2: $3n=22.68$ Composite Section Properties with Transformed Deck	47
Table 13 Section G2-2: $n=7.56$ Composite Section Properties with Transformed Deck	48
Table 14 Section G2-2: $3n$ Composite Section Properties with Longitudinal Steel Reinforcement	48
Table 15 Section G2-2: n Composite Section Properties with Longitudinal Steel Reinforcement	48
Table 16 Unfactored Analysis Results for the Design of Field Splice #1 on Girder G2.....	128

1.0 INTRODUCTION

Tub girders are often selected over I-girders because of their pleasing appearance offering a smooth, uninterrupted, cross section. Bracing, web stiffeners, utilities, and other structural and nonstructural components are typically hidden from view within the steel tub girder, leading to a clean, uncluttered appearance. Additionally, steel tub girder bridges offer advantages over other superstructure types in terms of span range, stiffness, durability, and future maintenance.

Steel tub girders can potentially be more economical than steel plate I-girders in long span applications due to the increased bending strength offered by their wide bottom flanges, and because they require less field work due to handling fewer pieces. Steel tub girders can also be suitable in short span ranges as well, especially when aesthetic preferences or constructibility considerations preclude the use of other structure types. However, tub girders should be no less than 5 feet deep to allow access for inspection, thus limiting their efficiency in short span applications.

Tub girders, as closed-section structures, provide a more efficient cross section for resisting torsion than I-girders. The increased torsional resistance of a closed composite steel tub girder also results in an improved lateral distribution of live loads. Tub girders offer some distinct advantages over I-girders in particular for horizontally curved bridges since the torsional stiffness of a tub girder is much larger than the torsional stiffness of an I-girder. The high torsional resistance of individual tub-girder sections permits the tub girder to carry more of the load applied to it rather than shifting the load to the adjacent tub girder with greater radius, as is the case for torsionally weaker I-girders. The tendency to more uniformly share gravity loads reduces the relatively large and often troubling deflection of the girder on the outside of the curve. Also less material needs to be added to tub girders to resist the torsional effects. Torsion in tub sections is resisted mainly by St. Venant torsional shear flow. The warping constant for closed-box sections is approximately equal to zero. Thus, warping shear and normal stresses due to warping torsion are typically quite small and are usually neglected.

The exterior surfaces of tub girders are less susceptible to corrosion since there are fewer details for debris to accumulate, in comparison to an I-girder structure. For tub girders, stiffeners and most diaphragms are located within the tub girder, protected from the environment. Additionally, the interior surface of the tub girder is protected from the environment, further reducing the likelihood of deterioration. Tub girder bridges tend to be easy to inspect and maintain since much of the inspection can occur from inside the tub girder, with the tub serving as a protected walkway.

Erection costs for tub girders may be lower than that of I-girders because the erection of a single tub girder, in a single lift, is equivalent to the placement and connection of two I-girders. Tub girders are also inherently more stable during erection, due to the presence of lateral bracing between the top flanges. Overall, the erection of a tub girder bridge may be completed in less time than that of an I-girder counterpart because there are fewer pieces to erect, a fewer number of external diaphragms to be placed in the field, and subsequently fewer field connections to be made. This is a significant factor to consider when available time for bridge erection is limited by schedule or site access.

In many instances, these advantages are not well reflected in engineering cost estimates based solely on material quantity comparisons. Consequently, tub girder bridges have historically been considered more economical than I-girder bridges only if their use resulted in a reduction in the total number of webs in cross section, particularly for straight bridges. However, if regional fabricators have the experience and equipment to produce tub girders efficiently, the competitiveness of tub girders in a particular application can be enhanced. Therefore, the comparative economies of I- and tub girder systems should be evaluated on a case-by-case basis, and the comparisons should reflect the appropriate costs of shipping, erection, future inspection and maintenance as well as fabrication.

Furthermore, designers should not feel limited by overly-strict reading of the AASHTO design provisions for tub girders in some cases. For example, there are currently cross-sectional limitations placed on the use of approximate live load distribution factors for straight tub girders in the *AASHTO LRFD Bridge Design Specifications* [1]. Limiting the proportions of tub girder cross-sections solely to allow the use of these approximate live load distribution factors (to allow the use of simplified analysis methods) may reduce the efficiency and competitiveness of a tub-girder cross-section. However, these cross-section proportion limitations do not apply when a refined analysis is employed; thus the use of a refined analysis method allows the designer to explore additional, and perhaps more economical, design options.

This design example demonstrates the design of a horizontally curved three-span continuous composite tub girder bridge with a span arrangement of 160'-0" – 210'-0" – 160'-0". This example illustrates the flexural design of a section in positive flexure, the flexural design of a section in negative flexure, computation of distortional stresses, the shear design of the web, the design of the bottom flange longitudinal stiffener, the design of an internal diaphragm, the design of a top flange lateral bracing member, the design of a bolted field splice, as well as other design and analysis related topics.

The bridge cross-section consists of two trapezoidal tub girders with the top flanges of each tub spaced at 10'-0" on centers, 12'-6" between the centerline of adjacent top tub flanges, and 4'-0" overhangs for a deck width of 40'-6" out-to-out. For the sake of brevity, only the AASHTO LRFD Strength I and Service II load combinations are demonstrated in this design example. The effects of wind loads are not considered. The reader may refer to *Design Example 1: Three-Span Continuous Straight Composite I-Girder* for information regarding additional load combination cases and wind load effects.

The example calculations provided herein comply with the current *AASHTO LRFD Bridge Design Specifications* (7th Edition, 2014), but the analysis described herein was not performed as part of this design example. The analysis results and general superstructure details contained within this design example were taken from the design example published as part of the National Cooperative Highway Research Program (NCHRP) Project 12-52 published in 2005, titled "AASHTO-LRFD Design Example: Horizontally Curved Steel Box Girder Bridge, Final Report" [2].

2.0 OVERVIEW OF LRFD ARTICLE 6.11

The design of tub girder flexural members is contained within Article 6.11 of the Seventh Edition of the *AASHTO LRFD Bridge Design Specifications* [1], referred to herein as *AASHTO LRFD (7th Edition, 2014)*. The provisions of Article 6.11 are organized to correspond to the general flow of the calculations necessary for the design of tub girder flexural members. Most of the provisions are written such that they are largely self-contained, however to avoid repetition, some portions of Article 6.11 refer to provisions contained in Article 6.10 for the design of I-girder sections when applicable (particularly those pertaining to tub girder top flange design, which is fundamentally similar to I-girder design). The provisions of Article 6.11 are organized as follows:

- 6.11.1 General
- 6.11.2 Cross-Section Proportion Limits
- 6.11.3 Constructibility
- 6.11.4 Service Limit State
- 6.11.5 Fatigue and Fracture Limit State
- 6.11.6 Strength Limit State
- 6.11.7 Flexural Resistance - Sections in Positive Flexure
- 6.11.8 Flexural Resistance - Sections in Negative Flexure
- 6.11.9 Shear Resistance
- 6.11.10 Shear Connectors
- 6.11.11 Stiffeners

It should be noted that Article 6.11, and specifically Article 6.11.6.2, does not permit the use of Appendices A6 and B6 because the applicability of these provisions to tub girders has not been demonstrated; however, Appendices C6 and D6 are generally applicable. Flow charts for flexural design of steel girders according to the LRFD provisions, along with an outline giving the basic steps for steel-bridge superstructure design, are provided in Appendix C6. Appendix C6 provides a useful reference for tub girder design. Fundamental calculations for flexural members are contained within Appendix D6.

Example calculations demonstrating the provisions of Article 6.10, pertaining to I-girder design, are provided in Example 1 for a straight I-girder bridge, and Example 4 for a horizontally curved I-girder bridge within this Steel Bridge Design Handbook. This design example will highlight several of the provisions of the *AASHTO LRFD (7th Edition, 2014)* as they relate to horizontally curved tub girder design.

One significant difference between the *AASHTO LRFD (7th Edition, 2014)* and earlier LRFD Specifications (prior to the Third Edition) is the inclusion of the flange lateral bending stress in the design checks. The provisions of Articles 6.10 and 6.11 provide a unified approach for consideration of major-axis bending and flange lateral bending for both straight and curved bridges. Bottom flange lateral bending stresses in tub girders tend to be quite small, due to the width of the bottom flange, and can typically be neglected. Top flange lateral bending is caused by the outward thrust due to web inclination, wind load, temporary support brackets for deck overhangs, curvature, and from loads applied by the lateral bracing system.

In addition to providing adequate strength, the constructibility provisions of Article 6.11.3 ensure that nominal yielding does not occur and that there is no reliance on post-buckling resistance for main load-carrying members during critical stages of construction. The *AASHTO LRFD (7th Edition, 2014)* specifies that for critical stages of construction, both compression and tension flanges must be investigated, and the effects of top flange lateral bending should be considered when deemed necessary by the Engineer. For noncomposite top flanges in compression, constructibility design checks ensure that the maximum combined stress in the flange will not exceed the specified minimum yield strength, the member has sufficient strength to resist lateral torsional and flange local buckling, and that web-bend buckling will not occur. For noncomposite bottom flanges in compression, during critical stages of construction, local buckling of the flange is checked in addition to the web bend-buckling resistance. For noncomposite top and bottom flanges in tension, constructibility design checks make certain that the maximum combined stress will not exceed the specified minimum yield strength of the flanges during construction.

One additional requirement specified particularly for tub girders sections is in regard to longitudinal warping and transverse bending stresses. When tub girders are subjected to torsion, their cross-sections become distorted, resulting in secondary bending stresses. Therefore, as specified in Article 6.11.5, longitudinal warping stresses and transverse bending stresses due to cross-section distortion are to be considered for:

- Single tub girders in straight or horizontally curved bridges;
- Multiple tub girders in straight bridges that do not satisfy requirements of Article 6.11.2.3;
- Multiple tub girders in horizontally curved bridges; or
- Any single or multiple tub girder with a bottom flange that is not fully effective according to the provisions of Article 6.11.1.1.

In accordance with Article 6.11.1.1, transverse bending stresses due to cross section distortion are to be considered for fatigue as specified in Article 6.11.5, and at the strength limit state. Transverse bending stresses at the strength limit state are not to exceed 20.0 ksi. Longitudinal warping stresses due to cross-section distortion are to be considered for fatigue as specified in Article 6.11.5, but may be ignored at the strength limit state. Article C6.11.1.1 allows the use of the beam-on-elastic-foundation (BEF) analogy developed by Wright and Abdel-Samad [3] for determining the transverse bending stresses and the longitudinal warping stresses due to cross-section distortion. The BEF analogy is discussed in more detail within the calculations provided in this design example.

Even though the longitudinal warping stresses and transverse stresses are generally considered small and could be neglected, there are bridge designs where such an assumption may not be the case. There may be particular designs where these stresses warrant consideration by designer for the strength limit state for the tub girder as well as field splices. These bridge types may include those with small radii of curvature, skewed supports, and/or long spans.

3.0 DESIGN PARAMETERS

The following data apply to this design example:

Specifications:	2014 AASHTO LRFD Bridge Design Specifications, Customary U.S. Units, Seventh Edition [1]
Structural Steel:	AASHTO M270, Grade 50W (ASTM A709, Grade 50W) uncoated weathering steel with $F_y = 50$ ksi, and conservatively $F_u = 65$ ksi
Concrete:	$f'_c = 4.0$ ksi, $\gamma = 150$ pcf
Slab Reinforcing Steel:	AASHTO M31, Grade 60 (ASTM A615, Grade 60) with $F_y = 60$ ksi

The bridge has spans of 160'-0" – 210'-0" – 160'-0" measured along the centerline of the bridge. Span lengths are arranged to give relatively equal positive dead load moments in the end spans and center span. The radius of the bridge is 700 ft at the centerline of the bridge.

The out-to-out deck width is 40.5 ft, and the bridge is to be designed for three 12 ft traffic lanes. The roadway is superelevated at 5 percent. All supports are radial to the roadway. The framing consists of two trapezoidal tub girders with the top of the webs in each tub spaced 10 ft apart at the top of the tub and with a deck span of 12.5 ft between the top of the interior webs of the two adjacent tubs.

Structural steel having a specified minimum yield stress of 50 ksi is used throughout the bridge. The deck is a conventional cast-in-place concrete deck, with a specified minimum 28-day compressive strength of 4,000 psi. The structural deck thickness is 9.5 inches, and there is no integral wearing surface assumed. The deck haunch is 4.0 inches thick, measured from the top of the web to the bottom of the deck, and is constant throughout the structure. The width of the haunch is assumed to be 20.0 inches for weight computations.

Shear connectors are provided along the entire length of each top flange, therefore the tub girders in this example are composite throughout the entire span, including regions of negative flexure. The shear connectors are 7/8 inch diameter by 6 inches in length. All tub girders (whether straight or curved) are subject to torsional loading, and the use of shear connectors along the entire length of a tub girder bridge (in both the positive and negative moment regions) is required to ensure an adequate and continuous load path for St. Venant torsional shear flows along the entire length of the girder.

Permanent steel stay-in-place deck forms are used between the girders; the forms are assumed to weigh 15.0 psf since it is assumed concrete will be in the flutes of the deck forms. In this example, the steel stay-in-place deck forms are used between the top flanges of individual tub girders and between the top flanges of adjacent girders. Sequential placement of the concrete deck is considered in this design example.

An allowance for a future wearing surface of 30.0 psf is incorporated in the design. Parapets are each assumed to weigh 495 lb/ft.

The bridge is designed for HL-93 live load, in accordance with Article 3.6.1.2. Multiple presence factors are accounted for in the analysis, as specified in Article 3.6.1.1.2 Live load for fatigue is taken as defined in Article 3.6.1.4. The bridge is designed for a 75-year fatigue life, and single lane Average Daily Truck Traffic (ADTT)_{SL} in one direction is assumed to be 1,000 trucks per day.

The bridge site is assumed to be located in Seismic Zone 1, and so seismic effects are not considered in this design example.

4.0 GENERAL STEEL FRAMING CONSIDERATIONS

Composite tub girder bridges fabricated using uncoated weathering steel have performed successfully without any interior corrosion protection. However, the interiors of tub girders should always be coated in a light color to aid visibility during girder inspection. Without owner direction towards a specific coating and preparation, girder interiors should receive a light brush blast and be painted with a white or light colored paint capable of telegraphing cracks in the steel section. Specified interior paint should be tolerant of minimal surface preparation. At the Engineer's discretion, an allowance may be made for the weight of the paint.

Provisions for adequate draining and ventilation of the interior of the tub are essential. As suggested in the NSBA Publication *Practical Steel Tub Girder Design* [4], bottom flange drain holes should be 1 ½ inches in diameter and spaced along the low side of the bottom flange every 50 feet, and be placed 4 inches away from the web plate. Access holes must be provided to allow for periodic structural inspection of the interior of the tub. The access holes should provide easy access for authorized inspectors. Solid doors can be used to close the access holes, however they should be light in weight, and they should be hinged and locked, but not bolted. Wire mesh screens should always be placed over copes and clips in end plates, and over the bottom flange drain holes to prevent entry of wildlife and insects. Wire mesh should be 10 gage to withstand welding and blasting and have a weave of approximately ½ inch by ½ inch.

Additional detailing guidelines can be found at the NSBA's Website (www.steelbridges.org), with particular attention given to document AASHTO/NSBA Steel Bridge Collaboration document G1.4, *Guidelines for Design Details* [5]. Four other detailing references offering guidance include the NSBA Publication *Practical Steel Tub Girder Design* [4], the Texas Steel Quality Council's *Preferred Practices for Steel Bridge Design, Fabrication, and Erection* [6], the Mid-Atlantic States Structural Committee for Economic Fabrication (SCEF) Standards, and the AASHTO/NSBA Steel Bridge Collaboration document *Guidelines for Design for Constructibility* [7].

4.1 Span Arrangement

Often, site-specific features will influence the span arrangement required. Careful consideration of the layout of the steel framing is an important part of the design process and involves the investigation of alternative span arrangements based on the superstructure and substructure costs to arrive at the most economical solution. In the absence of site constraints, choosing a balanced span arrangement for continuous steel bridges (end spans approximately 80% of the length of the center spans) will typically provide an efficient design. The span arrangement for this example bridge has spans of 160 feet – 210 feet – 160 feet. The framing plan of the bridge for this example is shown in Figure 1.

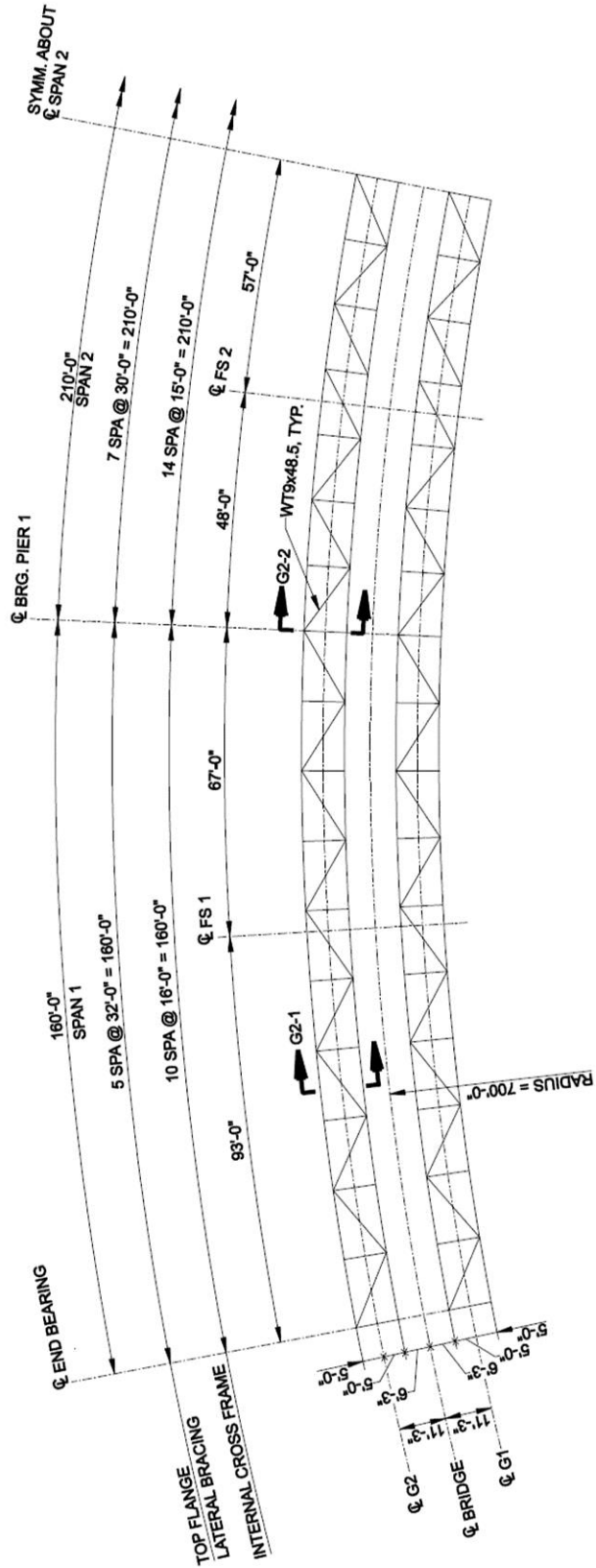


Figure 1 Framing Plan of the Tub Girder Bridge (all lengths shown are taken along the centerline of the bridge)

4.2 Field Section Sizes

The lengths of field sections are generally dictated by shipping (weight and length) restrictions. Generally, the weight of a single shipping piece is restricted to 200,000 lbs, while the piece length is limited to a maximum of 140 feet, with an ideal piece length of 120 feet. However, shipping requirements are typically dictated by state or local authorities, in which additional restrictions may be placed on piece weight and length. Handling issues during erection and in the fabrication shop also need to be considered in the determination of field section lengths, as they may govern the length of field sections. Therefore, the Engineer should consult with contractors and fabricators regarding any specific restrictions that might influence the field section lengths.

Field section lengths should also be determined with consideration given to the number of field splices required, as well as the locations of the field splices. It is desirable to locate field splices as close as possible to dead load inflection points, so as to reduce the forces that must be carried by the field splice. Field splices located in higher moment regions can become quite large, with cost increasing proportionally to their size. The Engineer should determine an economical solution for the particular span arrangement. For complex and longer span bridges, the fabricator's input can be helpful in reaching an economical solution.

The final girder field section lengths are shown on the framing plan in Figure 1. The longest field section is the field section of Girder G2 over the pier, and has a length of approximately 116.75 feet. This field section is also the heaviest field section, with a total approximate weight of 99,000 pounds (including internal cross frames, top flange lateral bracing, and other steel details).

In curved girder bridges, the Engineer must also consider the girder sweep and the subsequent total width when determining the lengths of the field sections. The curvature combined with the girder length can cause the field section to be too wide to transport, depending on shipping routes and local requirements. In the case of the field section of Girder G2 over the pier, the total width of the tub girder including girder sweep and the width of the top flanges is approximately 13.90 feet.

4.3 Bridge Cross Section and Girder Spacing

When developing the bridge cross-section, the designer will evaluate the number of girder lines required, relative to the overall cost. Specifically, the total cost of the superstructure is a function of steel quantity, details, and erection costs. Developing an efficient bridge cross-section should also give consideration to providing an efficient deck design, which is generally influenced by girder spacing and overhang dimensions. Specifically, with the exception of an empirical deck design, girder spacing significantly affects the design moments in the deck slab. In the case of tub girder bridges, which are comprised of torsionally stiff units, the deck should be designed to accommodate the transverse bending associated with differential girder deflection as shown in Figure C9.7.2.4-1 of the *AASHTO LRFD (7th Edition, 2014)*. Larger deck overhangs result in a greater load on the exterior web of the tub girder. Larger overhangs will increase the

bending moment in the deck, caused by the cantilever action of the overhang, resulting in additional deck slab reinforcing for the overhang region of the deck.

In addition, wider deck spans between top flanges can become problematic for several reasons. Some owners have economical deck detail standards for cast-in-place decks that may not be suited, or even permitted, for wider deck spans. At the same time, wider deck spans are progressively more difficult to form and construct. Wider deck spans also limit options for future deck replacement and partial deck removal. If bolder spacings and/or overhangs are used, a vaulted precast deck with transverse post-tensioning may be the most economical choice.

As shown in Figure 2, the example bridge cross-section consists of two trapezoidal tub girders with top flanges spaced at 10.0 feet within each tub girder, 12.5 feet between the centerline of adjacent top flanges, with 4.0 feet deck overhangs, and an out-to-out deck width of 40.5 feet. The 37.5 feet roadway width can accommodate up to three 12-foot-wide design traffic lanes. The total thickness of the cast-in-place concrete deck is 9.5 inches with no integral wearing surface. The concrete deck haunch is 4 inch deep measured from the top of the web to the bottom of the deck.

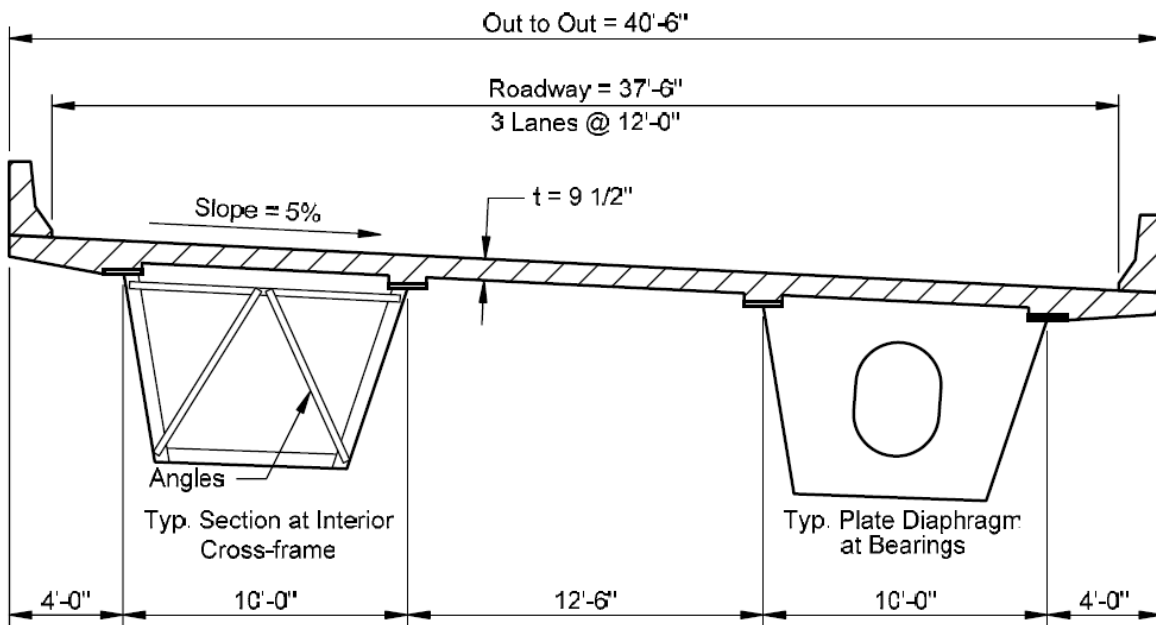


Figure 2 Cross Section of the Tub Girder Bridge [2]

4.4 Intermediate Internal and External Cross-Frames

Internal intermediate cross-frames are provided in tub girders to control cross-sectional distortion. Cross-sectional distortion results due to the St. Venant torsion shear flow changing direction at the corners of the tub. Cross-sectional distortion introduces additional stresses in the tub girder and, therefore, should be minimized. The distortion stresses basically occur because the section is not perfectly round. The shear flow must change direction at the corners, which tends to warp the cross-section. Adequate internal cross-bracing usually controls the magnitude of these stresses in tub girders of typical proportion such that they are not critical to the ultimate

resistance of the tub section at the strength limit state. As a minimum, internal cross-frames should be placed at points of maximum moment within a span and at points adjacent to field splices in straight bridges. Spacing of internal diaphragms, considered during development of the framing plan, should be influenced by factors such as the angle and length of the lateral bracing members.

Most cross-frames in modern tub girder bridges are K-frames, which allow better access during construction and inspection. Slenderness requirements (KL/r) generally govern the design of cross-frame members, however handling and strength requirements should always be investigated. When refined analysis methods are used and the cross-frame members are included in the structural model to determine force effects, the cross-frame members are to be designed for the calculated force effects. Consideration should be given to the cross-frame member forces during construction. When simplified analysis methods are used, such cross-frame forces due to dead and live loads are typically difficult to calculate. Therefore, the cross-frame members should at least be designed to transfer wind loads and carry construction loads due to deck overhang brackets, control tub girder cross section distortion, and satisfy appropriate slenderness requirements.

External intermediate cross-frames may be incorporated to control the differential displacements and rotations between individual tub girders during deck placement. In a finished bridge, when the tub girders are fully closed and the concrete deck effectively attaches the girders together, twist rotation is expected to be small and external cross-frames are not necessarily required.

External intermediate cross-frames typically utilize a K-frame configuration, with the depth closely matching the girder depth for efficiency and simplification of supporting details. At locations of external intermediate cross-frames, there should be bracing inside the tub girder to receive the forces of the external bracing. In some cases, for aesthetic reasons, it may be desirable to remove the external intermediate cross-frames after the deck has hardened. However, extreme care should be taken in evaluating the effects that the removal of external intermediate cross-frames has on the structure. The NSBA Publication *Practical Steel Tub Girder Design* [4] offers discussion on this topic.

Based on the preceding considerations, the internal cross-frame spacings shown on the framing plan in Figure 1 were chosen for this example. The tub girders are braced internally at intermediate locations with K-type cross-frames, where the diagonals intersect the top strut at the top flange level. The internal cross-frames are uniformly spaced in the end span and center span field sections. Internal cross-frame spacing in the center span positive flexure region is 15 feet. The top struts, both the individual struts and the ones that are part of internal cross-frames, also serve as part of the top flange lateral bracing system. Article C6.11.3.2 allows top lateral bracing attached to the flanges at points where only struts exist between the flanges to be considered as brace points at the discretion of the Engineer.

The design of the internal cross frame members is not shown in this example. Internal cross frames were modeled as truss members in the three-dimensional analysis, with a cross-sectional area of 5.0 square inches. There are no intermediate external cross frames provided between the tub girders in this design example.

4.5 Diaphragms at the Supports

Internal diaphragms at points of support are typically full-depth plates with a top flange. These diaphragms are subjected to bending moments which result from the shear forces in the inclined girder webs. If a single bearing is used at the support, and the bearing sole plate does not span the full width of the girder bottom flange, bending of the internal diaphragm over the support will result, causing bending stresses in the top flange of the diaphragm and the bottom flange of the tub girder. Additionally, a torsional moment reaction in the tub girder at the support will induce a shear flow along the circumference of the internal diaphragm. In order to provide the necessary force transfer between the tub girder and the internal diaphragms, the internal diaphragms should be connected to the web and top flanges of the tub girder.

Inspection access at the interior supports must also be provided through the internal diaphragm. Typically, an access hole will be provided within the internal diaphragm; however care must be taken in determining the location and size of the hole. The Engineer must investigate the flow of stress at the location of the hole in order to verify the sufficiency of the web near the access hole, or if reinforcing of the web may be required at the access hole.

Similar to internal diaphragms, external diaphragms are typically full-depth plate sections, but with top and bottom flanges. As acknowledged in the NSBA publication *Practical Steel Tub Girder Design* [4], the behavior of an external diaphragm at a point of support is highly dependent on the bearing arrangement at that location. If dual bearings used at each girder sufficiently prevent transverse rotation, external diaphragms at the point of support should theoretically be stress free. The force couple behavior of a dual bearing system resists the torsion that would otherwise be resisted by the external diaphragm and, in turn, minimizes the bending moments applied to the external diaphragm.

In accordance with Article 6.7.4.3, full-depth internal and external diaphragms are provided at the support lines in this design example. The web plates for the internal and external diaphragms in the three-dimensional analysis are assumed to have a thickness of 0.5 inches. The external diaphragm top and bottom flanges are assumed to have an area of 8.0 square inches for each flange.

4.6 Top Flange Lateral Bracing

In accordance with Article 6.7.5.3, for horizontally curved tub girders, a full-length lateral bracing system between common flanges of individual tub sections is to be provided, and the stability of compression flanges between panel points of the lateral bracing system is to be investigated during the deck placement. Generally, lateral bracing will not be required between adjacent tub girders.

Top flange lateral bracing creates a quasi-closed section, which increases the torsional stiffness of tub girder sections during erection, handling, and deck casting. For composite tub girders closed by the deck slab, the cross-section of the tub is torsionally stiff. However, prior to

placement of the deck slab, the open tub is torsionally more flexible and subject to rotation or twist. The top flange lateral bracing, then, forms a quasi-closed section resisting shear flow from the noncomposite loading.

Top lateral bracing is to be designed to resist shear flow in the pseudo box section due to factored loads before the concrete deck has hardened or is made composite. Forces in the bracing due to flexure of the tub girder should also be considered during construction based on the Engineer's assumed construction sequence. The top lateral bracing member forces can be determined using a refined three-dimensional analysis where the bracing members are explicitly modeled. Or, in the absence of a refined analysis, design equations have been developed to evaluate the bracing member forces due to tub girder major-axis bending [8 and 9].

The lateral bracing is typically comprised of WT or angle sections and is often configured in a single diagonal arrangement, such as a Warren-type or Pratt-type truss system. The diagonal bracing members commonly frame into the work point of the girder top flange and internal diaphragm or strut connection. Alternatively, the length between internal cross-frames can be divided into multiple lateral bracing panels. Such framing arrangements usually include a single transverse strut at intermediate brace locations. The plane of the top flange lateral bracing system should be detailed to be as close as possible to the plane of the girder top flanges so as to increase the torsional stiffness of the section, while at the same time reducing connection eccentricities and excessive out-of-plane bending in the web. In most cases the top flange lateral bracing is often attached directly to the top flange of the tub girders.

Single diagonal top lateral bracing systems are preferred over X-type systems because there are fewer pieces to fabricate and erect, and fewer connections. Warren-type and Pratt-type systems offer some advantages with regard to the behavior of each top flange lateral bracing system. In a Warren-type system, the bracing members alternate directions along the length of the bridge (see Figure 3). In most cases, the bracing forces will alternate from tension to compression along the length of the bridge. The tension and compression forces result from a combination of girder major-axis bending and girder torsion. If necessary, the flange lateral bending stresses and forces in the lateral bracing members can often be effectively mitigated by the judicious placement of parallel single-diagonal members in a Pratt-type configuration. In a Pratt-type system, the bracing members should be oriented based on the sign of the torque so that the forces induced in these members due to torsion offset the compressive or tensile forces induced in the same members due to major-axis bending of the tub section, thus allowing for smaller brace sizes (see Figure 4).

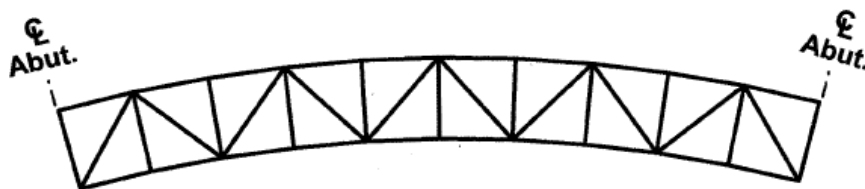


Figure 3 Plan View of a Warren-type truss lateral bracing system [1]

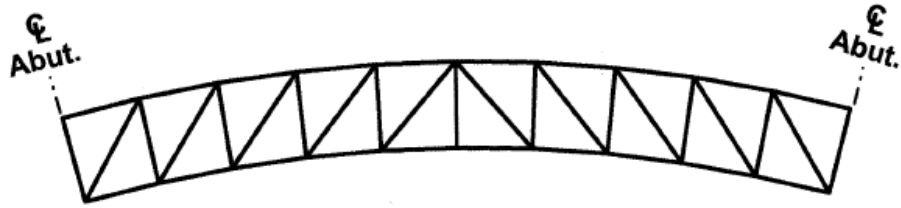


Figure 4 Plan View of a Pratt-type truss lateral bracing system [1]

As shown in Figure 1, a Warren-Type single diagonal top lateral bracing system is used in this design example. The bracing is assumed to be directly connected to the flanges at each internal cross frame and internal top strut; thus the bracing is assumed to lie in the plane of the top flange in the design calculations. The connection of the top flange lateral bracing directly to the flanges may require wider flanges than might otherwise be required by design, however this approach may still be more economical considering the high fabrication cost associated with gusset plates for the connections.

Truss members with an area of 8.0 square inches were assumed for the top flange lateral bracing members in the three-dimensional analysis. However, design calculations show that a WT9x48.5 is required, which has a cross-sectional area of 14.3 square inches. Although not done in this example, the designer should perform a second iteration of the analysis with this larger cross-sectional area, as the larger cross-sectional area will affect the load distribution in the bracing system in the noncomposite condition.

5.0 FINAL DESIGN

5.1 AASHTO LRFD Limit States

AASHTO LRFD (7th Edition, 2014) requires that bridges be designed for specified limit states to achieve the objectives of constructibility, safety, and serviceability. These objectives are met through the strength, service, fatigue and fracture, and extreme-event limit states. These limit states are intended to provide a safe, constructible, and serviceable bridge capable of carrying the appropriate design loads for a specified service life. A brief discussion of these limit states is provided herein, but the reader can refer to Steel Bridge Design Handbook topic on Limit States for more detailed discussion.

5.1.1 Strength Limit State

The strength limit states ensure strength and stability of the bridge and its components under the statistically predicted maximum loads during the 75-year life of the bridge. The strength limit states are not based upon durability or serviceability. There are five different strength limit state load combinations that must be considered by the designer.

In general, Strength I is the load combination used for checking the strength of a component under normal loading, in the absence of wind. To check the strength of a member or component under special permit loadings in the absence of wind, the Strength II load combination is used. The Strength III load combination is used for checking the strength of a component assuming the bridge is exposed to a wind velocity exceeding 55 miles per hour in the absence of live load. The Strength IV load combination basically relates to bridges with very high dead-to-live load force effect ratios. The Strength V load combination is used to check the strength of a component assuming the bridge is exposed to wind velocity equal to 55 miles per hour under normal loading.

5.1.2 Service Limit State

The service limit state ensures the durability and serviceability of the bridge and its components under typical “everyday” loads, traditionally termed service loads. The *AASHTO LRFD (7th Edition, 2014)* includes four service limit state load combinations of which only two are applicable to steel bridges.

The Service I load combination relates to normal operational use of the bridge and would be used primarily for crack control in reinforced concrete structures. However, the live load portion of the Service I load combination is used for checking live load deflection in steel bridges. The Service II load combination only applies to steel superstructures, and is intended to control yielding of steel structures and slip of slip-critical connections due to vehicular live load.

5.1.3 Fatigue and Fracture Limit State

The fatigue and fracture limit state is treated separately from the strength and service limit states since it represents a more severe consequence of failure than the service limit states, but not

necessarily as severe as the strength limit states. Fatigue cracking is certainly more serious than loss of serviceability as unchecked fatigue cracking can lead to brittle fracture, yet many passages of trucks may be necessary to cause a critically-sized fatigue crack while only one heavy truck can lead to a strength limit state failure. The fatigue and fracture limit state is only applicable where the detail under consideration experiences a net applied tensile stress.

The Fatigue I load combination is related to infinite load-induced fatigue life, and the Fatigue II load combination is related to finite load-induced fatigue life.

5.1.4 Extreme Event Limit State

Structural survival of the bridge must be ensured during an extreme event, such as an earthquake, flood, vessel collision, vehicle collision, or ice flow. The Extreme Event I load combination is related to earthquake loading, while the Extreme Event II load combination relates to the other possible extreme events.

5.1.5 Constructibility

Although not a specific limit state, the bridge must be safely erected and have adequate strength and stability during all phases of construction, as constructibility is one of the basic objectives of the *AASHTO LRFD (7th Edition, 2014)*. Specific design provisions are given in Articles 6.10.3 and 6.11.3 for I- and tub-girders, respectively, to help ensure constructibility. The constructibility checks are typically performed on the steel section only under the factored noncomposite dead loads using appropriate strength load combinations, especially when considering the deck placement sequence. Article 3.4.2 provides further guidance on the specific strength load combinations to be considered in the constructibility checks, and on the load factors to use for construction loads.

5.2 Loads

5.2.1 Dead Load

As defined in Article 3.5.1, dead loads are permanent loads that include the weight of all components of the structure, appurtenances and utilities attached to the structure, earth cover, wearing surfaces, future overlays and planned widenings.

The component dead load (DC) consists of all the structure dead load except for non-integral wearing surfaces, if anticipated, and any specified utility loads. For composite steel-girder design, DC is further divided into:

- Non-composite dead load (DC_1) is the portion of loading resisted by the non-composite section. DC_1 represents the permanent component load that is applied before the concrete deck has hardened or is made composite.
- Composite dead load (DC_2) is the portion of loading resisted by the long-term composite section. DC_2 represents the permanent component load that is applied after the concrete deck has hardened or is made composite.

The self-weight of the steel girders, cross-frames, diaphragms, lateral bracing and other attachments is applied to the erected steel structure in the three-dimensional model through the use of body forces in the various finite elements used to model the structure. A steel density of 490 pounds per cubic foot is assumed for all structural steel components. The analysis assumes that the steel is fit and erected in the no-load condition. The steel self-weight is a non-composite dead load (DC_1).

The concrete deck weight is assumed to be placed at one time on the noncomposite steel structure for the strength limit state checks. A separate deck placement sequence analysis is performed, where the analysis results are used for constructibility checks. The deck placement sequence is discussed later in this section. The deck weight includes the deck and concrete haunches, as well as an assumed weight of 15 pounds per square foot for the permanent metal deck forms inside the tub girders and between the two tub girders. The concrete deck weight, haunch weight, and permanent metal deck form weight are all considered to be non-composite dead loads (DC_1).

The composite dead load (DC_2), also referred to as a superimposed dead load, includes the weight of the parapets. The parapets are assumed to weigh 495 pounds per linear foot. The parapet weight is applied as line loads along the edges of the deck elements in the three-dimensional analysis.

The component dead load (DW) consists of the dead load of any non-integral wearing surfaces and any utilities, which can also be considered as superimposed dead loads. DW is applied as a surface load on the deck in the 3D analysis. For this example, a future wearing surface of 30 pounds per square foot of roadway is assumed, but no utilities are included.

For computing flexural stresses from composite dead loads DC_2 and DW , the stiffness of the long-term composite section in regions of positive flexure is calculated by transforming the concrete deck using a modular ratio of $3n$ (Article 6.10.1.1.1b). In regions of negative flexure, the long-term composite section is typically assumed to consist of the steel section plus the longitudinal reinforcement within the effective width of the concrete deck (Article 6.10.1.1.1c).

5.2.2 Deck Placement Sequence

The deck is considered to be placed in the following sequence for the constructibility limit state design checks, which is also illustrated in Figure 5. The concrete is first cast from the left abutment to a location near the dead load inflection point in Span 1. The concrete between approximate dead load inflection points in Span 2 is cast second. The concrete beyond the approximate dead load inflection point to the abutment in Span 3 is cast third. Finally, the concrete over the two piers is cast. In the analysis, earlier concrete casts are assumed fully composite for each subsequent cast.

For the constructibility limit state design checks, the noncomposite section is checked for the moments resulting from the deck placement sequence or the moments computed assuming the entire deck is cast at one time, whichever is larger.

The weight of the fresh concrete on the overhang brackets, along with other loads applied to the brackets, produces lateral forces on the outermost top flange of G2 and the innermost top flange of G1. This eccentric loading and subsequent lateral forces on the top flanges must be considered in the constructibility limit state design checks.

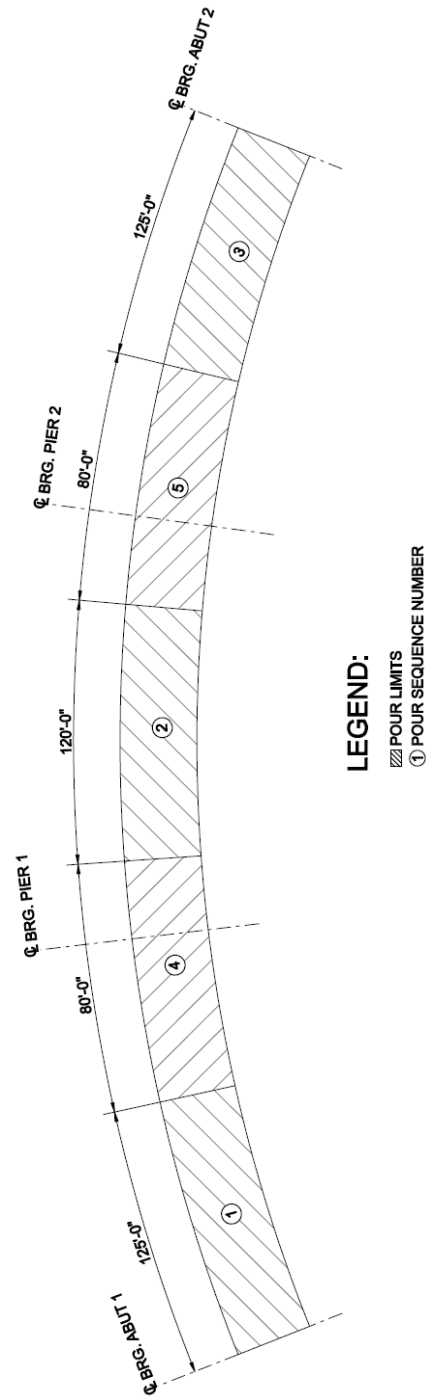


Figure 5 Diagram showing deck placement sequence

5.2.3 Live Load

Live loads are assumed to consist of gravity loads (vehicular live loads, rail transit loads and pedestrian loads), the dynamic load allowance, centrifugal forces, and braking forces. Live loads illustrated in this example include the HL-93 vehicular live load and a fatigue load, with the appropriate dynamic load allowance and centrifugal force (see Section 5.3) effects included.

Influence surfaces are utilized to determine the live load force effects in this design example. More details regarding influence surfaces and the live load analysis associated with the 3D analysis model are provided in Section 6.1.2 of this example.

Live loads are considered to be transient loads applied to the short-term composite (n) section. For computing flexural stresses from transient loading, the short-term composite (n) section in regions of positive flexure is calculated by transforming the concrete deck using a modular ratio of n (Article 6.10.1.1.1b). In regions of negative flexure, the short-term composite (n) section is assumed to consist of the steel section plus the longitudinal reinforcement within the effective width of the concrete deck (Article 6.10.1.1.1c), except as permitted otherwise for the fatigue and service limit states (see Articles 6.6.1.2.1 and 6.10.4.2.1).

When computing longitudinal flexural stresses in the concrete deck (see Article 6.10.1.1.1d), due to permanent and transient loads, the short-term composite section should be used.

Design Vehicular Live Load (Article 3.6.1.2)

The design vehicular live load is designated as the HL-93 and consists of a combination of the following placed within each design lane:

- a design truck *or* design tandem.
- a design lane load.

The design vehicular live load is discussed in detail within Example 1 of the Steel Bridge Design Handbook.

Fatigue Load (Article 3.6.1.4)

The vehicular live load for checking fatigue consists of a single design truck (without the lane load) with a constant rear-axle spacing of 30 feet (Article 3.6.1.4.1). The fatigue live load is discussed in detail within Example 1 of the Steel Bridge Design Handbook.

5.3 Centrifugal Force Computation

The centrifugal force is determined according to Article 3.6.3. The centrifugal force has two components, the radial force and the overturning force. The radial component of the centrifugal force is assumed to be transmitted from the deck through the end cross frames or diaphragms and to the bearings and the substructure.

The overturning component of centrifugal force occurs because the radial force is applied at a distance above the top of the deck. The center of gravity of the design truck is assumed to be 6

feet above the roadway surface according to the provisions of Article 3.6.3. The transverse spacing of the wheels is 6 feet per Figure 3.6.1.2.2-1. The overturning component causes the exterior (with respect to curvature) wheel line to be more than half the weight of the truck and the interior wheel line to be less than half the weight of the truck by the same amount. Thus, the outside of the bridge is more heavily loaded. The effect of superelevation, which reduces the overturning effect of centrifugal force, is considered, as permitted by Article 3.6.3. Figure 6 shows the relationship between the centrifugal force and the superelevation effect. The dimensions denoted by s and h in Figure 6 are both equal to 6 feet.

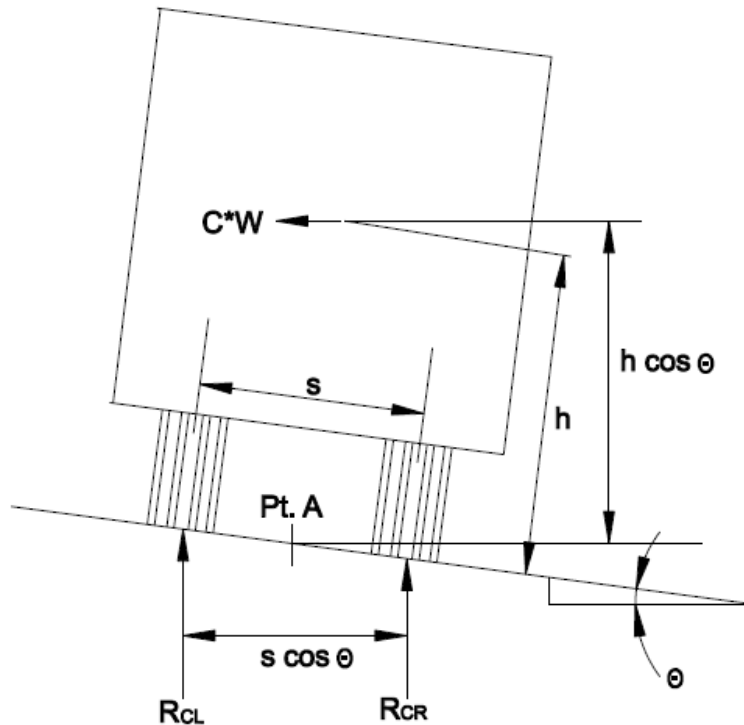


Figure 6 Vehicular Centrifugal Force Wheel-Load Reactions

Article 3.6.3 states that the centrifugal force is to be taken as the product of the axle weights of the design truck or tandem and the factor C , taken as:

$$C = f \frac{v^2}{g R} \quad \text{Eq. (3.6.3-1)}$$

where:

- f = 4/3 for load combinations other than fatigue and 1.0 for fatigue
- v = highway design speed (ft/sec)
- g = gravitational acceleration = 32.2 ft/sec²
- R = radius of curvature (ft)

Use the average bridge radius, $R = 700$ ft, in this case. For the purpose of this design example, the design speed is assumed to be $35 \text{ mph} = 51.3 \text{ ft/s}$. Therefore, for the HL-93 Design Truck:

$$C = \frac{4}{3} \left[\frac{51.3^2}{(32.2)(700)} \right] = 0.156$$

The next step is to compute the wheel load reaction, R_{CL} and R_{CR} , due to centrifugal force effects, as shown in Figure 6. In the case of the design truck, the wheel spacing, s , and the height of the radial force, h , are both equal to 6.0 feet. Therefore, summing moments about Point A (Figure 6) and enforcing equilibrium, the wheel load reactions, R_{CL} and $-R_{CR}$ are simply equal to C multiplied by W , as follows:

$$R_{CL} = -R_{CR} = (C * W) \frac{h \cos(\theta)}{2 \left(\frac{s}{2} \cos(\theta) \right)} = C * W = 0.156W$$

where:

$$W = \text{axle weight (kips)}$$

R_{CL} is an upward reaction for the left wheel, and R_{CR} is an equal but opposite downward reaction for the right wheel.

As permitted by Article 3.6.3, the effects of superelevation on the individual wheel load reactions can be computed and combined with the centrifugal force effects. For the 5% deck cross slope, the angle θ is equal to:

$$\theta = \tan^{-1}(0.05) = 2.86^\circ$$

The wheel load reactions due to superelevation, R_{SL} and R_{SR} , as shown in Figure 7, are computed by summing the moments about the left wheel, as follows:

$$R_{SR} = \frac{\left[\frac{s}{2} \cos(\theta) + h \sin(\theta) \right] W}{s \cos(\theta)} = \frac{\left[\left(\frac{6}{2} \right) \cos(2.86^\circ) + (6) \sin(2.86^\circ) \right] W}{(6) \cos(2.86^\circ)} = 0.550W$$

$$R_{SL} = 1.0W - R_{SR} = 1.0W - 0.550W = 0.450W$$

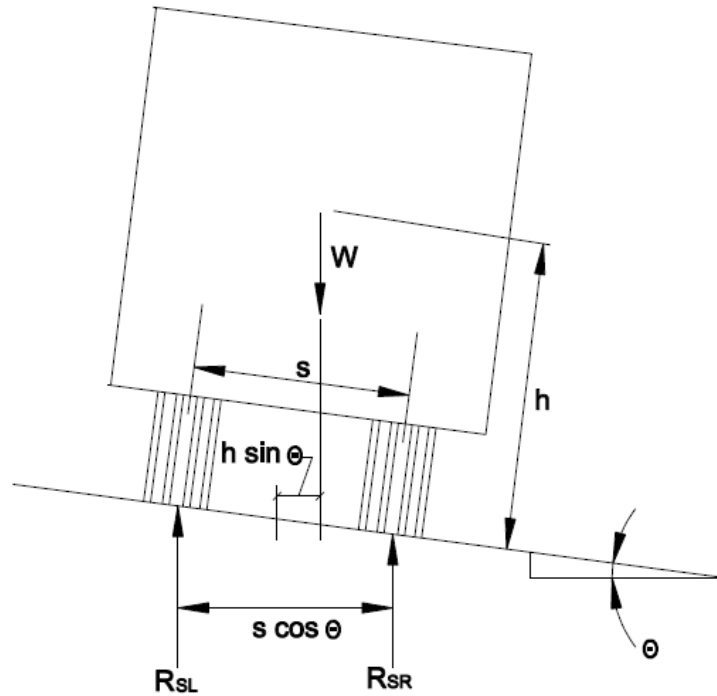


Figure 7 Effects of Superelevation of the Wheel-Load Reactions

For a refined analysis, as used in this design example, unit wheel load factors can be computed based on the sum of the wheel load reaction due to the centrifugal force and superelevation effects. The unit wheel load factors are applied to the appropriate wheels in the analysis. Unit wheel load factors due to the combined effects of centrifugal force and superelevation can be computed for the left wheels, F_L , and the right wheels, F_R . The sum of F_L and F_R must equal 2.0, as there are two wheel loads per one axle. The left and right unit wheel load factors, F_L and F_R , are computed as follows:

$$F_L = 2.0 \frac{R_{CL} + R_{SL}}{W} = 2.0 \frac{0.156W + 0.450W}{W} = 1.212$$

$$F_R = 2.0 \frac{R_{CR} + R_{RL}}{W} = 2.0 \frac{-0.156W + 0.550W}{W} = 0.788$$

As shown in Figure 8, F_L and F_R represent the factors that must be multiplied by the left wheel and right wheel load, respectively, in the analysis to take into account the combined effects of both centrifugal force and superelevation. In this case, since F_L is greater than F_R , the outermost girder will receive a slightly higher load and the innermost girder will receive slightly lower load from the design truck. Therefore, it is also necessary to compute the condition with no centrifugal force, i.e., a stationary vehicle, and select the worst case. In the live load analysis performed for this design example, force effects from an analysis due to live load cases with centrifugal force effects included (F_L equals 1.212 and F_R equals 0.788) are compared to force effects due to cases with no centrifugal force effects included (F_L and F_R equal 1.0), and the maximum/minimum force effect is selected.

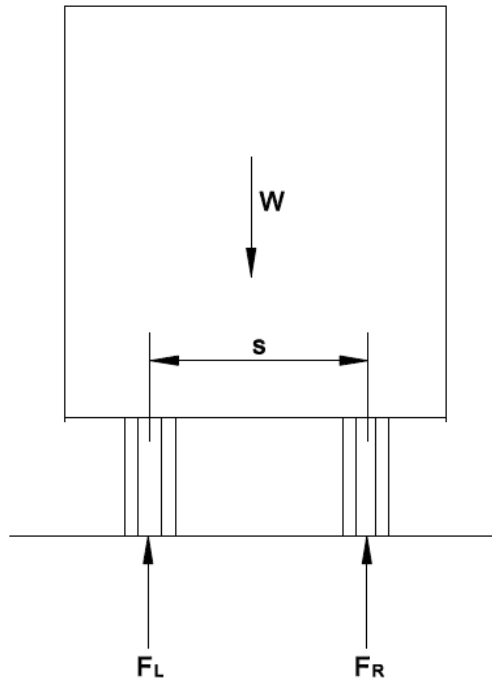


Figure 8 Unit Wheel Load Factors due to Combined Effects of Centrifugal Force and Superelevation

In accordance with Article C3.6.3, centrifugal force is not required to be applied to the design lane load, as the spacing of vehicles at high speed is assumed to be large, resulting in a low density of vehicles following and/or preceding the design truck.

From separate calculations for the fatigue limit state, similar to those shown previously, the centrifugal force factor C is equal to 0.117, and the unit wheel load factors, F_L and F_R , are 1.134 and 0.866, respectively.

5.4 Load Combinations

AASHTO LRFD (7th Edition, 2014) Table 3.4.1-1 is used to determine load combinations for strength according to Article 3.4. Strength I loading is used for design of most members for the strength limit state. However, Load Combinations Strength III and V and Service I and II from Table 3.4.1-1 are also checked for temperature and wind loadings in combination with vertical loading.

The following load combinations and load factors are typically checked in a girder design similar to this design example. In some design instances, other load cases may be critical, but for this example, these other load cases are assumed not to apply.

From Table 3.4.1-1 (minimum load factors of Table 3.4.1-2 are not considered here):

Strength I	$\eta \times [1.25(DC) + 1.5(DW) + 1.75((LL + IM) + CE + BR) + 1.2(TU)]$
Strength III	$\eta \times [1.25(DC) + 1.5(DW) + 1.4(WS) + 1.2(TU)]$
Strength V	$\eta \times [1.25(DC) + 1.5(DW) + 1.35((LL + IM) + CE + BR) + 0.4(WS) + 1.0(WL) + 1.2(TU)]$
Service I	$\eta \times [DC + DW + (LL + IM) + CE + BR + 0.3(WS) + WL + 1.2(TU)]$
Service II	$\eta \times [DC + DW + 1.3((LL + IM) + CE + BR) + 1.2(TU)]$
Fatigue I	$\eta \times [1.5((LL + IM) + CE)]$
Fatigue II	$\eta \times [0.75((LL + IM) + CE)]$

where:

η	=	Load modifier specified in Article 1.3.2
DC	=	Dead load: components and attachments
DW	=	Dead load: wearing surface and utilities
LL	=	Vehicular live load
IM	=	Vehicular dynamic load allowance
CE	=	Vehicular centrifugal force
WS	=	Wind load on structure
WL	=	Wind on live load
TU	=	Uniform temperature
BR	=	Vehicular braking force

In addition to the above load combinations, two additional load combinations for the constructibility checks are defined in Article 3.4.2 as follows:

$$\text{Construction: } \eta \times [1.25(D) + 1.5(C) + 1.25(WC)]$$
$$\eta \times [1.4(D + C)]$$

where:

D	=	Dead load
C	=	Construction loads
WC	=	Wind load for construction conditions from an assumed critical direction. Magnitude of wind may be less than that used for final bridge design.

In this design example, for brevity, only the first of these load combinations is considered/illustrated in the constructibility checks. Wind load effects during construction are also not considered herein.

For the purpose of this example, it has been assumed that the Strength I load combination governs for the strength limit state, so only Strength I loads are checked in the sample calculations for the strength limit state included herein. Also, the load modifier, η , is assumed to be 1.0 throughout this example unless noted otherwise. Furthermore, from a separate analysis, the girder demands due to thermal loading are determined to be quite small, and are neglected throughout these computations.

6.0 ANALYSIS

Article 4.4 of the *AASHTO LRFD (7th Edition, 2014)* requires that the analysis be performed using a method that satisfies the requirements of equilibrium and compatibility, and utilizes stress-strain relationships for the proposed materials. Article 4.6.1.2 provides additional guidelines for structures that are curved in plan. The moments, shears, and other force effects required to proportion the superstructure components are to be based on a rational analysis of the entire superstructure. Equilibrium of horizontally curved I-girders is developed by the transfer of load between the girders, thus the analysis must recognize the integrated behavior of structural components. Equilibrium of curved tub girders can be somewhat less dependent on the interaction between girders, as there are typically fewer external bracing members between adjacent tub girders as compared to I-girder bridges.

Furthermore, in accordance with Article 4.6.1.2, the entire superstructure, including bearings, is to be considered as an integral structural unit in the analysis. Boundary conditions should represent the articulations provided by the bearings and/or integral connections used in the design.

In most cases, small deflection elastic theory is acceptable for the analysis of horizontally curved steel girder bridges. However, curved girders, especially I-girders, are prone to deflect laterally when the girders are insufficiently braced during erection, and this behavior may not be appropriately recognized by small deflection theory. In curved tub girder bridges, there is typically sufficient bracing provided during steel erection so that deflections do not invalidate the use of small deflection elastic theory.

In general, three levels of analysis exist for horizontally curved girder bridges: approximate methods of analysis, 2D (two-dimensional) methods of analysis, and 3D (three-dimensional) methods of analysis. The V-load method and the M/R methods are approximate analysis methods that are typically used to analyze curved I-girder bridges and curved tub girder bridges, respectively. Both methods are developed based on the understanding of the distribution of forces through the curved bridge system. The two primary types of 2D analysis models are the traditional grid (or grillage) model and the plate and eccentric beam model. In 2D analysis models, the girders and external cross frames and diaphragms are modeled using beam elements, with the nodes for the grid representing the steel superstructure in a single horizontal plane. A 3D model recognizes the depth of the superstructure. Two planes of nodes are typically used for each girder, one in the plane of the top flanges and the second in the plane of the bottom flanges. Further details regarding these methods of analysis can be found in the Steel Bridge Design Handbook topic on Structural Analysis.

6.1 Three-Dimensional Finite Element Analysis

A three-dimensional finite element analysis is used to analyze the superstructure in this design example. The girder webs and bottom flanges are modeled using plate elements. The top flanges of each tub girder are modeled with beam elements. The girder elements connect to nodes that are placed in two horizontal planes; one plane at the top flange level and one plane at the bottom flange level. The horizontal curvature of the girders is represented by a series of straight

elements connected at the nodes, rather than by curved elements. Nodes are placed on all flanges along the girder at each internal cross frame and top flange lateral bracing location, and typically at the middle of each top flange lateral bracing bay.

The composite deck is modeled using a series of eight-node solid elements attached to the girder top flanges with rigid beam elements, which represent the shear studs.

Bearings are modeled with dimensionless elements called “foundation elements.” These dimensionless elements can provide six different stiffnesses, with three for translation and three for rotation. If a guided bearing is orientated along the tangential axis of a girder, a translational stiffness of zero is assigned to the stiffness in the tangential direction. The translational stiffness of the bearing, and supporting structure if not explicitly modeled, is assigned to the direction orthogonal to the tangential axis.

Internal cross frame members are modeled with individual truss elements connected to the nodes at the top and bottom flange of the girders. Internal solid-plate diaphragms at the supports are modeled with a single plate element. External solid-plate diaphragms at the supports are modeled using three full-depth plate elements along the length of the diaphragm, and three beam elements placed at the top and bottom of the web representing the top and bottom flanges of the diaphragm. Since the plate and beam elements are isoparametric, three sets of elements are used to model the web and flanges of the external diaphragm to allow for the possibility of reverse curvature.

Top flange lateral bracing members are modeled with individual truss elements connected to nodes at the top flanges of the tub girders.

6.1.1 Bearing Orientation and Arrangement

The orientation and lateral restraint of bearings affects the behavior of most girder bridges for most load conditions, and is particularly true for curved and skewed girder bridges. Furthermore, in tub girder bridges, one or two bearings can be use under each tub girder at each support.

The use of two bearings to support an individual girder at a support allows the girder torsion to be directly removed through the force couple provided by the bearings, and reduces the reaction demand in the bearings. Two-bearing systems typically work well with radial supports, but are impractical with supports skewed more than a few degrees where the tub girder and/or diaphragm stiffnesses work against the achievement of uniform bearing contact during various stages of girder erection and deck slab construction [4].

The use of one bearing to support an individual girder at a support optimizes contact between the girder and the bearing. One-bearing systems also tend to be more forgiving of construction tolerances, and at skewed supports, one-bearing systems are demonstrably better than two-bearing systems [4]. A disadvantage of one-bearing systems is that stiff cross frames or diaphragms between girders are required to resolve the girder torsion into the bearings.

In this example, two bearings are used at each girder support location. The centerline of each bearing is located 28.5 inches from the girder centerline at the support. Furthermore, the bearings at Pier 1 are assumed fixed against translation in both the radial and longitudinal directions (Fixed Bearings). The bearings at the abutments and at Pier 2 are assumed fixed against radial movement but free in the longitudinal direction (Guided Bearings). The longitudinal direction at each support varies, as in this case the longitudinal direction is taken along a straight line chord line between the fixed support (Pier 1) and each expansion bearing. Curved girder bridges do not expand and contract along the girder line, but more so along the aforementioned chord lines. Orientating the bearings in the manner discussed significantly reduces the longitudinal stresses in the girders that can occur due to thermal loading. Therefore, due to the bearing orientation and from a separate analysis, the girder demands due to thermal loading are determined to be quite small, and are neglected throughout these computations. In all designs, the thermal demands must be considered and properly addressed.

6.1.2 Live Load Analysis

The use of live load distribution factors is typically not appropriate for curved steel tub girder bridges, because these structures are best analyzed as a system. Therefore, influence surfaces are most often utilized to more accurately determine the live load force effects in curved girder bridges. Influence surfaces are an extension of influence lines, such that an influence surface not only considers the longitudinal position of the live loads, but the transverse position as well.

Influence surfaces provide influence ordinates over the entire deck. The influence ordinates are determined by applying a series of unit vertical loads, one at a time, at selected longitudinal and transverse positions on the bridge deck surface. The magnitude of the response for the unit vertical load is the magnitude of the ordinate of the influence surface for the particular response at the point on the deck where the load is applied. The entire influence surface is created by curve fitting between calculated ordinates. Specified live loads are then placed on the surface, mathematically, at the critical locations, as allowed by the governing specification, to determine the maximum and minimum effects. The actual live load effect is determined by multiplying the live load by the corresponding ordinate. In the case of an HL-93 truck load, a different ordinate will exist for each wheel load. The total HL-93 truck live load effect is the summation of all the wheel loads times their respective ordinates. For the design lane load, the effect is determined by integrating the area of the influence surface under the load and multiplying it by the intensity of the load.

In curved girder bridges, influence surfaces are generally needed for all live load force results, such as major-axis bending moments, flange lateral bending moments, girder shear, reactions, torques, deflections, cross-frame forces, diaphragm forces, lateral bracing forces, etc.

Unless noted otherwise, all live load force effects in this example are computed using influence surfaces, developed using the three-dimensional analysis. The dynamic load allowance (impact) is included in the analysis, and is applied to the live-load force effects in accordance with Article 3.6.2 for strength, service, and fatigue as required. Multiple presence factors are also included within the analysis, and thus are incorporated into the analysis results. Also, as appropriate,

centrifugal force effects are also included in the analysis results, using wheel-load factors as shown in Section 5.3 of this design example.

6.2 Analysis Results

This section shows the results from the three-dimensional analysis of the superstructure. Analysis results are provided for the moments, shears, and torques for girders G1 and G2. All analysis results are unfactored. Live load results included multiple presence factors, dynamic load allowance (impact), and centrifugal force effects.

Specific analysis results for design Section G2-1, which is located approximately 57 feet from the centerline of the bearings at abutment 1, are provided in Table 7. The analysis results are used in the design computations associated with Section G2-1, provided later within this design example.

Table 1 Girder G1 Unfactored Shears by Tenth Point

Girder G1 Unfactored Shears									
10th Point	Span Length (ft)	Dead Load				LL+I		Fatigue LL+I	
		DC1 _{STEEL}	DC1 _{CONC}	DC2	DW	Pos.	Neg.	Pos.	Neg.
		(kip)	(kip)	(kip)	(kip)	(kip)	(kip)	(kip)	(kip)
0	0.00	27	114	25	33	139	-24	52	-4
1	15.74	19	80	12	15	115	-29	41	-6
2	31.49	10	45	8	10	94	-35	34	-9
3	47.23	5	23	5	6	78	-41	28	-12
4	62.97	-6	-25	-3	-4	53	-52	22	-16
5	78.71	-11	-44	-6	-7	40	-63	16	-22
6	94.46	-16	-69	-8	-11	31	-83	13	-27
7	110.20	-23	-98	-13	-17	25	-101	10	-34
8	125.94	-28	-116	-18	-23	21	-116	7	-40
9	141.69	-34	-137	-24	-32	19	-127	7	-43
10	157.43	-44	-171	-40	-54	14	-163	4	-53
10	0.00	45	175	41	55	171	-15	58	-4
11	20.66	31	128	23	31	140	-23	44	-6
12	41.33	25	110	16	21	124	-26	39	-7
13	61.99	17	72	10	13	101	-37	31	-12
14	82.65	11	47	5	6	78	-45	27	-15
15	103.31	0	0	0	0	58	-57	22	-22
16	123.98	-11	-47	-5	-6	43	-78	15	-27
17	144.64	-17	-72	-10	-14	36	-101	12	-31
18	165.30	-25	-110	-16	-21	26	-124	6	-39
19	185.96	-31	-127	-23	-31	23	-140	6	-46
20	206.63	-45	-175	-41	-55	14	-166	4	-55
20	0.00	44	171	40	54	167	-15	56	-4
21	15.74	34	137	24	32	128	-19	43	-7
22	31.49	28	116	18	23	116	-21	40	-7
23	47.23	23	98	13	17	101	-25	34	-10
24	62.97	16	69	8	11	83	-31	27	-13
25	78.71	11	44	6	7	64	-38	22	-16
26	94.46	6	25	3	4	51	-52	16	-22
27	110.20	-5	-23	-5	-6	41	-77	12	-28
28	125.94	-10	-45	-8	-10	32	-92	9	-34
29	141.69	-19	-80	-12	-16	27	-113	6	-41
30	157.43	-27	-114	-25	-34	24	-139	4	-52

Note: Reported shears are the vertical shears and are for major-axis bending plus torsion in the critical tub girder web.

Table 2 Girder G2 Unfactored Shears by Tenth Point

Girder G2 Unfactored Shears									
10th Point	Span Length (ft)	Dead Load				LL+I		Fatigue LL+I	
		DC1 _{STEEL}	DC1 _{CONC}	DC2	DW	Pos.	Neg.	Pos.	Neg.
		(kip)	(kip)	(kip)	(kip)	(kip)	(kip)	(kip)	(kip)
0	0.00	31	110	39	52	128	-26	61	-12
1	16.26	19	74	17	22	110	-29	52	-12
2	32.51	11	44	11	15	93	-35	44	-12
3	48.77	5	21	6	8	75	-44	36	-12
4	65.03	-7	-26	-3	-5	54	-52	25	-18
5	81.29	-11	-45	-6	-8	40	-67	18	-27
6	97.54	-17	-69	-12	-16	36	-85	13	-34
7	113.80	-24	-97	-17	-23	33	-102	12	-43
8	130.06	-29	-117	-22	-29	26	-114	7	-49
9	146.31	-35	-137	-27	-35	16	-127	4	-53
10	162.57	-46	-185	-41	-55	13	-155	4	-61
10	0.00	47	185	44	58	160	-14	65	-4
11	21.34	32	130	28	37	135	-22	55	-4
12	42.68	26	105	22	29	120	-33	49	-9
13	64.01	17	69	15	20	100	-42	41	-13
14	85.35	12	46	7	10	78	-46	33	-16
15	106.69	0	0	0	0	57	-57	24	-24
16	128.03	-12	-46	-7	-10	46	-78	16	-33
17	149.36	-17	-69	-15	-20	41	-99	13	-41
18	170.70	-26	-105	-22	-29	33	-120	9	-50
19	192.04	-32	-130	-28	-37	22	-135	4	-55
20	213.38	-47	-185	-44	-58	14	-159	4	-64
20	0.00	46	185	41	55	158	-14	64	-4
21	16.26	35	137	27	35	128	-15	53	-4
22	32.51	29	117	22	29	115	-26	49	-7
23	48.77	24	97	17	23	102	-33	41	-12
24	65.03	17	69	12	16	85	-36	33	-13
25	81.29	11	45	6	8	67	-40	27	-18
26	97.54	7	26	3	5	52	-54	18	-25
27	113.80	-5	-21	-6	-8	44	-75	12	-36
28	130.06	-11	-44	-11	-15	34	-93	12	-44
29	146.31	-19	-74	-17	-22	28	-111	12	-52
30	162.57	-31	-110	-39	-52	26	-129	12	-61

Note: Reported shears are the vertical shears and are for major-axis bending plus torsion in the critical tub girder web.

Table 3 Girder G1 Unfactored Major-Axis Bending Moments by Tenth Point

Girder G1 Unfactored Major-Axis Bending Moments									
10th Point	Span Length (ft)	Dead Load				LL+I		Fatigue LL+I	
		DC1 _{STEEL}	DC1 _{CONC}	DC2	DW	Pos.	Neg.	Pos.	Neg.
		(kip-ft)	(kip-ft)	(kip-ft)	(kip-ft)	(kip-ft)	(kip-ft)	(kip-ft)	(kip-ft)
0	0.00	0	0	0	0	0	0	0	0
1	15.74	521	2191	340	450	2472	-469	748	-98
2	31.49	882	3666	592	785	4330	-938	1252	-196
3	47.23	1049	4321	724	960	5412	-1408	1477	-293
4	62.97	1047	4320	734	972	5863	-1878	1545	-385
5	78.71	851	3503	620	821	5777	-2338	1502	-471
6	94.46	493	2043	387	514	5189	-2795	1367	-553
7	110.20	-75	-315	36	47	4109	-3915	1108	-667
8	125.94	-837	-3461	-434	-576	2602	-4547	714	-813
9	141.69	-1781	-7206	-1014	-1343	1252	-5559	270	-991
10	157.43	-2969	-11629	-1762	-2335	1061	-7784	231	-1249
10	0.00	-2969	-11629	-1762	-2335	1061	-7784	231	-1249
11	20.66	-1422	-5845	-802	-1062	1310	-4411	363	-810
12	41.33	-326	-1516	-95	-125	2993	-3033	924	-618
13	61.99	493	1881	425	563	4784	-2275	1324	-470
14	82.65	977	3900	733	972	5926	-2008	1556	-367
15	103.31	1118	4442	836	1108	6304	-1749	1616	-279
16	123.98	976	3900	733	972	5928	-2013	1556	-369
17	144.64	492	1880	424	562	4775	-2279	1326	-471
18	165.30	-327	-1519	-95	-127	3000	-3021	923	-616
19	185.96	-1422	-5848	-803	-1064	1315	-4421	381	-810
20	206.63	-2969	-11633	-1762	-2336	1062	-7788	233	-1230
20	0.00	-2969	-11633	-1762	-2336	1062	-7788	233	-1230
21	15.74	-1780	-7203	-1014	-1345	1248	-5556	270	-997
22	31.49	-837	-3459	-436	-577	2591	-4532	714	-810
23	47.23	-74	-312	34	46	4099	-3900	1107	-665
24	62.97	493	2044	386	511	5181	-2783	1367	-551
25	78.71	851	3504	618	819	5769	-2328	1502	-462
26	94.46	1047	4320	732	971	5855	-1868	1544	-378
27	110.20	1048	4321	723	958	5405	-1402	1477	-286
28	125.94	882	3666	591	784	4326	-993	1252	-191
29	141.69	521	2189	339	449	2470	-466	748	-96
30	157.43	0	0	0	0	0	0	0	0

Table 4 Girder G2 Unfactored Major-Axis Bending Moments by Tenth Point

Girder G2 Unfactored Major-Axis Bending Moments									
10th Point	Span Length (ft)	Dead Load				LL+I		Fatigue LL+I	
		DC1 _{STEEL}	DC1 _{CONC}	DC2	DW	Pos.	Neg.	Pos.	Neg.
		(kip-ft)	(kip-ft)	(kip-ft)	(kip-ft)	(kip-ft)	(kip-ft)	(kip-ft)	(kip-ft)
0	0.00	0	0	0	0	0	0	0	0
1	16.26	555	2268	351	465	2606	-484	796	-95
2	32.51	938	3868	610	808	4559	-967	1330	-191
3	48.77	1116	4632	742	984	5687	-1446	1564	-289
4	65.03	1115	4633	745	988	6152	-1931	1630	-390
5	81.29	905	3780	622	824	6059	-2416	1579	-498
6	97.54	525	2207	373	494	5434	-2907	1427	-616
7	113.80	-79	-256	-1	-1	4308	-4097	1148	-757
8	130.06	-892	-3579	-501	-665	2751	-4768	750	-917
9	146.31	-1896	-7599	-1122	-1488	1305	-5836	287	-1110
10	162.57	-3154	-12272	-1923	-2550	1114	-8127	256	-1384
10	0.00	-3154	-12272	-1923	-2550	1114	-8127	256	-1384
11	21.34	-1513	-6169	-906	-1201	1401	-4629	388	-902
12	42.68	-348	-1473	-160	-211	3176	-3197	933	-692
13	64.01	525	2077	384	509	5018	-2366	1345	-527
14	85.35	1040	4196	704	934	6205	-2070	1587	-393
15	106.69	1190	4826	813	1077	6598	-1786	1655	-277
16	128.03	1039	4195	704	934	6204	-2065	1585	-391
17	149.36	525	2075	384	509	5001	-2355	1344	-524
18	170.70	-348	-1476	-159	-211	3166	-3165	932	-690
19	192.04	-1514	-6173	-906	-1200	1393	-4627	399	-901
20	213.38	-3155	-12275	-1922	-2547	1114	-8128	255	-1378
20	0.00	-3155	-12275	-1922	-2547	1114	-8128	255	-1378
21	16.26	-1895	-7595	-1121	-1485	1312	-5843	289	-1113
22	32.51	-891	-3577	-500	-662	2762	-4778	751	-923
23	48.77	-79	-253	1	2	4320	-4106	1151	-760
24	65.03	525	2208	375	496	5445	-2917	1430	-621
25	81.29	906	3781	624	827	6068	-2424	1581	-495
26	97.54	1115	4634	747	990	6160	-1936	1631	-387
27	113.80	1116	4632	743	986	5689	-1451	1564	-287
28	130.06	938	3867	611	810	4560	-971	1330	-190
29	146.31	555	2266	351	465	2607	-487	797	-95
30	162.57	0	0	0	0	0	0	0	0

Table 5 Girder G1 Unfactored Torques by Tenth Point

Girder G1 Unfactored Torques							
10th Point	Span Length (ft)	Dead Load				LL+I	
		DC1 _{STEEL} (kip-ft)	DC1 _{CONC} (kip-ft)	DC2 (kip-ft)	DW (kip-ft)	Pos. (kip-ft)	Neg. (kip-ft)
0	0.00	42	286	-62	-83	660	-398
1	15.74	82	398	-54	-71	775	-448
2	31.49	34	189	-40	-53	756	-482
3	47.23	30	153	-40	-52	597	-389
4	62.97	-1	9	-23	-31	389	-307
5	78.71	-29	-125	-13	-17	309	-354
6	94.46	-33	-158	0	0	360	-479
7	110.20	-54	-262	21	28	462	-636
8	125.94	-25	-165	46	62	569	-766
9	141.69	-10	-135	83	110	668	-866
10	157.43	-22	-231	126	168	1049	-922
10	0.00	36	294	-144	-191	1049	-922
11	20.66	4	105	-89	-117	995	-702
12	41.33	60	309	-52	-68	919	-598
13	61.99	39	205	-22	-30	716	-464
14	82.65	61	261	-9	-11	555	-383
15	103.31	0	0	0	0	446	-430
16	123.98	-64	-261	9	11	413	-540
17	144.64	-39	-205	22	29	500	-724
18	165.30	-60	-309	52	68	625	-906
19	185.96	-4	-105	89	117	713	-991
20	206.63	-36	-294	144	190	928	-1046
20	0.00	22	231	-127	-169	928	-1046
21	15.74	10	134	-85	-112	874	-657
22	31.49	25	166	-47	-62	770	-549
23	47.23	54	262	-22	-29	640	-434
24	62.97	33	158	0	-1	482	-319
25	78.71	30	125	12	17	375	-281
26	94.46	1	-10	23	30	346	-378
27	110.20	-30	-153	39	51	434	-591
28	125.94	-34	-190	39	52	512	-751
29	141.69	-82	-398	57	75	503	-772
30	157.43	-42	-285	75	99	399	-662

Table 6 Girder G2 Unfactored Torques by Tenth Point

Girder G1 Unfactored Torques							
10th Point	Span Length (ft)	Dead Load				LL+I	
		DC1 _{STEEL} (kip-ft)	DC1 _{CONC} (kip-ft)	DC2 (kip-ft)	DW (kip-ft)	Pos. (kip-ft)	Neg. (kip-ft)
0	0.00	42	286	-62	-83	660	-398
1	15.74	82	398	-54	-71	775	-448
2	31.49	34	189	-40	-53	756	-482
3	47.23	30	153	-40	-52	597	-389
4	62.97	-1	9	-23	-31	389	-307
5	78.71	-29	-125	-13	-17	309	-354
6	94.46	-33	-158	0	0	360	-479
7	110.20	-54	-262	21	28	462	-636
8	125.94	-25	-165	46	62	569	-766
9	141.69	-10	-135	83	110	668	-866
10	157.43	-22	-231	126	168	1049	-922
10	0.00	36	294	-144	-191	1049	-922
11	20.66	4	105	-89	-117	995	-702
12	41.33	60	309	-52	-68	919	-598
13	61.99	39	205	-22	-30	716	-464
14	82.65	61	261	-9	-11	555	-383
15	103.31	0	0	0	0	446	-430
16	123.98	-64	-261	9	11	413	-540
17	144.64	-39	-205	22	29	500	-724
18	165.30	-60	-309	52	68	625	-906
19	185.96	-4	-105	89	117	713	-991
20	206.63	-36	-294	144	190	928	-1046
20	0.00	22	231	-127	-169	928	-1046
21	15.74	10	134	-83	-111	874	-657
22	31.49	25	166	-47	-62	770	-549
23	47.23	54	262	-22	-29	640	-434
24	62.97	33	158	0	-1	482	-319
25	78.71	30	125	12	17	375	-281
26	94.46	1	-10	23	30	346	-378
27	110.20	-30	-153	39	51	434	-591
28	125.94	-34	-190	39	52	512	-751
29	141.69	-82	-398	57	75	503	-772
30	157.43	-42	-285	75	99	399	-662

Table 7 Section G2-1 Unfactored Major-Axis Bending Moments and Torques

Unfactored Demands at Section G2-1 (10th Point = 3.5)									
Demand	Dead Load					LL+I		Fatigue LL+I	
	DC1_{STEEL}	DC1_{CONC}	DC1_{CAST1}	DC2	DW	Pos.	Neg.	Pos.	Neg.
Moment (kip-ft)	1144	4747	2979	765	1006	5920	-1689	-290	1525
Torque (kip-ft)	59	205	464	41	54	525	-409	-113	232

7.0 DESIGN

Sample design calculations at selected critical locations of Girder G2 are provided within this section. The calculations are intended to illustrate the application of some of the more significant provisions of the *AASHTO LRFD (7th Edition, 2014)*. As such, complete calculations for each girder section and all bridge components are not shown. Two critical girder section checks are provided: Section G2-1 represents a girder section checked for positive moment, and Section G2-2 represents a girder section at an interior pier and the maximum negative moment location. The sample girder design calculations illustrate provisions that need to be checked at the Strength, Service, Fatigue, and Constructibility limit states. Also, sample calculations for determining tub girder distortional stresses based on the beam-on-elastic-foundation analogy are provided.

Sample design calculations are also provided for the longitudinal bottom flange stiffener design, internal full-depth diaphragm design, bearing stiffener design, top flange lateral bracing member design, and a bolted field splice design. The sample design calculations make use of moments, shears, and torques provided in tables shown in Section 6.2 of this design example, and section properties that are computed in the sections that follow. In the calculations of major-axis bending stress throughout the sample calculations, compressive stresses are always shown as negative values and tensile stresses are always shown as positive values.

7.1 Girder Section Proportioning

Figure 9 illustrates the Girder G2 elevation, showing the flange and web sizes employed in this design example. The same flange and web sizes of Girder G2 are used on Girder G1, but with plate lengths radially proportional to the plate lengths for Girder G2.

7.1.1 Girder Web Depth

Proper proportioning of tub girders involves a study of various girder depths versus girder weight to arrive at the least weight solution that meets all performance and handling requirements. The overall weight of the tub girder can vary dramatically based on web depth. Therefore, selection of the proper girder depth is an extremely important consideration affecting the economy of steel girder design. The NSBA Publication, *Practical Steel Tub Girder Design* [3] points out that a traditional rule of thumb for steel tub girder bridge depths is $L/25$, however designers should not be reluctant to exceed this ratio. Tangent steel tub girders have approached $L/35$ while meeting all code requirements for strength and deflection. Furthermore, tub girders are generally stiffer than I-girders because an individual tub nearly acts as two I-girders for major-axis bending. For torsion, an individual tub girder is significantly stiffer than two-I-girders.

Article 2.5.2.6.3 provides suggested minimum span-to-depth ratios for I-girders, but does not specifically address tub girder sections. The suggested minimum total depth of a composite I-girder, in a continuous span, is given as $0.032L$, where L is the span length in feet. This criterion may be applied to determine a starting depth of the tub girder for the depth studies. The length of the center span of the outside girder, Girder G2, is 213.38 feet (measured along the centerline of the tub section), which is the longest effective span in this design example. Therefore the suggested minimum depth of the composite section is:

$$0.032(213.38) = 6.828 \text{ ft} = 81.9 \text{ in.}$$

Considering that 81.9 inches is the suggested minimum depth of the composite section including the depth of the concrete deck, a vertical web depth of 78.0 inches is chosen in this design example.

Tub girders typically employ inclined webs, as they are advantageous in reducing the width of the bottom flange. Article 6.11.2.1 specifies that the web inclination should not exceed 1:4 (horizontal:vertical). Because progressively deeper webs may result in a narrower and potentially thicker bottom flange plate (at location of maximum flexure), it is generally necessary for the Engineer to explore a wide range of web depths and web spacing options in conjunction with bottom flange requirements to determine the optimal solution.

The maximum recommended web inclination of 1:4 is used for this design example, so as to minimize the bottom flange width. Based on the previously mentioned web depth study, a vertical web depth of 78.0 inches is selected, resulting in a distance of 81 inches between the centerline of the webs at the bottom flange. The actual bottom flange width is 83 inches in order to provide a 1.0-inch flange extension on the outside of each web, which permits welding of the webs to the bottom flange. However, it should be noted, according to the *AASHTO/NSBA Steel Bridge Collaboration Document: Guidelines for Design Details* [5], most fabricators prefer a bottom flange extension of 1.5 inches, and 1.0 inch is the minimum.

7.1.2 Cross-section Proportions

Proportion limits for webs of tub girders are specified in Article 6.11.2.1. Provisions for webs with and without longitudinal stiffeners are presented. For this example a longitudinally stiffened web is not anticipated. The web plate must be proportioned such that the web plate thickness (t_w) meets the requirement:

$$\frac{D}{t_w} \leq 150 \quad \text{Eq. (6.11.2.1.2-1)}$$

where D is the distance along the web. For inclined webs, Article 6.11.2.1.1 states that the distance along the web is to be used for all design checks. The web thickness used along the entire length of both girders in this design example is 0.5625 inches. Determine the web depth along the incline:

$$D = 78 \left(\frac{4.123}{4.0} \right) = 80.40 \text{ in.}$$

Checking Eq. (6.11.2.1.2-1):

$$\frac{D}{t_w} = \frac{80.40}{0.5625} = 142.9 \leq 150 \quad \text{OK}$$

Cross-section proportion limits for top flanges of tub girders are specified in Article 6.11.2.2. The smallest top flange employed in this design example is 1.0 in. x 16.0 in. The minimum width of flanges is specified as:

$$b_f \geq \frac{D}{6} = \frac{80.40}{6} = 13.4 \text{ in.} \quad \text{Eq. (6.11.2.2-2)}$$

Therefore, the minimum top flange width of 16.0 in. satisfies the requirements of Eq. (6.11.2.2-2). The minimum thickness of the top flange must satisfy the following two provisions:

$$\frac{b_f}{2t_f} \leq 12.0 \quad \text{Eq. (6.11.2.2-1)}$$

$$\frac{b_f}{2t_f} = \frac{16.0}{2(1.0)} = 8.0 \leq 12.0 \quad \text{OK}$$

and,

$$t_f \geq 1.1 t_w \quad \text{Eq. (6.11.2.2-3)}$$

$$t_f = 1.0 \text{ in.} \geq 1.1 t_w = 1.1(0.5625) = 0.62 \text{ in.} \quad \text{OK}$$

Although not required in this design example, it should be noted that the AASHTO/NSBA Steel Bridge Collaboration document *Guidelines for Design for Constructibility* [7] recommends a minimum flange thickness of 0.75 inches to enhance girder stability during handling and erection.

This example utilizes the provisions of the *AASHTO LRFD (7th Edition, 2014)* to size the bottom flanges, which impose no limitations with regard to the b/t ratio of bottom flanges in tension. However, the design engineer should consider current industry practice regarding sizing the bottom flange of tub girders in positive moment regions. For positive moment regions, past and current literature has suggested a lower bound limit for the bottom flange thickness. These “rules of thumb” have suggested that a bottom flange in tension have a maximum b/t ratio of 120 or an even more restrictive ratio of 80. These limits are intended to address several fabrication concerns, including waviness and warping effects during welding of the bottom flange to the webs. Additional discussion concerning this issue can be found in the NSBA publication *Practical Steel Tub Girder Design* [4].

Furthermore, the designer should be aware that it is possible that the bottom flange in tension in the final condition may be in compression during lifting of the tub girder during erection, possibly causing buckling of the slender bottom flange. Slenderness limits for the bottom tension flange have also been suggested to limit local vibrations, especially in very wide flanges that do not utilize any stiffening elements.

The designer should consult with fabricators if it is determined that a bottom flange thickness that does not satisfy these previously discussed rules of thumb will be utilized in the final design of the structure. It should be verified that a tub girder with the selected bottom flange thickness can be fabricated without causing handling and distortion concerns. For this particular example, tension flange thicknesses that do not satisfy the suggested maximum b/t ratio of 120 are utilized (maximum b/t = $81/0.625 = 129.6$), as they are allowed by *AASHTO LRFD (7th Edition, 2014)*.

7.2 Section Properties

The calculation of the section properties for Sections G2-1 and G2-2 is illustrated below. In computing the composite section properties, the structural slab thickness, or total thickness minus the thickness of the integral wearing surface, should be used. However, in the case of this design example, there is no integral wearing surface assumed, therefore the total structural thickness of the deck slab is 9.50 in.

For all section property calculations, the haunch depth of 4.00 in. is considered in computing the section properties, but the area of the haunch is not included. Since the actual depth of the haunch concrete may vary from its theoretical value to account for construction tolerances, some designers ignore the haunch concrete depth in all calculations. For composite section properties including only longitudinal reinforcement, a haunch depth is considered when determining the vertical position of the reinforcement relative to the steel girder. The longitudinal reinforcement

steel area is assumed to be equal to 20.0 in.² per girder, and is assumed to be placed at the mid-depth of the effective structural deck thickness.

The section properties also include the longitudinal component of the top flange lateral bracing area, the longitudinal bottom flange stiffener (where present), and the 1 in. bottom flange extensions beyond the webs. A single top flange lateral bracing member of 8.0 in.² placed at an angle of 30 degrees from the girder tangent is assumed in this design example.

The composite section must consist of the steel section and the transformed area of the effective width of the concrete deck. Therefore, compute the modular ratio, n (Article 6.10.1.1.1b):

$$n = \frac{E}{E_c} \quad \text{Eq. (6.10.1.1.1b-1)}$$

where E_c is the modulus of elasticity of the concrete determined as specified in Article 5.4.2.4. A unit weight of 0.150 kcf is used for the concrete in the calculation of the modular ratio.

$$E_c = 33,000 K_1 w_c^{1.5} \sqrt{f'_c} \quad \text{Eq. (5.4.2.4-1)}$$

$$E_c = 33,000 (1.0) (0.150)^{1.5} \sqrt{4.0} = 3,834 \text{ ksi}$$

$$n = \frac{29,000}{3,834} = 7.56$$

Even though Article C6.10.1.1.1b permits n to be taken as 8 for concrete with f'_c equal to 4.0 ksi, $n = 7.56$ will be used in all subsequent computations in this design example.

7.2.1 Section G2-1: Span 1 Positive Moment Section Properties

Section G2-1 is located in Span 1, approximately 57 feet from the centerline of the bearing at abutment 1. The cross section for Section G2-1 is shown in Figure 10. For this section, the longitudinal reinforcement is conservatively neglected in computing the composite section properties as is typically assumed in design.

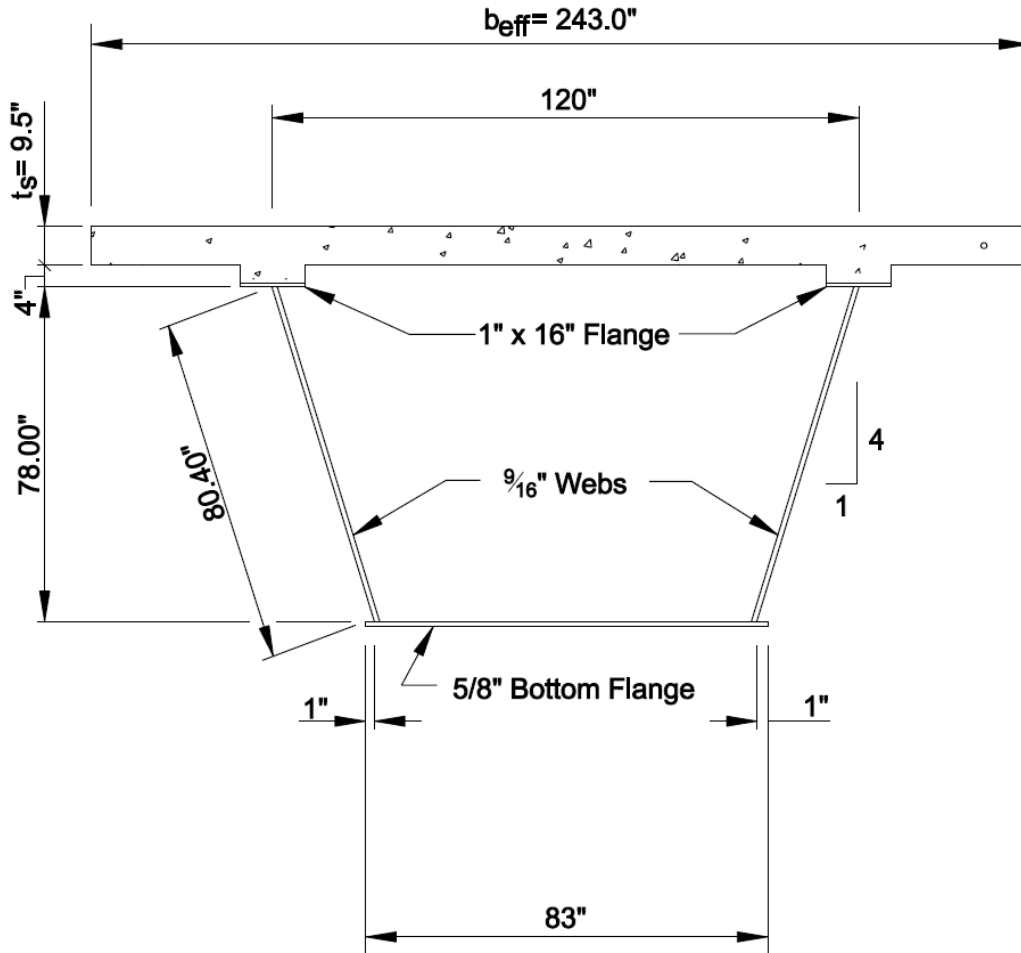


Figure 10 Sketch of Tub-Girder Cross-Section at Section G2-1

7.2.1.1 Effective Width of Concrete Deck

As specified in Article 6.10.1.1.1e, the effective flange width is to be determined as specified in Article 4.6.2.6. According to Article 4.6.2.6, the deck slab effective width may be taken as the tributary width perpendicular to the axis of the member for determining cross-section stiffnesses for analysis and for determining flexural resistances. In a typical two tub girder cross-section, the tributary width of the deck slab over each girder is taken as the distance between the two webs of the girder, plus half the distance from one web to the adjacent web of the adjacent girder plus the full overhang width. Therefore, the deck slab effective width, b_{eff} , for Girder G2 is:

$$b_{eff} = 4.00 + 10.00 + \frac{12.50}{2} = 20.25 \text{ ft} = 243 \text{ in.}$$

7.2.1.2 Elastic Section Properties: Section G2-1

For tub sections with inclined webs, the area of the inclined webs should be used in computing all section properties. Also, as shown in Figure 11, the moment of inertia of a single inclined web, I_{ow} , with respect to a horizontal axis at mid-depth if the web is computed as:

$$I_{ow} = \frac{S^2}{S^2 + 1} I_w$$

where: S = web slope with respect to the horizontal (equal to 4.00 in this example)

I_w = moment of inertia of each inclined web with respect to an axis normal to the web

$$I_{ow} = \left(\frac{4.0^2}{4.0^2 + 1} \right) \frac{1}{12} (0.5625)(80.4)^3 = 22,929 \text{ in.}^4$$

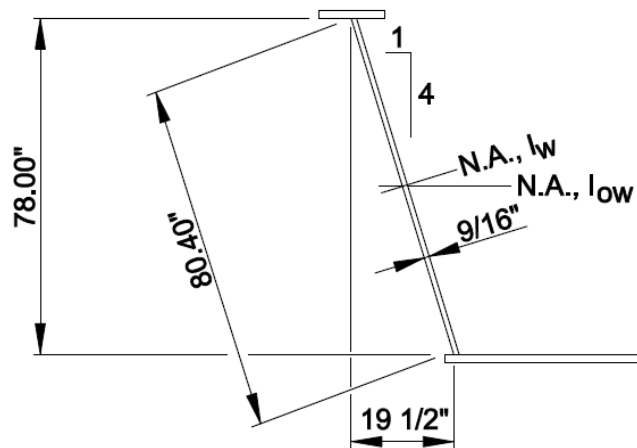


Figure 11 Moment of Inertia of an Inclined Web

In the calculations of the section properties that follow in Table 8 to Table 10, d is measured vertically from a horizontal axis through the mid-depth of the web to the centroid of each element of the tub girder.

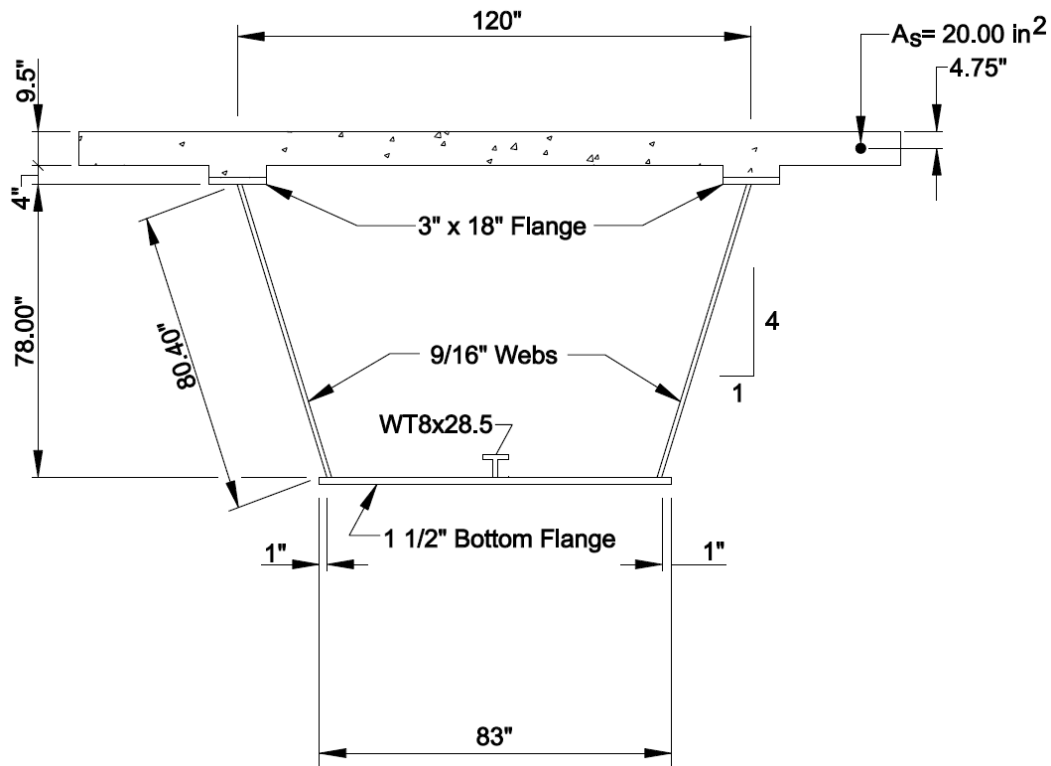


Figure 12 Sketch of Tub-Girder Cross-Section at Section G2-2

7.2.2.1 Elastic Section Properties: Section G2-2

Furthermore, for members with shear connectors provided throughout their entire length that also satisfy the provisions of Article 6.10.1.7, Articles 6.6.1.2.1 and 6.10.4.2.1 permit the concrete deck to also be considered effective for negative flexure when computing stress ranges and flexural stresses acting on the composite section at all sections in the member at the fatigue and service limit states, respectively. Therefore, section properties for the short-term and long-term composite section, including the concrete deck but neglecting the longitudinal reinforcement, are also determined for later use in the calculations of Section G2-2 at these limit states.

Although not required by the *AASHTO LRFD (7th Edition, 2014)*, for stress calculations involving the application of long-term loads to the composite section in regions of negative flexure in this example, the area of the longitudinal reinforcement is conservatively adjusted for the effects of concrete creep by dividing the area by 3 (i.e. $20.00 \text{ in.}^2/3 = 6.67 \text{ in.}^2$). The concrete is assumed to transfer the force from the longitudinal deck reinforcement to the rest of the cross-section and concrete creep acts to reduce that force over time.

As shown in Figure 10, a single WT 8x28.5 is utilized as a bottom flange longitudinal stiffener with the stem welded to the bottom flange, and is placed at the centerline of the bottom flange. The WT 8x28.5 is considered in the section property computations.

Table 13 Section G2-2: $n=7.56$ Composite Section Properties with Transformed Deck

Component	A	d	Ad	Ad ²	I _o	I
Steel Section	338.3		-568.8			440,225
Concrete Slab (9½" x 243")/7.56	305.4	47.75	14,583	696,331	2,297	698,628
	643.7		14,014			1,139,372
					-21.77(14,014) =	-305,085
					$I_{NA} =$	833,768 in. ⁴

$d_n = \frac{14,014}{643.7} = 21.77 \text{ in.}$
 $d_{\text{TOPOFSTEEL}} = 42.00 - 21.77 = 20.23 \text{ in.}$
 $S_{\text{TOPOFSTEEL}} = \frac{833,768}{20.23} = 41,234 \text{ in.}^3$
 $d_{\text{BOTOFSTEEL}} = 40.50 + 21.77 = 62.27 \text{ in.}$
 $S_{\text{BOTOFSTEEL}} = \frac{833,768}{62.27} = 13,390 \text{ in.}^3$

Table 14 Section G2-2: $3n$ Composite Section Properties with Longitudinal Steel Reinforcement

Component	A	d	Ad	Ad ²	I _o	I
Steel Section	338.3		--568.8			440,225
Longitudinal Reinforcement	6.67	47.75	318.5	15,208		15,208
	345.0		-250.3			455,940
					$-(-0.73)(-250.3) =$	-183
					$I_{NA} =$	455,250 in. ⁴

$d_{3n} = \frac{-250.3}{345.0} = -0.73 \text{ in.}$
 $d_{\text{TOPOFSTEEL}} = 42.00 + 0.73 = 42.73 \text{ in.}$
 $S_{\text{TOPOFSTEEL}} = \frac{455,250}{42.73} = 10,654 \text{ in.}^3$
 $d_{\text{BOTOFSTEEL}} = 40.50 - 0.73 = 39.77 \text{ in.}$
 $S_{\text{BOTOFSTEEL}} = \frac{455,250}{39.77} = 11,447 \text{ in.}^3$

Table 15 Section G2-2: n Composite Section Properties with Longitudinal Steel Reinforcement

Component	A	d	Ad	Ad ²	I _o	I
Steel Section	338.3		-568.8			440,225
Longitudinal Reinforcement	20.0	47.75	955.0	45,601		45,601
	358.3		386.2			486,333
					$-1.06(378.5) =$	-417
					$I_{NA} =$	485,409 in. ⁴

$d_n = \frac{386.2}{358.3} = 1.08 \text{ in.}$
 $d_{\text{TOPOFSTEEL}} = 42.00 - 1.08 = 40.94 \text{ in.}$
 $S_{\text{TOPOFSTEEL}} = \frac{485,409}{40.92} = 11,862 \text{ in.}^3$
 $d_{\text{BOTOFSTEEL}} = 40.50 + 1.08 = 41.58 \text{ in.}$
 $S_{\text{BOTOFSTEEL}} = \frac{485,409}{41.58} = 11,674 \text{ in.}^3$

7.2.3 Check of Minimum Negative Flexure Concrete Deck Reinforcement (Article 6.10.1.7)

To control concrete deck cracking in regions of negative flexure, Article 6.10.1.7 specifies that the total cross-sectional area of the longitudinal reinforcement must not be less than 1 percent of the total cross-sectional area of the deck. The minimum longitudinal reinforcement must be provided wherever the longitudinal tensile stress in the concrete deck due to either the factored construction loads or Load Combination Service II exceeds ϕf_r . ϕ is to be taken as 0.9 and f_r is to be taken as the modulus of rupture of the concrete determined as follows:

- For normal weight concrete: $f_r = 0.24\sqrt{f'_c}$
- For lightweight concrete: f_r is calculated as specified in Article 5.4.2.6.

It is further specified that the reinforcement is to have a specified minimum yield strength not less than 60 ksi and a size that should not exceed No. 6 bars. The reinforcement should be placed in two layers uniformly distributed across the deck width, and two-thirds should be placed in the top layer. The individual bars should be spaced at intervals not exceeding 12 inches.

Article 6.10.1.1.1c states that for calculating stresses in composite sections subjected to negative flexure at the strength limit state, the composite section for both short-term and long-term moments is to consist of the steel section and the longitudinal reinforcement within the effective width of the concrete deck. Referring to the cross-section shown in Figure 2:

$$A_{\text{deck}} = (\text{entire width of 9.5" thick deck}) + (\text{triangular portion of overhang})$$

$$A_{\text{deck}} = \frac{9.5}{12}(40.5) + 2 \left[\frac{1}{2} \left(\frac{4.0}{12} \right) \left(4.0 - \frac{16.0}{2} \right) \right] = 33.17 \text{ ft}^2 = 4,777 \text{ in.}^2$$

$$0.01(4,777) = 47.77 \text{ in.}^2$$

$$\frac{47.77}{40.5} = 1.18 \text{ in.}^2/\text{ft} = 0.098 \text{ in.}^2/\text{in.}$$

$$0.098(2430) = 23.81 \text{ in.}^2 \text{ per tub girder}$$

Therefore, the assumption of 20.00 in.² for the longitudinal deck reinforcement used in the calculation of the section properties for Section G2-1 is conservative and is left as shown in Table 14 and Table 15, as the longitudinal deck reinforcement to be used is more than that assumed in the section property calculations. In the actual deck, the longitudinal reinforcement should have a minimum cross-sectional area of 23.81 in.² per tub girder. If the reinforcement is detailed, #6 bars at 6 inches are placed in the top layer, and in the bottom layer use #4 bars at 6 inches. Therefore, the total area of deck reinforcement steel in the given effective width of concrete deck is:

$$A_s = (0.44 + 0.44 + 0.20 + 0.20) \left(\frac{243.0}{12} \right) = 25.92 \text{ in.}^2 > 23.81 \text{ in.}^2$$

Also, approximately two-thirds of the reinforcement is in the top layer: $\frac{0.44 + 0.44}{1.28} = 0.69 \approx \frac{2}{3}$

7.3 Girder Check: Section G2-1, Constructibility (Article 6.11.3)

Article 6.11.3 directs the engineer to Article 6.10.3 for discussion regarding the constructibility checks of tub girders. For critical stages of construction, the provisions of Articles 6.10.3.2.1 through 6.10.3.2.3 are to be applied to the top flanges of the tub girder. The noncomposite bottom tub flange in compression or tension is to satisfy the requirements specified in Article 6.11.3.2. Web shear is to be checked in accordance with Article 6.10.3.3, with the shear to be taken along the slope of the web in accordance with the provisions of Article 6.11.6.

As specified in Article 6.10.3.4, sections in positive flexure that are composite in the final condition, but noncomposite during construction, are to be investigated during the various stages of deck placement. The effects of forces from deck overhang brackets acting on the fascia girders are also to be considered. Wind load effects on the noncomposite structure prior to and during casting are also an important consideration during construction. The presence of construction equipment may also need to be considered. Lastly, the potential for uplift at bearings should be investigated at each critical construction stage. For this design example, the effects of wind load on the structure and the presence of construction equipment are not considered.

Calculate the maximum flexural stresses in the flanges of the steel section due to the factored loads resulting from the application of steel self-weight and Cast #1 of the deck placement sequence. Cast #1 yields the maximum positive moment for the noncomposite Section G2-1. As specified in Article 6.10.1.6, for design checks where the flexural resistance is based on lateral torsional buckling, f_{bu} is to be determined as the largest value of the compressive stress throughout the unbraced length in the flange under consideration, calculated without consideration of flange lateral bending. For design checks where the flexural resistance is based on yielding, flange local buckling or web bend-buckling, f_{bu} may be determined as the stress at the section under consideration. From Figure 1, brace points adjacent to Section G2-2 are located at intervals of approximately 16.3 feet, and the largest stress occurs within this unbraced length.

In accordance with Article 3.4.2.1, when investigating Strength I, III, and V during construction, load factors for the weight of the structure and appurtenances, DC and DW, are not to be taken to be less than 1.25. Also, as discussed previously, the η factor is taken equal to 1.0 in this example. As shown in Table 7 the unfactored moments due to steel self-weight and Cast #1 are 1,144 k-ft and 2,979 k-ft, respectively. Therefore,

For Construction Strength I:

$$\text{General: } f_{bu} = \frac{\eta \gamma M_{DC}}{S_{nc}}$$

$$\text{Top Flange: } f_{bu} = \frac{1.0(1.25)(1,144 + 2,979)(12)}{4,334} = -14.27 \text{ ksi}$$

$$\text{Bot. Flange: } f_{bu} = \frac{1.0(1.25)(1,144 + 2,979)(12)}{5,029} = 12.30 \text{ ksi}$$

As mentioned previously in Section 5.4, in the interest of brevity, the special load combination specified in Article 3.4.2.1 for DC loads and construction loads, C, applied to the fully erected steelwork during construction, i.e., 1.4(DC + C), is not considered herein.

7.3.1 Deck Overhang Bracket Load

During construction, the weight of the deck overhang wet concrete is resisted by the deck overhang brackets. Other loads supported by the overhang brackets during construction include the formwork, screed rail, railing, worker walkway, and possibly the deck finishing machine.

The deck overhang construction loads are typically applied to the non-composite section, and removed once the concrete deck has become composite with the steel girders. The deck overhang bracket imparts a lateral force on the top and bottom flanges, resulting in lateral bending of the flanges. The lateral bending of the top flange that must be considered as part of the constructibility check, however in a tub girder bridge, the flange lateral bending of the bottom flange is typically ignored due to the large section modulus of the bottom flange in the lateral direction. Also, it should be noted that if the bottom of the bracket does not bear on the web near the junction of the web and bottom flange, additional support and/or stiffening of the web may be warranted.

Since G2 is a fascia girder, one-half of the deck overhang weight is assumed to be carried by the girder and one-half is assumed placed on the overhang brackets, as shown in Figure 13.

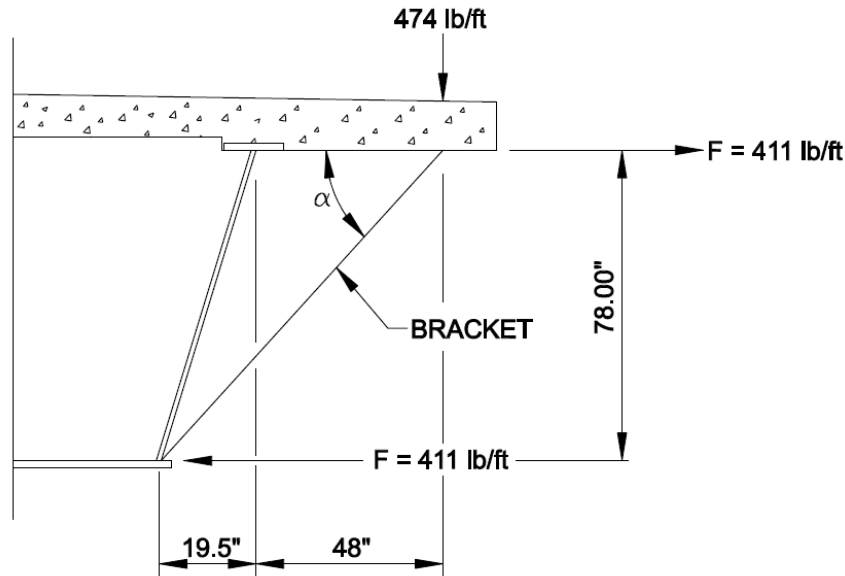


Figure 13 Deck Overhang Bracket Loading

The deck overhang bracket loads are assumed to be applied uniformly to the top flange, even though the brackets are actually spaced at approximately 3 feet along the length of the girder.

The unbraced length of the top flange is approximately 16.3 ft in Span 1. The deck thickness in the overhang area is assumed to be 10 inches, and the weight of the deck finishing machine is not considered in these calculations. Therefore, the vertical load on the deck overhang brackets is computed as:

$$\text{Deck Overhang: } \left(\frac{1}{2}\right)(4.0)\left(\frac{10}{12}\right)(150) = 250 \text{ lbs/ft}$$

$$\text{Deck Forms + Screed Rail} = 224 \text{ lbs/ft (assumed)}$$

$$\text{Total Uniform Load on Brackets} = 474 \text{ lbs/ft}$$

According to Article 3.4.2.1, the load factor for construction loads is to be taken as 1.50 for the Strength I load combination. The factored Strength I lateral force on the top flange is therefore computed as:

$$\alpha = \tan^{-1}\left(\frac{78.0}{67.5}\right) = 49.1^\circ$$

$$F_\ell = \frac{1.25(250) + 1.50(224)}{\tan(49.1^\circ)} = 562 \text{ lb/ft} = 0.562 \text{ kip/ft}$$

The flange lateral bending moment on the exterior web top flange due to the deck overhang bracket is computed. The flange lateral moment at the brace points due to the overhang forces is negative in the top flange of Girder G2 on the outside of the curve in regions of positive flexure because the stress due to the lateral moment is compressive on the convex side of the flange at the brace points. The opposite would be true on the convex side of the Girder G1 top flange on the inside of the curve in regions of positive flexure at the brace points. In the absence of a more refined analysis, the equations given in Article C6.10.3.4 may be used to estimate the maximum flange lateral bending moments in the discretely braced compression flange due to the lateral bracket forces. Assuming the flange is continuous with the adjacent unbraced lengths and that the adjacent unbraced lengths are approximately equal, the factored Strength I lateral bending moment due to a statically equivalent uniformly distributed lateral bracket force may be estimated as:

$$M_{\ell} = \frac{F_{\ell} L_b^2}{12} = - \left[\frac{0.562(16.3)^2}{12} \right] = -12.4 \text{ kip} \cdot \text{ft} \quad \text{Eq. (C6.10.3.4-2)}$$

7.3.2 Flange Lateral Bending Due to Horizontal Component of Web Shear

In addition to the lateral bending moment due to the overhang brackets, the inclined webs of the tub girder cause a lateral force on the top flanges. However, in this example this force and subsequent lateral bending effects are relatively small and are ignored in these computations.

7.3.3 Flange Lateral Bending Due to Curvature

Another source of lateral bending is due to curvature, which can either be taken from the analysis results, or estimated by the approximate V-load equation given in Article C4.6.1.2.4b. The V-load equation assumes the presence of a cross frame at the point under investigation and a constant major-axis moment over the distance between the brace points. Although the V-load equation is intended for application to I-girders and is not theoretically pure for tub girders or at locations in-between brace points, it may conservatively be used to estimate the flange lateral bending moments at the cross-frames in the top flanges of a tub.

The top flange size is constant between brace points in this region under investigation. In positive moment regions, the largest value of the major-axis bending stress (f_{bu}) may not necessarily be at either brace point. Generally in positive moment regions, f_{bu} will not be significantly larger than the value at adjacent brace points, which is the case in this example. Therefore, the computed value of f_{bu} at Section G2-1 and the lateral bending moment at the brace points are conservatively combined for this constructibility check.

For this example, and illustration purposes, the V-load equation is used to compute the flange lateral bending moment due to curvature. For a single tub girder flange, consider only one-half of the girder major-axis moment due to steel self-weight and Cast #1 of the deck placement sequence.

$$M = \frac{(1,144 + 2,979)}{2} = 2,062 \text{ kip - ft}$$

$$M_{LAT} = \frac{M \ell^2}{N R D} = - \left[\frac{(2,062)(16.3)^2}{(12)(716.25)(6.5)} \right] = -9.8 \text{ kip - ft} \quad \text{Eq. (C4.6.1.2.4b-1)}$$

where:

- M_{LAT} = flange lateral bending moment (kip-ft)
- M = major-axis bending moment (kip-ft)
- ℓ = unbraced length (ft)
- N = a constant taken as 10 or 12 in past practice; 12 is recommended for use herein
- R = girder radius (ft)
- D = web depth (ft)

The flange lateral moment at the brace points due to curvature is negative when the top flanges are subjected to compression because the stress due to the lateral moment is in compression on the convex side of the flange at the brace points. The opposite is true whenever the top flanges are subjected to tension. Thus, the flange lateral moments due to the overhang loads in the top flange of Girder G2 on the outside of the curve in regions of positive flexure are additive to those due to curvature (see below); the opposite is true in the top flange of Girder G1 on the inside of the curve in regions of positive flexure. The total factored Strength I lateral moment and stress in the top flange of Girder G2, including the factored lateral moment from the overhang bracket is:

$$M_{TOT_LAT} = (1.25)(-9.8) + (-12.4) = -24.7 \text{ kip - ft}$$

$$f_{\ell} = \frac{M_{TOT_LAT}}{S_{\ell}} = \frac{-24.7(12)}{(1.00)(16)^2/6} = -6.95 \text{ ksi}$$

It should be noted that another significant source of flange lateral bending results from forces that develop in single-diagonal top flange bracing members resulting from major-axis bending of the tub girder. This effect is recognized in flange lateral moments that are taken directly from a finite element analysis. In the absence of a refined analysis, equations have been developed to evaluate bracing member forces and the forces imparted on the top flange in tub girders due to major-axis bending [8 and 9]. The flange lateral bending due to the forces in the top lateral bracing is not considered in these computations.

7.3.4 Top Flange Lateral Bending Amplification

According to Article 6.10.1.6, lateral bending stresses determined from a first-order analysis may be used in discretely braced compression flanges for which:

$$L_b \leq 1.2L_p \sqrt{\frac{C_b R_b}{f_{bu}/F_{yc}}} \quad \text{Eq. (6.10.1.6-2)}$$

L_p is the limiting unbraced length specified in Article 6.10.8.2.3 determined as:

$$L_p = 1.0r_t \sqrt{\frac{E}{F_{yc}}} \quad \text{Eq. (6.10.8.2.3-4)}$$

where r_t is the effective radius of gyration for lateral torsional buckling specified in Article 6.10.8.2.3 determined as:

$$r_t = \frac{b_{fc}}{\sqrt{12 \left(1 + \frac{1}{3} \frac{D_c t_w}{b_{fc} t_{fc}} \right)}} \quad \text{Eq. (6.10.8.2.3-9)}$$

For the steel section, the depth of the web in compression in the elastic range, D_c , at Section G2-1 is computed along the web (not vertical) as follows:

Note that for the steel section only: $d_{\text{TOP OF STEEL}} = 42.77$ in.

$$D_c = (d_{\text{TOP OF STEEL}} - t_f) \sqrt{\frac{S^2 + 1}{S^2}}$$

$$D_c = (42.77 - 1.00) \sqrt{\frac{4^2 + 1}{4^2}} = 43.06 \text{ in.}$$

It should be noted that values of D_c and D are taken as distances along the web, in accordance with Article 6.11.2.1.1. Therefore,

$$r_t = \frac{16}{\sqrt{12 \left(1 + \frac{1}{3} \frac{43.06(0.5625)}{16(1.00)} \right)}} = 3.77 \text{ in.}$$

$$L_p = \frac{1.0(3.77)}{12} \sqrt{\frac{29,000}{50}} = 7.57 \text{ ft}$$

C_b is the moment gradient modifier specified in Article 6.10.8.2.3 and may conservatively be taken equal to 1.0 in regions of positive flexure. According to Article 6.10.1.10.2, the web load-shedding factor, R_b , is to be taken equal to 1.0 when checking constructibility. Finally, f_{bu} is the largest value of the compressive stress due to the factored loads throughout the unbraced length

in the flange under consideration, calculated without consideration of flange lateral bending. In this case, use $f_{bu} = -14.27$ ksi, as computed earlier for the Construction Strength I load combination. Therefore:

$$1.2(7.57) \sqrt{\frac{1.0(1.0)}{\frac{-14.27}{50}}} = 17.00 \text{ ft} > L_b = 16.3 \text{ ft} \quad \text{Eq. (6.10.1.6-2)}$$

Therefore, Eq. 6.10.1.6-2 is satisfied, and amplification of the first-order elastic compression-flange lateral bending stresses is not required. The flange lateral bending stress, f_ℓ , determined from the first-order elastic analysis is sufficient; thus $f_\ell = -6.95$ ksi. The factored flange lateral bending stress is less than the limit of $0.6F_{yf} = 0.6(50) = 30.0$ ksi specified in Article 6.10.1.6.

7.3.5 Flexure (Article 6.11.3.2)

For critical stages of construction, Article 6.11.3.2 directs the engineer to the provisions of Article 6.10.3.2 to compute the resistance of top flanges of tub sections. The unbraced length should be taken as the distance between interior cross frames or diaphragms. However as stated in the commentary to Article 6.11.3.2, top lateral bracing attached to the flanges at points where only struts exist between the flanges may be considered as brace points at the discretion of the engineer.

Article 6.10.3.2.1 requires that discretely braced flanges in compression satisfy the following:

$$f_{bu} + f_\ell \leq \phi_f R_h F_{yc} \quad \text{Eq. (6.10.3.2.1-1)}$$

$$f_{bu} + \frac{1}{3}f_\ell \leq \phi_f F_{nc} \quad \text{Eq. (6.10.3.2.1-2)}$$

$$f_{bu} \leq \phi_f F_{crw} \quad \text{Eq. (6.10.3.2.1-3)}$$

Article 6.11.3.2 requires that the noncomposite box flange (bottom flange) in tension satisfy:

$$f_{bu} \leq \phi_f R_h F_{yf} \Delta \quad \text{Eq. (6.11.3.2-3)}$$

where: ϕ_f = resistance factor for flexure from Article 6.5.4.2 ($\phi_f = 1.0$)
 R_h = hybrid factor specified in Article 6.10.1.10.1 (1.0 at homogeneous Section G2-1)
 F_{crw} = nominal elastic bend-buckling resistance for webs determined as specified in Article 6.10.1.9
 F_{nc} = nominal flexural resistance of the compression flange determined as specified in Article 6.10.8.2 (i.e. local or lateral torsional buckling resistance, as applicable). The provisions of Article A6.3.3 are not to be used to determine the lateral torsional buckling resistance of top flanges of tub girders with compact or noncompact webs, as specified in Article 6.11.3.2.

Δ = a factor dependent on the St. Venant torsional shear stress in the bottom flange. St. Venant torsional shear stress will be addressed later in this example.

7.3.5.1 Top Flange

7.3.5.1.1 Top Flange: Yielding

First, check that the top flanges satisfy Eq. 6.10.3.2.1-1 as follows:

$$f_{bu} + f_{\ell} \leq \phi_f R_h F_{yc} \quad \text{Eq. (6.10.3.2.1-1)}$$

$$f_{bu} + f_{\ell} = |-14.27| + |-6.95| = 21.22 \text{ ksi}$$

$$\phi_f R_h F_{yc} = 1.0(1.0)(50) = 50.0 \text{ ksi} > 21.22 \text{ ksi} \quad \text{OK} \quad (\text{Ratio} = 0.424)$$

7.3.5.1.2 Top Flange: Local Buckling Resistance (Article 6.10.8.2.2)

Determine the slenderness ratio of the top flange:

$$\lambda_f = \frac{b_{fc}}{2t_{fc}} \quad \text{Eq. (6.10.8.2.2-3)}$$

$$\lambda_f = \frac{16}{2(1.00)} = 8.00$$

Determine the limiting slenderness ratio for a compact flange (alternatively see table C6.10.8.2.2-1):

$$\lambda_{pf} = 0.38 \sqrt{\frac{E}{F_{yc}}} \quad \text{Eq. (6.10.8.2.2-3)}$$

$$\lambda_{pf} = 0.38 \sqrt{\frac{29,000}{50}} = 9.15$$

Since $\lambda_f < \lambda_{pf}$,

$$F_{nc} = R_b R_h F_{yc} \quad \text{Eq. (6.10.8.2.2-1)}$$

Since R_b is taken as 1.0 for constructibility,

$$F_{nc} = (1.0)(1.0)(50) = 50 \text{ ksi}$$

Check Eq. 6.10.3.2.1-2 as follows:

$$|-14.27| + \frac{1}{3}|-6.95| = 16.59\text{ksi} \leq (1.0)(50.0) = 50.0\text{ ksi} \quad \text{OK} \quad (\text{Ratio} = 0.332)$$

7.3.5.1.3 Top Flange: Lateral Torsional Buckling Resistance (Article 6.10.8.2.3)

The limiting unbraced length, L_p , was computed earlier to be 7.57 feet. The effective radius of gyration for lateral torsional buckling, r_t , for the noncomposite Section G2-1 was also computed earlier to be 3.77 inches. The computations for L_p and r_t are shown in Section 7.3.4 discussing the top flange lateral bending amplification.

Determine the limiting unbraced length, L_r :

$$L_r = \pi r_t \sqrt{\frac{E}{F_{yr}}} \quad \text{Eq. (6.10.8.2.3-5)}$$

$$L_r = \frac{\pi(3.77)}{12} \sqrt{\frac{29,000}{0.7(50)}} = 28.41\text{ ft}$$

Since $L_p = 7.57\text{ feet} < L_b = 16.30\text{ feet} < L_r = 28.41\text{ feet}$, Eq. (6.10.8.2.3-2) is used to compute the lateral torsional buckling resistance.

$$F_{nc} = C_b \left[1 - \left(1 - \frac{F_{yr}}{R_h F_{yc}} \right) \left(\frac{L_b - L_p}{L_r - L_p} \right) \right] R_b R_h F_{yc} \leq R_b R_h F_{yc} \quad \text{Eq. (6.10.8.2.3-2)}$$

Compute the moment-gradient modifier, C_b , to be used in Eq. (6.10.8.2.3-2), where

$$C_b = 1.0 \text{ for members where } f_{\text{mid}}/f_2 > 1 \text{ or } f_2 = 0 \quad \text{Eq. (6.10.8.2.3-6)}$$

$$\text{Otherwise: } C_b = 1.75 - 1.05 \left(\frac{f_1}{f_2} \right) + 0.3 \left(\frac{f_1}{f_2} \right)^2 \leq 2.3 \quad \text{Eq. (6.10.8.2.3-7)}$$

where:

f_{mid} = flange stress without the consideration of lateral bending at the middle of the unbraced length of the flange under consideration. f_{mid} shall be due to factored loads and shall be taken as positive in compression and negative in tension.

f_2 = largest compressive flange stress without consideration of lateral bending at either end of the unbraced length of the flange under consideration. f_2 shall be due to factored loads and shall be taken as positive. If the flange stress is zero or tensile

in the flange under consideration at both ends of the unbraced length, f_2 shall be taken as zero.

$f_1 =$ in the case of Section G2-1, the moment diagram along the entire length between brace points is concave in shape, and therefore, $f_1 = f_0$, and is the stress without consideration of lateral bending at the brace point opposite to the one corresponding to f_2 .

The largest compressive stress at the end of the unbraced length under consideration is at the brace point 65.04 ft into span 1. From calculations not shown herein, the unfactored moments at 65.04 ft due to steel self-weight and Cast #1 are 1,115 k-ft and 3,361 k-ft, respectively. Therefore, f_2 is calculated as:

$$f_2 = \frac{1.0(1.25)(1,115 + 3,361)(12)}{4,334} = 15.49 \text{ ksi}$$

f_{mid} is the compressive stress at the location under investigation, previously computed as 14.27 ksi in compression. Check the f_{mid}/f_2 ratio:

$$\frac{f_{\text{mid}}}{f_2} = \frac{14.27}{15.49} = 0.92 < 1.0$$

Therefore, C_b can be calculated using Eq. (6.10.8.2.3-7). First, it is necessary to compute f_1 , which is the flange stress at the opposite brace point from f_2 . From calculations not shown herein, the unfactored moments at 48.77 ft due to steel self-weight and Cast #1 are 1,116 k-ft and 2,588 k-ft, respectively. Therefore, f_1 is calculated as:

$$f_1 = \frac{1.0(1.25)(1,116 + 2,588)(12)}{4,334} = 12.82 \text{ ksi}$$

C_b is computed as:

$$C_b = 1.75 - 1.05 \left(\frac{12.82}{15.49} \right) + 0.3 \left(\frac{12.82}{15.49} \right)^2 = 1.09 \leq 2.3$$

Therefore, the lateral torsional buckling resistance is:

$$F_{\text{nc}} = (1.09) \left[1 - \left(1 - \frac{0.7(50)}{(1.0)(50)} \right) \left(\frac{16.30 - 7.57}{28.41 - 7.57} \right) \right] (1.0)(1.0)(50) = 47.7 \text{ ksi} \leq (1.0)(1.0)(50) = 50 \text{ ksi}$$

Check Eq. 6.10.3.2.1-2 as follows:

$$|-14.27| + \frac{1}{3} |-6.95| = 16.59 \text{ ksi} \leq (1.0)(47.7) = 47.7 \text{ ksi} \quad \text{OK} \quad (\text{Ratio} = 0.348)$$

Although not necessary in this case, if a larger lateral torsional buckling resistance had been required, then the equations of Article D6.4.1 could have alternatively been used to potentially obtain a larger resistance since C_b is greater than 1.0.

7.3.5.1.4 Top Flange: Web Bend-Buckling Resistance (Article 6.10.1.9)

Determine the nominal elastic web bend-buckling resistance at Section G2-1 according to the provisions of Article 6.10.1.9.1 as follows:

$$F_{crw} = \frac{0.9Ek}{\left(\frac{D}{t_w}\right)^2} \leq \min\left(R_h F_{yc}, \frac{F_{yw}}{0.7}\right) \quad \text{Eq. (6.10.1.9.1-1)}$$

where:

$$k = \frac{9}{(D_c/D)^2} \quad \text{Eq. (6.10.1.9.1-2)}$$

In earlier calculations, D_c was computed as 43.06 in. along the inclined web.

$$k = \frac{9}{\left(\frac{43.06}{80.04}\right)^2} = 31.1$$

Therefore,

$$F_{crw} = \frac{0.9(29,000)(31.1)}{\left(\frac{80.4}{0.5625}\right)^2} = 39.73 \text{ ksi} < R_h F_{yc} = 50 \text{ ksi}$$

Check Eq. (6.10.3.2.1-3),

$$|-14.27| = 14.27 \text{ ksi} \leq (1.0)(40.11) = 40.11 \text{ ksi} \quad \text{OK} \quad (\text{Ratio} = 0.356)$$

It should be noted that the web bend-buckling resistance is generally checked against the maximum compression flange stress due factored loads, without consideration of flange lateral bending, as shown in the previous calculation. Since web-bend buckling is a check of the web, the maximum flexural compression stress in the web could be calculated and used for comparison against the bend-buckling resistance. However, the precision associated with making the distinction between the stress in the compression flange and the maximum compressive stress in the web is typically not warranted.

7.3.5.2 Bottom Flange

Noncomposite tub flanges in tension, in this particular case the bottom flange, must satisfy the following requirement:

$$f_{bu} \leq \phi_f R_h F_{yf} \Delta \quad \text{Eq. (6.11.3.2-3)}$$

where:

$$\Delta = \sqrt{1 - 3 \left(\frac{f_v}{F_{yf}} \right)^2} \quad \text{Eq. (6.11.3.2-4)}$$

The term f_v is the factored St. Venant torsional shear stress in the flange at the section under consideration, and is taken as:

$$f_v = \frac{T}{2 A_o t_f} \quad \text{Eq. (6.11.3.2-5)}$$

where:

- T = internal torque due to factored loads (kip-in.)
- A_o = enclosed area within the box section (in.³)
- t_f = bottom flange thickness (in.)

Compute the enclosed area of the noncomposite box section, A_o .

$$A_o = \frac{[120 + (83 - 2(1))]}{2} \left(\frac{1.00}{2} + 78 + \frac{0.625}{2} \right) = 7,921 \text{ in.}^2$$

As shown in Table 7 the unfactored torques due to steel self-weight and Cast #1 are 59 kip-ft and 464 kip-ft, respectively. Therefore,

$$f_v = \frac{(1.25)(59 + 464)(12)}{2(7,921)(1.00)} = 0.50 \text{ ksi}$$

$$\Delta = \sqrt{1 - 3 \left(\frac{f_v}{F_{yf}} \right)^2} = \sqrt{1 - 3 \left(\frac{0.50}{50} \right)^2} = 1.00$$

The factored bottom flange major-axis bending stress, calculated previously, is 12.30 ksi. Check Eq. 6.11.3.2-3 as follows:

$$f_{bu} = 12.30 \text{ ksi} \leq \phi_f R_h F_{yf} \Delta = (1.0)(1.0)(50)(1.0) = 50.0 \text{ ksi} \quad \text{OK} \quad (\text{Ratio} = 0.246)$$

Although the check here of the bottom flange is illustrated for completeness, the bottom flange will typically not govern the constructibility check in regions of positive flexure.

7.3.6 Shear (Article 6.10.3.3)

Article 6.10.3.3 requires that interior panels of stiffened webs satisfy the following requirement:

$$V_u \leq \phi_v V_{cr} \quad \text{Eq. (6.10.3.3-1)}$$

where: ϕ_v = resistance factor for shear = 1.0 (Article 6.5.4.2)

V_u = shear in the web at the section under consideration due to the factored permanent loads and factored construction loads applied to the noncomposite section

V_{cr} = shear buckling resistance determined from Eq. (6.10.9.3.3-1)

Only the interior panels of stiffened webs are checked because the shear resistance of the end panel of stiffened webs and the shear resistance of unstiffened webs are already limited to the shear buckling resistance at the strength limit state.

For this example, the web is unstiffened in the positive moment regions. Therefore, the constructibility check for shear is not required at this section.

7.3.7 Concrete Deck (Article 6.10.3.2.4)

Generally, the entire deck is not placed in a single pour. Typically, for continuous span bridges, the positive flexure regions are placed first. Thus positive flexure regions may become composite prior to casting the other sections of the bridge. As the deck placement operation progresses, tensile stresses can develop in previously cast regions that will exceed the allowable rupture strength (ϕ_f) in the hardened deck. When cracking is predicted, longitudinal deck reinforcing as specified in Article 6.10.1.7 is required to control cracking. Otherwise, alternative deck casting sequences must be employed to minimize the anticipated stresses to acceptable levels. This check is illustrated in Example 1.

7.4 Girder Check: Section G2-1, Service Limit State (Article 6.11.4)

Article 6.11.4 directs the Engineer to Article 6.10.4, which contains provisions related to the control of elastic and permanent deformations at the Service Limit State.

7.4.1 Permanent Deformations (Article 6.10.4.2)

Article 6.10.4.2 contains criteria intended to control permanent deformations that would impair rideability. As specified in Article 6.10.4.2.1, these checks are to be made under the Service II load combination.

Article 6.10.4.2.2 requires that flanges of composite sections satisfy the following:

$$\text{Top flange of composite sections: } f_f \leq 0.95R_h F_{yf} \quad \text{Eq. (6.10.4.2.2-1)}$$

$$\text{Bottom flange of composite sections: } f_f + \frac{f_\ell}{2} \leq 0.95R_h F_{yf} \quad \text{Eq. (6.10.4.2.2-2)}$$

The term f_f is the flange stress at the section under consideration due to the Service II loads calculated without consideration of flange lateral bending. The f_ℓ term, the flange lateral bending stress, in Eq. 6.10.4.2.2-2 is to be taken equal to zero, in accordance with Article 6.11.4, for tub girder bottom flanges. A resistance factor is not included in these equations because Article 1.3.2.1 specifies that the resistance factor be taken equal to 1.0 at the service limit state.

It should be noted that in accordance with Article 6.11.4 redistribution of negative moment due to the Service II loads at the interior-pier sections in continuous span flexural members using the procedures specified in Appendix B6 is not to be applied to tub girder sections. The applicability of the Appendix B6 provisions to tub girder sections has not been demonstrated; hence, the procedures are not permitted for the design of tub girder sections.

Furthermore, according to Article C6.11.4, under the load combinations specified in Table 3.4.1-1, Eqs. 6.10.4.2.2-1 and 6.10.4.2.2-2 need only be checked for compact sections in positive flexure. For sections in negative flexure and noncompact sections in positive flexure, these two equations do not control and need not be checked. Composite sections in all horizontally curved girder systems are to be treated as noncompact sections at the strength limit state, in accordance with Article 6.11.6.2.2. Therefore, for Section G2-1, Eqs. 6.10.4.2.2-1 and 6.10.4.2.2-2 do not need to be checked, and are not checked in this example.

7.4.2 Web Bend-Buckling

With the exception of composite sections in positive flexure in which the web satisfies the requirement of Articles 6.11.2.1.2 and 6.10.2.1.1 ($D/t_w \leq 150$), web bend-buckling of all sections under the Service II load combination is to be checked as follows:

$$f_c \leq F_{crw} \quad \text{Eq. (6.10.4.2.2-4)}$$

The term f_c is the compression-flange stress at the section under consideration due to the Service II loads calculated without consideration of flange lateral bending, and F_{crw} is the nominal elastic bend-buckling resistance for webs determined as specified in Article 6.10.1.9. Because Section G2-1 is a composite section subject to positive flexure satisfying Article 6.11.2.1.2, Eq. (6.10.4.2.2-4) need not be checked as $D/t_w = 142.9$ which is less than 150. An explanation as to why these particular sections are exempt from the above web bend-buckling check is given in Article C6.10.1.9.1.

7.5 Girder Check: Section G2-1, Fatigue Limit State (Article 6.11.5)

Article 6.11.5 directs the designer to Article 6.10.5, where details in tub girder section flexural members must be investigated for fatigue as specified in Article 6.6.1. As appropriate, the Fatigue I and Fatigue II load combinations specified in Table 3.4.1-1 and the fatigue live load specified in Article 3.6.1.4 are to be employed for checking load-induced fatigue in tub girder sections. The Fatigue I load combination is to be used in combination with design checks for infinite fatigue life. The Fatigue II load combination is to be used in combination with design checks for finite fatigue life.

As specified in Article 6.11.5, one additional requirement specified particularly for tub girders sections is in regard to longitudinal warping and transverse bending stresses. When tub girders are subjected to torsion, their cross-sections become distorted, resulting in secondary bending stresses. Therefore, longitudinal warping stresses and transverse bending stresses due to cross-section distortion are to be considered in the fatigue checks for:

- Single tub girders in straight or horizontally curved bridges;
- Multiple tub girders in straight bridges that do not satisfy requirements of Article 6.11.2.3;
- Multiple tub girders in horizontally curved bridges; or
- Any single or multiple tub girder with a bottom flange that is not fully effective according to the provisions of Article 6.11.1.1.

Therefore, in this design example for Section G2-1, the stress range due to longitudinal warping resulting from cross-section distortion in the girders is considered in checking the fatigue resistance of the base metal. For simplicity in this design example, it is assumed that the longitudinal warping stresses are approximately equal to 10 percent of the longitudinal stresses caused by the major-axis bending moment. Thus, for the calculations contained herein at Section G2-1, the fatigue vertical bending moments are simply increased by 10 percent in computing the stress range.

The transverse bending stress range is considered separately from the longitudinal warping stress range for evaluating the fatigue resistance of the base metal adjacent to flange-to-web fillet welds and adjacent to the termination of fillet welds connecting transverse elements to webs and box flanges. The transverse bending stress range is not computed in this design example for Section G2-1. More exact calculations to determine the stress range from longitudinal warping and transverse bending due to cross-section distortion can be carried out using the beam-on-elastic-foundation analogy (BEF) presented by Wright and Abdel-Samad [3]. Sample calculations for determining these distortional stresses based on the BEF analogy are presented in the 2003 *AASHTO Guide Specification for Horizontally Curved Steel Girder Highway Bridges* [10], which is superseded by the current AASHTO specifications. Calculations demonstrating the use of the BEF analogy to compute the longitudinal warping stress and transverse bending stress ranges are included as part of the fatigue check of Section G2-2.

At Section G2-1, it is necessary to check the bottom flange for the fatigue limit state. The base metal at the transverse stiffener weld terminations and internal cross frame connection plate welds at locations subject to a net tensile stress must be checked as a Category C' fatigue detail (reference Table 6.6.1.2.3-1). Only the bottom flange is checked herein, as a net tensile stress is not induced in the top flange by the fatigue loading at this location.

According to Table 3.6.2.1-1, the dynamic load allowance for fatigue loads is 15%. Centrifugal force effects are considered and included in the fatigue moments. As discussed previously, the 75-year single lane ADTT is assumed to be 1,000 trucks per day.

According to Eq. (6.6.1.2.2-1), $\gamma(\Delta f)$ must not exceed the nominal fatigue resistance, $(\Delta F)_n$. In accordance with Article C6.6.1.2.2, the resistance factor, ϕ , and the load modifier, η , are taken as 1.0 for the fatigue limit state.

$$\gamma(\Delta f) \leq (\Delta F)_n \quad \text{Eq. (6.6.1.2.2-1)}$$

From Table 6.6.1.2.3-2, the 75-year $(ADTT)_{SL}$ equivalent to infinite fatigue life for a Category C' fatigue detail is 745 trucks per day. Therefore, since the assumed $(ADTT)_{SL}$ for this design example is 1,000 trucks per day, the detail must be checked for infinite fatigue life using the Fatigue I load combination. In accordance with Article 6.6.1.2.5, the nominal fatigue resistance for infinite fatigue life is equal to the constant-amplitude fatigue threshold:

$$(\Delta F)_n = (\Delta F)_{TH} \quad \text{Eq. (6.6.1.2.5-1)}$$

where $(\Delta F)_{TH}$ is the constant-amplitude fatigue threshold, and is taken from Table 6.6.1.2.5-3. For a Category C' fatigue detail, $(\Delta F)_{TH} = 12.0$ ksi, and therefore:

$$(\Delta F)_n = 12.0 \text{ ksi}$$

As shown in Table 7 the unfactored negative and positive moments due to fatigue, including centrifugal force effects and the 15 percent dynamic load allowance, at Section G2-1 are -290 kip-ft and 1,525 kip-ft, respectively. The short-term composite section properties ($n = 7.56$) used to compute the stress at the bottom of the web (top of the bottom flange) are:

$$I_{NA(n)} = 478,009 \text{ in.}^4$$

$$d_{BOT \text{ OF WEB}} = d_{BOT \text{ OF STEEL}} - t_{f_BOT \text{ FLANGE}} = 68.56 \text{ in.} - 0.625 \text{ in.} = 67.94 \text{ in.}$$

As specified in Table 3.4.1-1, the load factor, γ , for the Fatigue I load combination is 1.5. The total factored stress range at the bottom of the web, including the 10 percent increase estimate for the longitudinal warping stress, is computed as follows:

$$\gamma(\Delta f) = (1.5) \left(\frac{(1.10)(|-290| + 1,525)(12)(67.94)}{478,009} \right) = 5.11 \text{ ksi}$$

Check Eq. (6.6.1.2.2-1) as follows:

$$\gamma(\Delta f) = 5.11 \text{ ksi} \leq (\Delta F)_n = 12.00 \text{ ksi} \quad \text{OK} \quad (\text{Ratio} = 0.426)$$

7.5.1 Special Fatigue Requirements for Webs

In accordance with Article 6.10.5.3, interior panels of stiffened webs must satisfy:

$$V_u \leq V_{cr} \quad \text{Eq. (6.10.5.3-1)}$$

where: V_u = shear in the web at the section under consideration, due to unfactored permanent loads plus the factored fatigue load (Fatigue I)

V_{cr} = shear buckling resistance determined from Eq. (6.10.9.3.3-1).

Satisfaction of Eq. (6.10.5.3-1) is intended to control elastic flexing of the web, such that the member is assumed to be able to sustain an infinite number of smaller loadings without fatigue cracking due to this effect. The live load shear in the special requirement is intended to represent the heaviest truck expected to cross the bridge in 75 years.

Only interior panels of stiffened webs are investigated because the shear resistance of end panels of stiffened webs and the shear resistance of unstiffened webs are limited to the shear buckling resistance at the Strength limit state.

The detailed check of this special fatigue requirement for webs is not illustrated in this example; however, similar checks are illustrated in Example 1.

7.6 Girder Check: Section G2-1, Strength Limit State (Article 6.11.6)

7.6.1 Flexure (Article 6.11.6.2)

According to Article 6.11.6.2.2, sections in horizontally curved steel tub girder bridges are to be considered noncompact sections and are to satisfy the requirements of Article 6.11.7.2. Furthermore, compact and noncompact sections in positive flexure must satisfy the ductility requirement specified in Article 6.10.7.3. The ductility requirement is intended to protect the concrete deck from premature crushing. The section must satisfy:

$$D_p \leq 0.42 D_t \quad \text{Eq. (6.10.7.3-1)}$$

Where D_p is the distance from the top of the concrete deck to the neutral axis of the composite section at the plastic moment, and D_t is the total depth of the composite section. Reference the section property computations for the location of the neutral axis of the composite section at the plastic moment. At Section G2-1:

$$D_p = 9.5 + 4.0 - 1.0 + 0.27 = 12.77 \text{ in.}$$

$$D_t = 0.625 + 78.0 + 4.0 + 9.5 = 92.13 \text{ in.}$$

$$0.42D_t = 0.42(92.13) = 38.69 \text{ in.} > 12.77 \text{ in.} \quad \text{OK} \quad (\text{Ratio} = 0.330)$$

For a horizontally curved steel tub girder at the strength limit state, noncompact sections in positive flexure must satisfy the provisions of Article 6.11.7.2. At the strength limit state, the compression flanges of tub sections must satisfy:

$$f_{bu} \leq \phi_f F_{nc} \quad \text{Eq. (6.11.7.2.1-1)}$$

where:

- f_{bu} = longitudinal flange stress at the section under consideration calculated without consideration of flange lateral bending or longitudinal warping
- ϕ_f = resistance factor for flexure as specified in Article 6.5.4.2 ($\phi_f = 1.0$)
- F_{nc} = nominal flexural resistance of the compression flange determined as specified in Article 6.11.7.2.2

Flange lateral bending is not considered for the compression flanges in positive bending at the strength limit state because the flanges are continuously supported by the concrete deck. In accordance with Article 6.11.1.1, longitudinal warping stresses may be ignored at the strength limit state. However, St. Venant torsion and cross-section distortion stresses in the bottom box flange must be considered for noncompact sections.

At the strength limit state, the tension flange must satisfy:

$$f_{bu} \leq \phi_f F_{nt} \quad \text{Eq. (6.11.7.2.1-2)}$$

where:

- F_{nt} = nominal flexural resistance of the tension flange determined as specified in Article 6.11.7.2.2

Lateral bending does not need to be considered for the tension flange, in this case the bottom flange, as lateral bending is typically negligible in bottom flanges of tub girders.

Furthermore, the maximum longitudinal compressive stress in the concrete deck at the strength limit state is not to exceed $0.6f'_c$. The longitudinal compressive stress in the deck is to be determined in accordance with Article 6.10.1.1d, which allows the permanent and transient load stresses in the concrete deck to be computed using the short-term section properties (i.e. modular ratio taken as n).

The unfactored bending moments at Section G2-1 are taken directly from the analysis and are shown below (see). The live load moment includes the centrifugal force and dynamic load allowance effects.

Noncomposite Dead Load:	M_{DC1}	= 5,891 kip-ft
Composite Dead Load:	M_{DC2}	= 765 kip-ft
Future Wearing Surface Dead Load:	M_{DW}	= 1,006 kip-ft

Live Load (incl. IM and CF): $M_{LL+IM} = 5,920$ kip-ft

Compute the factored flange flexural stresses at Section G2-1 for the Strength I load combination, without consideration of flange lateral bending. As discussed previously, the η factor is taken equal to 1.0 in this example. Therefore:

For Strength I:

Top Flange:

$$f_{bu} = -1.0 \left[\frac{1.25(5,891)}{4,334} + \frac{1.25(765)}{14,329} + \frac{1.5(1,006)}{14,329} + \frac{1.75(5,920)}{43,181} \right] 12 = -25.33 \text{ ksi}$$

Bottom Flange:

$$f_{bu} = 1.0 \left[\frac{1.25(5,891)}{5,029} + \frac{1.25(765)}{6,406} + \frac{1.5(1,006)}{6,406} + \frac{1.75(5,920)}{6,972} \right] 12 = 40.02 \text{ ksi}$$

In accordance with Article 6.11.1.1, the effects of both flexural and St. Venant torsional shear are to be considered in horizontally curved tub girder bridges. Therefore, compute the factored St. Venant torsional shear stress, f_v , in the bottom flange for the Strength I load combination. f_v is determined by dividing the St. Venant torsional shear flow [$f = T/(2A_o)$] by the thickness of the bottom flange:

$$f_v = \frac{T}{2 A_o t_f} \quad \text{Eq. (6.11.3.2-5)}$$

where:

T = internal torque due to factored loads (kip-in.)
 A_o = enclosed area within the box section (in.³)
 t_f = bottom flange thickness (in.)

The unfactored torques at Section G2-1 obtained directly from the analysis are shown below (see Table 7). The live load torque includes the centrifugal force and dynamic load allowance effects.

Noncomposite Dead Load: $T_{DC1} = 264$ kip-ft
 Composite Dead Load: $T_{DC2} = 41$ kip-ft
 Future Wearing Surface Dead Load: $T_{DW} = 54$ kip-ft
 Live Load (incl. IM and CF): $T_{LL+IM} = 525$ kip-ft

Article C6.11.1.1 indicates that for torques applied to the noncomposite section, A_o is to be computed for the noncomposite section. Since the top lateral bracing in this example is attached to the top flange, the vertical depth can be calculated as the distance between the mid-thicknesses

of the top and bottom flanges. Furthermore, for torques applied to the composite section, A_o is to be computed for the composite section, using the depth from the mid-thickness of the bottom flange to the mid-thickness of the concrete deck. In this example, the height of the deck haunch is considered.

Compute the enclosed area of the noncomposite tub section, A_{o_NC} .

$$A_{o_NC} = \frac{[120 + (83 - 2(1))]}{2} \left(\frac{1.00}{2} + 78 + \frac{0.625}{2} \right) = 7,921 \text{ in.}^2$$

Compute the enclosed area of the composite tub section, A_{o_C} .

$$A_{o_C} = \frac{[120 + (83 - 2(1))]}{2} \left(78 + \frac{0.625}{2} + 4.00 + \frac{9.50}{2} \right) = 8,750 \text{ in.}^2$$

Compute the factored Strength I St. Venant torsional shear stress on the noncomposite section:

$$f_{v_NC} = (1.0) \frac{(1.25)(264)(12)}{2(7,921)(0.625)} = 0.40 \text{ ksi}$$

Compute the factored Strength I St. Venant torsional shear stress on the composite section:

$$f_{v_C} = (1.0) \frac{[(1.25)(41) + (1.50)(54) + (1.75)(525)](12)}{2(8,750)(0.625)} = 1.15 \text{ ksi}$$

Therefore the total factored Strength I St. Venant torsional shear stress is computed as:

$$f_v = 0.40 + 1.15 = 1.55 \text{ ksi}$$

According to Article 6.11.1.1, the St. Venant torsional shear stress in box flanges due to factored loads at the strength limit state is not to exceed the factored torsional shear resistance of flange, F_{vr} , taken as:

$$F_{vr} = 0.75\phi_v \frac{F_{yf}}{\sqrt{3}} \quad \text{Eq. (6.11.1.1-1)}$$

where:

$$\phi_v = \text{resistance factor for shear specified in Article 6.5.4.2}$$

Therefore:

$$F_{vr} = 0.75(1.0) \frac{50}{\sqrt{3}} = 21.65 \text{ ksi} > f_v = 1.55 \text{ ksi} \quad \text{OK}$$

7.6.1.1 Top Flange Flexural Resistance in Compression

In accordance with Article 6.11.7.2.2, the nominal flexural resistance of the compression flanges of noncompact composite tub sections is to be taken as:

$$F_{nc} = R_b R_h F_{yc} \quad \text{Eq. (6.11.7.2.2-1)}$$

where:

R_b = web load-shedding factor determined as specified in Article 6.10.1.10.2

R_h = hybrid factor determined as specified in Article 6.10.1.10.1.

For a homogenous girder, the hybrid factor, R_h , is equal to 1.0. In accordance with Article 6.10.1.10.2, the web load-shedding factor, R_b , is equal to 1.0 for composite section in which the web satisfies the requirement of Article 6.11.2.1.2, such that $D/t_w \leq 150$.

$$\frac{D}{t_w} = \frac{80.40}{0.5625} = 142.9 \leq 150$$

Therefore:

$$F_{nc} = (1.0)(1.0)(50.0) = 50.00 \text{ ksi}$$

For Strength I:

$$f_{bu} \leq \phi_f F_{nc} \quad \text{Eq. (6.11.7.2.1-1)}$$

$$f_{bu} = |-25.33| \text{ ksi} \leq \phi_f F_{nc} = (1.0)(50.00) = 50.00 \text{ ksi} \quad \text{OK} \quad (\text{Ratio} = 0.507)$$

7.6.1.2 Bottom Flange Flexural Resistance in Tension

Article 6.11.7.2.2 states that the nominal flexural resistance of the tension flange of a noncompact tub section is to be taken as:

$$F_{nt} = R_h F_{yt} \Delta \quad \text{Eq. (6.11.7.2.2-5)}$$

in which:

$$\Delta = \sqrt{1 - 3 \left(\frac{f_v}{F_{yt}} \right)^2} \quad \text{Eq. (6.11.7.2.2-6)}$$

$$\Delta = \sqrt{1 - 3 \left(\frac{1.55}{50.0} \right)^2} = 0.999$$

Therefore:

$$F_{nt} = (1.0)(50.0)(0.999) = 49.93 \text{ ksi}$$

For Strength I:

$$f_{bu} \leq \phi_f F_{nt} \quad \text{Eq. (6.11.7.2.1-2)}$$

$$f_{bu} = 40.02 \text{ ksi} \leq \phi_f F_{nt} = (1.0)(49.93) = 49.93 \text{ ksi} \quad \text{OK} \quad (\text{Ratio} = 0.802)$$

Note that longitudinal warping stresses due to cross-section distortion do not need to be considered at the strength limit state. However, transverse bending stresses due to cross-section distortion do need to be considered at the strength limit state and are not to exceed 20.0 ksi as specified in Article 6.11.1.1. However, in this design example for Section G2-1, it is assumed that the transverse bending stresses at the strength limit state do not exceed 20.0 ksi. For more detailed calculations of the transverse bending stress at the strength limit state, see the computations for Section G2-2 in this design example.

7.6.1.3 Concrete Deck Stresses

According to Article 6.11.7.2.1, the maximum longitudinal compressive stress in the concrete deck at the strength limit state is not to exceed $0.6f'_c$. This limit is to ensure linear behavior of the concrete, which is assumed in the calculation of steel flange stresses. The longitudinal compressive stress in the deck is to be determined in accordance with Article 6.10.1.1d, which allows the permanent and transient load stresses in the concrete deck to be computed using the short-term section properties ($n = 7.56$ composite section properties). Referring to Table 10 of the section property calculations, the section modulus to the top of the concrete deck is:

$$S_{\text{deck}} = \frac{478,009}{92.13 - 68.56} = 20,280 \text{ in.}^3$$

Calculate the Strength I factored longitudinal compressive stress in the deck at this section, noting that the concrete deck is not subjected to noncomposite dead loads. The stress in the concrete deck is obtained by dividing the stress acting on the transformed section by the modular ratio, n .

$$f_{\text{deck}} = 1.0 \left[\frac{1.25(765) + 1.5(1,006) + 1.75(5,920)}{(20,280)(7.56)} \right] 12 = -1.00 \text{ ksi}$$

$$f_{\text{deck}} = |-1.00 \text{ ksi}| < 0.6f'_c = 0.6(4.0) = 2.40 \text{ ksi} \quad \text{OK} \quad (\text{Ratio} = 0.417)$$

7.7 Girder Check: Section G2-2, Constructibility (Article 6.11.3)

7.7.1 Flexure (Article 6.11.3.2)

The bottom flange, in regions of negative flexure, is to satisfy the requirements of Eqs. (6.11.3.2-1) and (6.11.3.2-2) for critical stages of construction. Generally these provisions will not control because the size of the bottom flange in negative flexure regions is normally governed by the Strength Limit State. In regard to construction loads, the maximum negative moment reached during the deck placement analysis, plus the moment due to the self-weight, typically does not significantly exceed the calculated noncomposite negative moments assuming a single stage deck pour. Nonetheless, the constructibility check is performed herein for completeness and to illustrate the constructibility checks required for a negative moment region. For this constructibility check, it is assumed that the concrete deck has not yet hardened at Section G2-2.

$$f_{\text{bu}} \leq \phi_f F_{\text{nc}} \quad \text{Eq. (6.11.3.2-1)}$$

$$f_{\text{bu}} \leq \phi_f F_{\text{crw}} \quad \text{Eq. (6.11.3.2-2)}$$

Additionally, the top flanges, which are considered discretely braced for constructibility (i.e. the deck is not hardened), must satisfy the requirement specified in Article 6.10.3.2.2. Because the top flange is discretely braced, flange lateral bending must be considered, as shown in Eq. 6.10.3.2.2-1.

$$f_{\text{bu}} + f_{\ell} \leq \phi_f R_h F_{\text{yt}} \quad \text{Eq. (6.10.3.2.2-1)}$$

To illustrate this constructibility check, from separate analysis results not shown, the unfactored major-axis bending moment due to the deck pour sequence is -12,272 kip-ft. As shown in Table 4, the unfactored major-axis moment due to steel self-weight is -3,154 kip-ft.

Calculate the factored major-axis flexural stresses in the flanges of the steel section due to the factored load resulting from the steel self-weight and the assumed deck pour sequence.

For Construction Strength I:

$$\text{Top Flange: } f_{\text{bu}} = -\frac{1.0(1.25)[(-3,154) + (-12,272)](12)}{10,057} = 23.01 \text{ ksi}$$

$$\text{Bot. Flange: } f_{bu} = \frac{1.0(1.25)[(-3,154) + (-12,272)](12)}{11,316} = -20.45 \text{ ksi}$$

For this example, and illustration purposes, the V-load equation is used to compute the top flange lateral bending moment due to curvature. For a single flange, consider only one-half of the girder major-axis moment due to steel self-weight and the deck placement sequence.

$$M = \frac{[(-3,154) + (-12,272)]}{2} = -7,713 \text{ kip - ft}$$

$$M_{LAT} = \frac{M \ell^2}{NRD} = \frac{(-7,713)(16.3)^2}{(12)(716.25)(6.5)} = 36.7 \text{ kip - ft} \quad \text{Eq. (C4.6.1.2.4b-1)}$$

Combine the flange lateral bending moment computed using the V-load equation with the factored lateral moment due to the overhang brackets, which was computed previously in the Section G2-1 calculations. Noting that the factored flange lateral bending moment due to the deck overhang bracket loads is 12.4 kip-ft, the factored flange lateral bending moment and flange lateral bending stress are computed as:

$$M_{TOT_LAT} = (1.25)(36.7) + 12.4 = 58.3 \text{ kip - ft}$$

$$f_{\ell} = \frac{M_{TOT_LAT}}{S_{\ell}} = \frac{(58.3)(12)}{(3.00)(18)^2/6} = 4.32 \text{ ksi}$$

Because the top flanges are subject to tension at Section G2-2, amplification of the first-order flange lateral bending stress is not required. The factored flange lateral bending stress is less than the limit of $0.6F_{yt} = 0.6(50) = 30.0$ ksi specified in Article 6.10.1.6.

It should be noted that another significant source of flange lateral bending results from forces that develop in the single-diagonal top flange bracing members resulting from the major-axis bending of the tub girder. This effect is recognized in flange lateral moments taken directly from a finite element analysis. In the absence of a refined analysis, Fan and Helwig [8] have developed equations to evaluate bracing member forces and the forces imparted on the top flanges of tub girders resulting from major-axis bending of the girder. The flange lateral bending due to the top lateral bracing is not considered in these computations. However, in an actual bridge design the top-flange lateral bending moments due to the forces in the top lateral bracing members resulting from major-axis bending should be considered, and can be computed using the procedures suggested by Fan and Helwig [8].

Compute the factored St. Venant torsional shear stress, f_v , in the bottom flange for the Strength I load combination.

$$f_v = \frac{T}{2 A_o t_f} \quad \text{Eq. (6.11.3.2-5)}$$

Compute the enclosed area of the noncomposite tub section, A_o .

$$A_o = \frac{[120 + (83 - 2(1))]}{2} \left(\frac{3.00}{2} + 78 + \frac{1.50}{2} \right) = 8,065 \text{ in.}^2$$

The unfactored torques due to steel self-weight and Cast #1 are -22 kip-ft and -33 kip-ft, respectively (note that results for Cast #1 at this location are not provided in the analysis results table). Therefore,

$$f_v = (1.0) \frac{(1.25)(22 + 33)(12)}{2(8,065)(1.50)} = 0.03 \text{ ksi}$$

7.7.1.1 Top Flange

Check that the top flange tension stress is in compliance with Article 6.10.3.2.2:

$$f_{bu} + f_\ell \leq \phi_f R_h F_{yt} \quad \text{Eq. (6.10.3.2.2-1)}$$

For Construction Strength I:

$$f_{bu} + f_\ell = 23.01 \text{ ksi} + 4.32 \text{ ksi} = 27.33 \text{ ksi}$$

$$\phi_f R_h F_{yt} = (1.0)(1.0)(50.0) = 50.0 \text{ ksi}$$

$$f_{bu} + f_\ell = 27.33 \text{ ksi} < \phi_f R_h F_{yt} = 50.0 \text{ ksi} \quad \text{OK} \quad (\text{Ratio} = 0.547)$$

7.7.1.2 Bottom Flange

7.7.1.2.1 Bottom Flange: Flexural Resistance in Compression – Stiffened Flange

Calculate the nominal flexural resistance of the bottom flange in compression, F_{nc} , in accordance with Article 6.11.8.2. Per Article 6.11.3.2, in computing F_{nc} for constructibility, the web load-shedding factor, R_b , is to be taken as 1.0. The bottom flange is longitudinally stiffened at this location with a single WT 8x28.5 stiffener, placed at the center of the bottom flange. Therefore, Article 6.11.8.2.3 applies.

Determine the slenderness ratio of the bottom flange:

$$\lambda_f = \frac{b_{fc}}{t_{fc}} \quad \text{Eq. (6.11.8.2.2-8)}$$

where, in this case:

$$b_{fc} = w = \text{larger of the width of the flange between the longitudinal flange stiffeners or the distance from a web to the nearest longitudinal flange stiffener.}$$

Since the longitudinal stiffener is at the center of the bottom flange, w is the distance from the longitudinal stiffener to the centerline of the web.

$$\lambda_f = \frac{\left(\frac{81}{2}\right)}{1.50} = 27.00$$

Calculate the first limiting slenderness ratio:

$$\lambda_p = 0.57 \sqrt{\frac{Ek}{F_{yc}\Delta}} \quad \text{Eq. (6.11.8.2.2-9)}$$

where k is computed in accordance with Article 6.11.8.2.3 for longitudinally stiffened flanges, and Δ is computed as specified in Article 6.11.8.2.2.

As specified in Article 6.11.8.2.3, since a single bottom flange stiffener is used, $n = 1$ and the plate-buckling coefficient for uniform normal stress, k , is to be taken as:

$$k = \left(\frac{8 I_s}{w t_{fc}^3}\right)^{\frac{1}{3}} \quad \text{Eq. (6.11.8.2.3-1)}$$

and:

$$\Delta = \sqrt{1 - 3 \left(\frac{f_v}{F_{yc}}\right)^2} \quad \text{Eq. (6.11.8.2.2-11)}$$

where:

- f_v = factored St. Venant torsional shear stress in the flange (ksi)
- n = number of equally spaced longitudinal flange stiffeners
- k = plate-buckling coefficient for uniform normal stress, $1.0 \leq k \leq 4.0$
- I_s = moment of inertia of a single longitudinal flange stiffener about an axis parallel to the flange and taken at the base of the stiffener (in.⁴)

Structural tees are efficient shapes for longitudinal stiffeners because they provide a high ratio of stiffness to cross-sectional area. For the WT 8x28.5 stiffener, $I_x = 48.7 \text{ in.}^4$, $A = 8.39 \text{ in.}^2$, and the elastic neutral axis (N.A.) is 6.28 in. from the tip of the stem. Therefore, I_s is computed as:

$$I_s = 48.7 + (8.39)(6.28)^2 = 379.6 \text{ in.}^4$$

Compute the plate-buckling coefficient k :

$$k = \left(\frac{8(379.6)}{\left(\frac{81}{2}\right)(1.50^3)} \right)^{\frac{1}{3}} = 2.81 \leq 4.0$$

Compute the Δ term:

$$\Delta = \sqrt{1 - 3\left(\frac{0.03}{50.0}\right)^2} = 1.00$$

Compute λ_p :

$$\lambda_p = 0.57 \sqrt{\frac{(29,000)(2.81)}{(50.0)(1.00)}} = 23.01$$

Since λ_f is greater than 23.01 ($\lambda_f = 27.00$), it is necessary to compute the second limiting slenderness ratio:

$$\lambda_r = 0.95 \sqrt{\frac{Ek}{F_{yr}}} \quad \text{Eq. (6.11.8.2.2-10)}$$

where:

$$F_{yr} = (\Delta - 0.3)F_{yc} \leq F_{yw} \quad \text{Eq. (6.11.8.2.2-13)}$$

$$F_{yr} = (1.0 - 0.3)(50) = 35.0 \text{ ksi} \leq F_{yw} = 50 \text{ ksi}$$

Compute λ_r :

$$\lambda_r = 0.95 \sqrt{\frac{(29,000)(2.81)}{35.0}} = 45.84$$

Since $\lambda_p < \lambda_f = 27.00 \leq \lambda_r$, then the nominal axial compression buckling resistance of the flange under compression alone, F_{cb} , is calculated as follows:

$$F_{cb} = R_b R_h F_{yc} \left[\Delta - \left(\Delta - \frac{\Delta - 0.3}{R_h} \right) \left(\frac{\lambda_f - \lambda_p}{\lambda_r - \lambda_p} \right) \right] \quad \text{Eq. (6.11.8.2.2-3)}$$

$$F_{cb} = (1.0)(1.0)(50) \left[1.0 - \left(1.0 - \frac{1.0 - 0.3}{1.0} \right) \left(\frac{27.00 - 23.01}{45.84 - 23.01} \right) \right]$$

$$F_{cb} = 47.38 \text{ ksi}$$

Compute the nominal flexural resistance of the compression flange:

$$F_{nc} = F_{cb} \sqrt{1 - \left(\frac{f_v}{\phi_v F_{cv}} \right)^2} \quad \text{Eq. (6.11.8.2.2-1)}$$

where:

F_{cv} = nominal shear buckling resistance of the flange under shear alone (ksi)

In order to compute F_{cv} , first calculate k_s , the plate-buckling coefficient for shear stress as specified in Article 6.11.8.2.3:

$$k_s = \frac{5.34 + 2.84 \left(\frac{I_s}{w t_{fc}^3} \right)^{\frac{1}{3}}}{(n+1)^2} \leq 5.34 \quad \text{Eq. (6.11.8.2.3-3)}$$

$$k_s = \frac{5.34 + 2.84 \left(\frac{379.6}{(40.5)(1.50^3)} \right)^{\frac{1}{3}}}{(1+1)^2} = 2.33 \leq 5.34$$

As specified in Article 6.11.8.2.2, if $\lambda_f \leq 1.12 \sqrt{\frac{E k_s}{F_{yc}}}$, then:

$$F_{cv} = 0.58 F_{yc} \quad \text{Eq. (6.11.8.2.2-5)}$$

$$\lambda_f = 27.00 \leq 1.12 \sqrt{\frac{(29,000)(2.33)}{50}} = 41.17$$

Therefore:

$$F_{cv} = 0.58(50) = 29.0 \text{ ksi}$$

Compute F_{nc} :

$$F_{nc} = 47.38 \sqrt{1 - \left(\frac{0.03}{(1.0)(29.0)} \right)^2} = 47.38 \text{ ksi}$$

Checking compliance with Eq. 6.11.3.2-1:

$$f_{bu} \leq \phi_f F_{nc} \quad \text{Eq. (6.11.3.2-1)}$$

For Construction Strength I:

$$f_{bu} = |-20.45 \text{ ksi}| < \phi_f F_{nc} = (1.00)(47.38) = 47.38 \text{ ksi} \quad \text{OK} \quad (\text{Ratio} = 0.432)$$

7.7.1.2.2 Bottom Flange: Flexural Resistance in Compression – Web Bend-Buckling

According to Article 6.11.3.2, for sections with compact or noncompact webs, the web bend-buckling check of Eq. 6.11.3.2-2 is not necessary. Therefore, check if the web satisfies the noncompact slenderness limit given in Article 6.10.6.2.3.

$$\frac{2D_c}{t_w} < 5.7 \sqrt{\frac{E}{F_{yc}}} \quad \text{Eq. (6.10.6.2.3-1)}$$

where:

D_c = depth of web in compression in the elastic range (in.).

For a tub girder, the depth of the web must be taken along the inclined web. Therefore:

$$\frac{2D_c}{t_w} = \frac{2(38.82 - 1.5)/\cos 14.04^\circ}{0.5625} = 136.8$$

$$5.7 \sqrt{\frac{E}{F_{yc}}} = 5.7 \sqrt{\frac{29,000}{50.0}} = 137.3$$

Since Eq. 6.10.6.2.3-1 is satisfied the web is noncompact, and the web bend-buckling check of Eq. 6.11.3.2.-2 does not need to be investigated for constructibility.

7.7.1.3 Shear (Article 6.11.3.3)

For constructibility, Article 6.10.3.3 requires that interior panels of stiffened webs satisfy the following requirement:

$$V_u \leq \phi_v V_{cr} \quad \text{Eq. (6.10.3.3-1)}$$

where:

ϕ_v = resistance factor for shear specified in Article 6.5.4.2 ($\phi_v = 1.0$)

V_u = shear in the web at the section under consideration due to the factored permanent loads and factored construction loads applied to the noncomposite section.

V_{cr} = shear-buckling resistance determined from Eq. (6.10.9.3.3-1).

The panel on the Span 2 side of Section G2-2 will be investigated herein. The transverse stiffener spacing at this location is 62 inches. The total factored shear will include the contribution of the noncomposite dead load, and should not only include the vertical shear due to flexure but also shear in the web due to torsion. Although not included herein, wind loads and construction live loads also need to be considered by the designer, as applicable. The shears used in the computations below are for flexure plus the torsional shear in the critical web. The critical web shear due to steel self-weight is 47 kips (see Table 2), and the critical web shear for Cast #1 is taken as 185 kips (analysis results not explicitly provided for Cast #1).

For Construction Strength I:

$$V_u = 1.0(1.25)(47 + 185) = 265 \text{ kips}$$

However, it is required that the shear be taken along the inclined web, in accordance with Article 6.11.9:

$$V_{ui} = \frac{V_u}{\cos(\theta_{WEB})} \quad \text{Eq. (6.11.9-1)}$$

$$V_{ui} = \frac{265}{\cos(14.04^\circ)} = 273 \text{ kips}$$

The shear-buckling resistance of the 62 inch panel is determined as:

$$V_n = V_{cr} = CV_p \quad \text{Eq. (6.10.9.3.3-1)}$$

C is the ratio of the shear-buckling resistance to the shear yield strength determined as specified in Article 6.10.9.3.2. First, compute the shear-buckling coefficient, k:

$$k = 5 + \frac{5}{\left(\frac{d_o}{D}\right)^2} = 5 + \frac{5}{\left(\frac{62}{80.4}\right)^2} = 13.41 \quad \text{Eq. (6.10.9.3.2-7)}$$

Since:

$$\frac{D}{t_w} = \frac{80.4}{0.5625} = 142.9 > 1.40 \sqrt{\frac{Ek}{F_{yw}}} = 1.40 \sqrt{\frac{29,000(13.41)}{50}} = 123.5$$

$$C = \frac{1.57}{\left(\frac{D}{t_w}\right)^2} \left(\frac{Ek}{F_{yw}}\right) \quad \text{Eq. (6.10.9.3.2-6)}$$

$$C = \frac{1.57}{(142.9)^2} \left(\frac{29,000(13.41)}{50}\right) = 0.598$$

V_p is the plastic shear force and is calculated as follows:

$$V_p = 0.58 F_{yw} D t_w \quad \text{Eq. (6.10.9.3.3-2)}$$

$$V_p = 0.58 (50.0)(80.4)(0.5625) = 1,311 \text{ kips}$$

Therefore,

$$V_n = V_{cr} = CV_p = (0.598)(1,311) = 784 \text{ kips}$$

$$\phi_V V_{cr} = 1.0(784) = 784 \text{ kips}$$

$$V_{ui} = 273 \text{ kips} \leq \phi_V V_{cr} = 784 \text{ kips} \quad \text{OK} \quad (\text{Ratio} = 0.348)$$

7.8 Girder Check: Section G2-2, Service Limit State (Article 6.11.4)

Article 6.11.4 directs the Engineer to Article 6.10.4, which contains provisions related to the control of elastic and permanent deformations at the Service Limit State.

7.8.1 Permanent Deformations (Article 6.10.4.2)

Article 6.10.4.2 contains criteria intended to control permanent deformations that would impair rideability. As specified in Article 6.10.4.2.1, these checks are to be made under the Service II load combination.

As stated previously for the Service limit state check of Section G2-1, Article 6.10.4.2.2 requires that flanges of composite sections satisfy the following:

$$\text{Top flange of composite sections: } f_f \leq 0.95R_h F_{yf} \quad \text{Eq. (6.10.4.2.2-1)}$$

$$\text{Bottom flange of composite sections: } f_f + \frac{f_\ell}{2} \leq 0.95R_h F_{yf} \quad \text{Eq. (6.10.4.2.2-2)}$$

However, according to Article C6.11.4, under the load combinations specified in Table 3.4.1-1, Eqs. 6.10.4.2.2-1 and 6.10.4.2.2-2 need only be checked for compact sections in positive flexure. For sections in negative flexure and noncompact sections in positive flexure, these two equations do not control and need not be checked. Therefore, for Section G2-2, Eqs. 6.10.4.2.2-1 and 6.10.4.2.2-2 do not need to be checked, and are not checked in this example.

7.8.2 Web Bend-Buckling

With the exception of composite sections in positive flexure in which the web satisfies the requirement of Articles 6.11.2.1.2 and 6.10.2.1.1 ($D/t_w \leq 150$), web bend-buckling of all sections under the Service II load combination is to be checked as follows:

$$f_c \leq F_{crw} \quad \text{Eq. (6.10.4.2.2-4)}$$

The term f_c is the compression-flange stress at the section under consideration due to the Service II loads calculated without consideration of flange lateral bending, and F_{crw} is the nominal elastic bend-buckling resistance for webs determined as specified in Article 6.10.1.9. Because Section G2-2 is a section in negative flexure, Eq. 6.10.4.2.2-4 must be checked.

Determine the nominal web bend-buckling resistance, F_{crw} , for Section G2-2 in accordance with Article 6.10.1.9.1, as follows:

$$F_{crw} = \frac{0.9 E k}{\left(\frac{D}{t_w}\right)^2} \quad \text{Eq. (6.10.1.9.1-1)}$$

However, F_{crw} is not to exceed the smaller of $R_h F_{yc}$ and $F_{yw}/0.7$. The bend-buckling coefficient, k , is computed as:

$$k = \frac{9}{(D_c / D)^2} \quad \text{Eq. (6.10.1.9.1-2)}$$

where:

D_c = depth of the web in compression in the elastic range (in.). For composite sections, D_c is to be determined as specified in Article D6.3.1.

In accordance with Article 6.10.4.2.1, for members with shear connectors provided throughout the entire length of the girder that also satisfy Article 6.10.1.7, the concrete deck may be assumed to be effective for both positive and negative flexure, provided that the corresponding longitudinal stresses in the concrete deck at the section under consideration under the Service II loads are smaller than $2f_r$, where f_r is the modulus of rupture of concrete specified in Article 6.10.1.7. The requirements of Article 6.10.1.7 related to the minimum one percent longitudinal reinforcement required in the concrete deck are satisfied for Section G2-2 in this design example.

$$f_r = 0.24\sqrt{f'_c} \qquad \text{Article 6.10.1.7}$$

Therefore,

$$2f_r = 2(0.24\sqrt{4}) = 0.960 \text{ ksi}$$

In accordance with Article 6.10.1.1.1d, the longitudinal flexural stresses in the concrete deck due to all permanent and transient loads are to be computed using the short-term modular ratio, n . The calculated stress on the transformed section is divided by n to obtain the longitudinal stress in the concrete deck. Since the deck is not subjected to noncomposite dead loads, the longitudinal stress in the deck at Section G2-2 is due to DC2, DW, and LL+I moments only. The unfactored major-axis bending moments at Section G2-2 are (see Table 4):

Noncomposite Dead Load:	M_{DC1}	= -15,426 kip-ft
Composite Dead Load:	M_{DC2}	= -1,923 kip-ft
Future Wearing Surface Dead Load:	M_{DW}	= -2,550 kip-ft
Live Load (incl. IM and CF):	M_{LL+IM}	= -8,127 kip-ft

The longitudinal compressive stress in the deck is to be determined in accordance with Article 6.10.1.1.1d, which allows the permanent and transient load stresses to be computed using the short-term section properties ($n = 7.56$ composite section properties). Referring to Table 13 of the section property calculations, the section modulus to the top of the concrete deck is:

$$S_{\text{deck}} = \frac{833,768}{93.00 - 62.27} = 27,132 \text{ in.}^3$$

Calculate the Service II factored longitudinal compressive stress in the deck at this section, noting that the concrete deck is not subjected to noncomposite dead loads. The stress in the concrete deck is obtained by dividing the stress acting on the transformed section by the modular ratio, n .

$$f_{\text{deck}} = -1.0 \left[\frac{1.00(-1,923) + 1.00(-2,550) + 1.30(-8,127)}{(27,132)(7.56)} \right] 12 = 0.880 \text{ ksi}$$

$$f_{\text{deck}} = 0.880 \text{ ksi} < 2f_r = 0.960 \text{ ksi}$$

Since f_{deck} is less than $2f_r$, for this Service limit state check, the flexural stresses in the composite section caused by the Service II load may be computed assuming that the concrete deck is effective in tension. Refer to Table 12 and Table 13 for the section properties assuming that the concrete deck is effective. The major-axis bending stresses in the top and bottom flanges for the Service II load combination are computed as follows (f_t = tension flange, f_c = compression flange):

For Service II:

Top Flange:

$$f_t = -1.0 \left[\frac{1.00(-15,426)}{10,057} + \frac{1.00(-1,923)}{19,574} + \frac{1.00(-2,550)}{19,574} + \frac{1.30(-8,127)}{41,214} \right] 12 = 24.22 \text{ ksi}$$

Bottom Flange:

$$f_c = 1.0 \left[\frac{1.00(-15,426)}{11,316} + \frac{1.00(-1,923)}{12,562} + \frac{1.00(-2,550)}{12,562} + \frac{1.30(-8,127)}{13,390} \right] 12 = -30.10 \text{ ksi}$$

In order to compute F_{crw} , it is first necessary to determine D_c , the depth of the web in compression, in accordance with Eq. D6.3.1-1, as required in Article D6.3.1 for composite sections in negative flexure whenever the deck is considered effective in tension at the service limit state:

$$D_c = \left(\frac{-f_c}{|f_c| + f_t} \right) d - t_{fc} \geq 0 \quad \text{Eq. (D6.3.1-1)}$$

where:

- f_c = sum of the compression flange stresses caused by DC1, DC2, DW, and LL+I; acting on their respective sections (ksi). Flange lateral bending is disregarded.
- f_t = sum of the tension flange stresses caused by DC1, DC2, DW, and LL+I; acting on their respective sections (ksi). Flange lateral bending is disregarded.
- d = depth of steel section (in.)
- t_{fc} = thickness of compression flange (in.)

Therefore:

$$D_c = \left(\frac{-(-30.10)}{|-30.10| + 24.22} \right) (82.50) - 1.50 = 44.22 \text{ in.} \geq 0$$

However, the depth of the web in compression, D_c , should be taken along the inclined web for computing the web bend-buckling resistance. Therefore:

$$D_{ci} = \frac{44.22}{\cos(14.04^\circ)} = 45.58 \text{ in.}$$

Compute the bend-buckling coefficient, k :

$$k = \frac{9}{(D_c/D)^2} = \frac{9}{(45.58/80.40)^2} = 28.00$$

Therefore, the nominal web bend-buckling resistance, F_{crw} , is computed as:

$$F_{crw} = \frac{0.9 E k}{\left(\frac{D}{t_w}\right)^2} = \frac{0.9 (29,000) (28.00)}{\left(\frac{80.40}{0.5625}\right)^2} = 35.77 \text{ ksi} < \min(R_h F_{yc}, F_{yw}/0.7) = 50.0 \text{ ksi}$$

Verify Eq. (6.10.4.2.2-4):

$$f_c = |-30.10| \text{ ksi} \leq F_{crw} = 35.77 \text{ ksi} \quad \text{OK} \quad (\text{Ratio} = 0.841)$$

7.8.3 Concrete Deck (Article 6.10.1.7)

Article 6.10.1.7 requires the minimum one-percent longitudinal reinforcement in the concrete deck wherever the longitudinal tensile stress in the deck due to the factored construction loads or due to the Service II load combination exceeds ϕf_r . This check is illustrated for the negative moment region in Example 4.

7.9 Girder Check: Section G2-2, Fatigue Limit State (Article 6.11.5)

Article 6.11.5 directs the designer to Article 6.10.5, where details in tub girder flexural members must be investigated for fatigue as specified in Article 6.6.1. The Fatigue I load combination specified in Table 3.4.1-1 and the fatigue live load specified in Article 3.6.1.4 are employed for checking load-induced fatigue at Section G2-2.

At Section G2-2, it is necessary to check the top flange for the fatigue limit state for major-axis bending. The base metal at the transverse stiffener weld terminations and internal cross frame connection plate welds at locations subject to a net tensile stress must be checked as a Category C' fatigue detail (reference Table 6.6.1.2.3-1). Additional consideration must be given to cross-section distortion stresses, as discussed in more detail later in this section.

According to Table 3.6.2.1-1, the dynamic load allowance for fatigue loads is 15%. Centrifugal force effects are considered and included in the fatigue moments. As discussed previously, the 75-year single lane ADTT is assumed to be 1,000 trucks per day.

According to Eq. (6.6.1.2.2-1), $\gamma(\Delta f)$ must not exceed the nominal fatigue resistance, $(\Delta F)_n$. In accordance with Article C6.6.1.2.2, the resistance factor, ϕ , and the load modifier, η , are taken as 1.0 for the fatigue limit state.

$$\gamma(\Delta f) \leq (\Delta F)_n \quad \text{Eq. (6.6.1.2.2-1)}$$

From Table 6.6.1.2.3-2, the 75-year $(ADTT)_{SL}$ equivalent to infinite fatigue life for a Category C' fatigue detail is 745 trucks per day. Therefore, since the assumed $(ADTT)_{SL}$ for this design example is 1,000 trucks per day, the detail must be checked for infinite fatigue life using the Fatigue I load combination. Per Article 6.6.1.2.5, the nominal fatigue resistance for infinite fatigue life is equal to the constant-amplitude fatigue threshold:

$$(\Delta F)_n = (\Delta F)_{TH} \quad \text{Eq. (6.6.1.2.5-1)}$$

where $(\Delta F)_{TH}$ is the constant-amplitude fatigue threshold and is taken from Table 6.6.1.2.5-3. For a Category C' fatigue detail, $(\Delta F)_{TH} = 12.0$ ksi, and therefore:

$$(\Delta F)_n = 12.0 \text{ ksi}$$

As shown in Table 4 the unfactored negative and positive moments due to fatigue, including the 15 percent dynamic load allowance, at Section G2-2 are -1,384 kip-ft and 256 kip-ft, respectively.

In accordance with Article 6.6.1.2.1, for flexural members that utilize shear connectors throughout the entire length that also have concrete deck reinforcement satisfying the provisions of Article 6.10.1.7, it is permissible to compute the flexural stresses and stress ranges assuming the concrete deck to be effective for both positive and negative flexure at the fatigue limit state.

As required by Articles 6.10.10.1 and 6.11.10, shear connectors are necessary along the entire length of horizontally curved tub girder bridges. Also, earlier calculations in this design example show that the deck reinforcement is in compliance with Article 6.10.1.7. Therefore, the concrete deck is assumed effective in computing the major-axis bending stresses for the fatigue limit state at Section G2-2. The short-term composite section properties ($n = 7.56$) used to compute the stress at the top of the web (bottom of the top flange) are:

$$I_{NA(n)} = 833,768 \text{ in.}^4$$

$$d_{TOP \text{ OF WEB}} = d_{TOP \text{ OF STEEL}} - t_{f_TOP \text{ FLANGE}} = 20.23 \text{ in.} - 3.00 \text{ in.} = 17.23 \text{ in.}$$

As specified in Table 3.4.1-1, the load factor, γ , for the Fatigue I load combination is 1.5. The factored stress range at the top of the web, without consideration of the flange lateral bending stress and distortional longitudinal warping stress since the top flange is continuously braced by the concrete deck, is computed as follows:

$$\gamma(\Delta f) = (1.5) \left(\frac{(|-1,384| + 256)(12)(17.23)}{833,768} \right) = 0.41 \text{ ksi} < (\Delta F)_{TH} = 12.0 \text{ ksi ok}$$

(Ratio = 0.034)

7.9.1 Cross-section Distortion Stresses

As stated previously for the fatigue limit state check of Section G2-1, additional requirements are placed on computing stresses due to fatigue loads for tub sections. In particular, Article 6.11.5 requires the consideration of longitudinal warping stresses and transverse bending stresses due to cross-section distortion in tub sections. When a tub section is subjected to torsion, the cross-section becomes distorted, resulting in these secondary stresses.

In accordance with Article 6.11.5, the stress range due to longitudinal warping should be considered when investigating the fatigue resistance of the base metal at all details in the tub section. For simplicity, the longitudinal warping stresses are added to the longitudinal major-axis bending stresses.

Also, as specified in Article 6.11.5, the stress range due to the transverse bending stresses is to be considered in the base metal adjacent to the termination of fillet welds connecting transverse elements to webs and box flanges. The transverse bending stresses are considered separately from the longitudinal warping stresses. Article C6.11.5 states that as a result of the transverse bending, a stress concentration occurs at the termination of the fillet welds connecting transverse elements to webs and box flanges. The fatigue resistance of this detail, when subject to transverse bending, is not currently quantified but is anticipated to be as low as a Category E detail.

Calculations to determine the stress range from longitudinal warping and transverse bending can be carried out using the beam-on-elastic-foundation (BEF) analogy presented by Wright and Abdel-Samad [3]. The *Designers Guide to Box Girder Bridges* by Bethlehem Steel Corporation [11] also presents the method developed by Wright and Abdel-Samad to estimate the transverse bending stresses using the BEF analogy. In this method, the moment in the BEF is analogous to the longitudinal warping stress and the deflection of the BEF is analogous to the transverse bending stress.

The BEF analogy for computing the distortional stresses is demonstrated for Section G2-2 in the calculations that follow. Equation and figure references relate to those shown in the *Designers Guide to Box Girder Bridges (DGBGB)* [11]. The calculations that follow are intended to simply illustrate the procedure for computing these stresses using the BEF analogy. At Section G2-2, the bottom flange is not subject to a net tensile stress by inspection, and the top flanges are continuously braced by the concrete deck. Thus, the effect of the distortional stresses may be ignored at Section G2-2 for fatigue. However, in an actual design of a horizontally curved tub

girder, these stresses should be considered in the base metal adjacent to welded details at or near the bottom flange at locations where the flange is subject to a net tensile stress.

From a separate analysis (all results not shown) the unfactored negative and positive torques due to fatigue loading, including the 15 percent dynamic load allowance, at Section G2-2 are -309 kip-ft and 339 kip-ft, respectively. The torque fatigue range is a result of placing the fatigue truck in two different positions on the bridge but on opposite sides of the tub section. Also, it is assumed that this range is larger than the range produced by a single passage of the fatigue truck for this design example. As indicated in Article 6.11.5, a factor of 0.75 can be applied to this torque range to account for the fact that two separate positions of the fatigue truck are required to cause the critical torque range (note: the preceding has since been superseded in the 2015 Interims to the 7th Edition – refer to Articles C6.11.5 and C6.6.1.2.1 regarding the computation of a more realistic fatigue torque range at transverse bracing members in tub girders in lieu of applying the 0.75 factor. The 0.75 factor will continue to be applied in this example). Therefore applying this 0.75 factor, and the load factor for the Fatigue I load combination ($\gamma = 1.5$), the factored fatigue torque range, T_{FAT} , is:

$$T_{FAT} = (0.75)(1.5)[|-309| + 339] = 729 \text{ kip - ft}$$

Other required constants that will be used in the calculations that follow are:

$$\begin{aligned} I_{NA(n)} &= 833,768 \text{ in.}^4 \\ t_c &= \text{web thickness} = 0.5625 \text{ in.} \\ t_b &= \text{bottom flange thickness} = 1.50 \text{ in.} \\ t_a &= \text{slab thickness} = 9.5 \text{ in.} \\ E_c &= 3,834 \text{ ksi} \\ E_s &= 29,000 \text{ ksi} \\ \mu_c &= \text{Poisson's ratio for concrete} = 0.20 \text{ (Article 5.4.2.5)} \\ \mu_s &= \text{Poisson's ratio for steel} = 0.30 \\ \ell &= \text{cross frame spacing} = 16.30 \text{ ft} = 196 \text{ in.} \\ &\text{Transverse stiffener spacing at Section G2-2} = 62 \text{ in.} \\ &\text{Transverse stiffener is } 0.5 \text{ in.} \times 5.5 \text{ in.} \end{aligned}$$

Calculate the transverse flexural rigidities, D_a and D_b , of the concrete deck and the bottom box flange, respectively.

$$D_a = \frac{E_c t_a^3}{12(1 - \mu_c^2)} = \frac{(3,834)(9.5)^3}{12(1 - 0.20^2)} = 285,345 \frac{\text{k - in.}^2}{\text{in.}} \quad \text{DGBGB Eq. (A3a)}$$

$$D_b = \frac{E_s t_b^3}{12(1 - \mu_s^2)} = \frac{(29,000)(1.50)^3}{12(1 - 0.30^2)} = 8,963 \frac{\text{k - in.}^2}{\text{in.}} \quad \text{DGBGB Eq. (A3b)}$$

Article 6.11.1.1 permits transverse stiffeners to be considered effective in resisting transverse bending. Therefore, the transverse flexural rigidity of the web, D_c , is computed considering the

stiffness of the transverse stiffener. Calculate the effective width of the web plate, d_o , that acts with the transverse stiffener (see Figure 14):

$$d_o = \frac{d \tanh\left(5.6 \frac{d}{h}\right)}{5.6 \frac{d}{h} (1 - \mu_s^2)} \quad \text{DGBGB Eq. (A4)}$$

where:

- d = spacing of transverse stiffeners = 62 in.
- h = web plate depth, along the inclined web = 80.40 in.

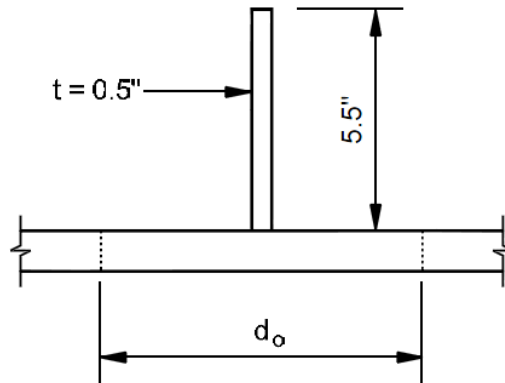


Figure 14 Effective Width of Web Plate, d_o , Acting with the Transverse Stiffener

Therefore,

$$d_o = \frac{(62) \tanh\left(5.6 \left(\frac{62}{80.40}\right)\right)}{5.6 \left(\frac{62}{80.40}\right) (1 - 0.30^2)} = 15.8 \text{ in.}$$

The transverse flexural rigidity of the web, D_c , considering the stiffness of the transverse stiffener is computed as:

$$D_c = \frac{E_s I_s}{d} \quad \text{DGBGB Eq. (A3d)}$$

where:

- I_s = moment of inertia of the effective stiffened web plate for transverse bending, including the transverse stiffener.

To compute I_s , first compute the location of the neutral axis of the effective section from the outer web face:

$$\begin{aligned} \text{Area of stiffener} &= (5.5)(0.5) &&= 2.75 \text{ in.}^2 \\ \text{Area of effective web} &= (15.8)(0.5625) &&= 8.89 \text{ in.}^2 \\ \text{Total Area} &&&= 11.64 \text{ in.}^2 \end{aligned}$$

$$\text{N.A.} = \frac{2.75\left(0.5625 + \frac{5.5}{2}\right) + 8.89\left(\frac{0.5625}{2}\right)}{11.64} = 1.0 \text{ in.}$$

Calculate the moment of inertia, I_s :

$$\begin{aligned} I_s &= \left(\frac{1}{12}\right)(0.5)(5.5)^3 + 2.75\left(\frac{5.5}{2} + 0.5625 - 1.0\right)^2 + \left(\frac{1}{12}\right)(15.8)(0.5625)^3 \\ &\quad + 8.89\left(\frac{0.5625}{2} - 1.0\right)^2 \end{aligned}$$

$$I_s = 26.5 \text{ in.}^4$$

Therefore,

$$D_c = \frac{(29,000)(26.5)}{62} = 12,395 \frac{\text{kip} \cdot \text{in.}^2}{\text{in.}}$$

The stiffness of the transverse stiffener is assumed to be distributed evenly along the web.

Compute the compatibility shear, v , at the center of the bottom (box) flange for unit loads applied at the top corners of a box section of a unit length:

$$v = \frac{\frac{1}{D_c} [(2a + b)abc] + \frac{1}{D_a} ba^3}{(a + b) \left(\frac{a^3}{D_a} + \frac{2c(a^2 + ab + b^2)}{D_c} + \frac{b^3}{D_b} \right)} \quad \text{DGBGB Eq. (A2)}$$

where a , b , and c are dimensional parameters of the tub section:

- a = distance between centerline of webs at top of tub section = 120 in.
- b = distance between centerline of webs at bottom of tub section = 81 in.
- c = height of web, along the incline = 80.40 in.

$$v = \frac{\frac{1}{12,395} [(2(120) + 81)(120)(81)(80.40)] + \frac{1}{285,345} (81)(120^3)}{(120 + 81) \left(\frac{120^3}{285,345} + \frac{2(80.40)(120^2 + (120)(81) + 81^2)}{12,395} + \frac{81^3}{8,963} \right)} = 0.22$$

Compute the box distortion per kip of load, δ_1 , assuming no cross-bracing or diaphragms are present:

$$\delta_1 = \frac{ab}{24(a+b)} \left[\frac{c}{D_c} \left(\frac{2ab}{a+b} - v(2a+b) \right) + \frac{a^2}{D_a} \left(\frac{b}{a+b} - v \right) \right] \quad \text{DGBGB Eq. (A1)}$$

$$\delta_1 = \frac{(120)(81)}{24(120+81)} \left[\frac{80.40}{12,395} \left(\frac{2(120)(81)}{120+81} - (0.22)(2(120)+81) \right) + \frac{120^2}{285,345} \left(\frac{81}{120+81} - 0.22 \right) \right]$$

$$\delta_1 = 0.36 \frac{\text{in.}^2}{\text{kip}}$$

The BEF stiffness parameter, β , is a measure of the torsional stiffness of the beam, and is analogous to the beam-foundation parameter in the BEF derivation. The BEF stiffness parameter, β , is calculated as:

$$\beta = \left(\frac{1}{E I_c \delta_1} \right)^{\frac{1}{4}} \quad \text{DGBGB Eq. (A5)}$$

$$\beta = \left(\frac{1}{(29,000)(833,768)(0.36)} \right)^{\frac{1}{4}} = 0.00327 \text{ in.}^{-1}$$

Multiplying the BEF stiffness parameter by the length between internal cross frames yields:

$$\beta \ell = (0.00327)(196.0) = 0.64$$

The transverse bending stress range at the top or bottom corners of the tub section may be determined as:

$$\sigma_t = C_t F_d \beta \frac{1}{2a} T_{\text{range}} \quad \text{DGBGB Eq. (A8)}$$

where:

C_t = BEF factor for determining the transverse distortional bending stress from DGBGB Figure A6 (see Figure 15)

$$\begin{aligned}
T_{\text{range}} &= \text{range of concentrated torque} = T_{\text{FAT}} \text{ (computed previously)} \\
a &= \text{distance between webs at the top of tub section} \\
F_d &= \frac{bv}{2S} \text{ for the bottom corner of tub section [DGBGB Eq. (A9a)]} \\
&= \left(\frac{a}{2S} \right) \left(\frac{b}{a+b} - v \right) \text{ for top corner of tub section [DGBGB Eq. (A9b)]} \\
S &= \text{section modulus of the transverse member (per inch)}
\end{aligned}$$

Calculate the section modulus, S , per unit length of the stiffened portion of the web. S is taken at the top of the transverse member. In the following equation, the section modulus is divided by the stiffener spacing, d ; and the distance from neutral axis of the stiffened web to the tip of the stiffener is c_s .

$$S_{\text{STIFFENED}} = \left(\frac{I}{c_s} \right) \left(\frac{1}{d} \right) = \left(\frac{26.5}{5.5 + 0.5625 - 1.0} \right) \left(\frac{1}{62} \right) = 0.084 \frac{\text{in.}^3}{\text{in.}}$$

Calculate the section modulus, S , per unit length of the unstiffened portion of the web taken at the mid-thickness of the web. In the equation that follows, b_{US} is taken as a unit 1.0 inch, so that the section modulus is computed per unit length.

$$S_{\text{UNSTIFFENED}} = \left(\frac{b_{\text{US}} h^2}{6} \right) = \left(\frac{(1.0)(0.5625)^2}{6} \right) = 0.0527 \frac{\text{in.}^3}{\text{in.}}$$

Compute the term F_d at the bottom corner of the tub section for the stiffened and unstiffened portions of the web:

$$\text{Stiffened Web: } F_d = \frac{bv}{2S} = \frac{(81)(0.22)}{2(0.084)} = 106 \text{ in.}^{-1}$$

$$\text{Unstiffened Web: } F_d = \frac{bv}{2S} = \frac{(81)(0.22)}{2(0.0527)} = 169 \text{ in.}^{-1}$$

Compute the term F_d at the top corner of the tub section for the stiffened and unstiffened portions of the web:

$$\text{Stiffened Web: } F_d = \left(\frac{a}{2S} \right) \left(\frac{b}{a+b} - v \right) = \left(\frac{120}{2(0.084)} \right) \left(\frac{81}{120+81} - 0.22 \right) = 131 \text{ in.}^{-1}$$

$$\text{Unstiffened Web: } F_d = \left(\frac{a}{2S} \right) \left(\frac{b}{a+b} - v \right) = \left(\frac{120}{2(0.0527)} \right) \left(\frac{81}{120+81} - 0.22 \right) = 208 \text{ in.}^{-1}$$

It is conservatively assumed that the transverse stiffeners are not attached to the top or bottom flanges. Therefore, F_d is equal to 208 in.^{-1} , as the larger value governs so as to produce a larger transverse bending stress.

In order to read C_t from Figure 15 (DGBGB Figure A6), the dimensionless ratio, q , must be calculated. The quantity q represents the ratio of cross frame / diaphragm brace stiffness to the tub section stiffness per unit length and is computed as:

$$q = \left[\frac{E_b A_b}{L_b \ell \delta_1} \right] \delta_b^2 \quad \text{DGBGB Eq. (A6)}$$

where:

- E_b = Young's modulus of the internal cross frame / diaphragm material
- A_b = cross-sectional area of one cross frame / diaphragm bracing member
- ℓ = internal cross frame / diaphragm spacing
- L_b = length of cross frame / diaphragm bracing member
- δ_b = deformation of the bracing member due to the applied torque and is calculated in accordance with DGBGB Eq. (A7)

$$\delta_b = \frac{2 \left(1 + \frac{a}{b} \right)}{\sqrt{1 + \left[\frac{a+b}{2h} \right]^2}} (\delta_1) \quad \text{DGBGB Eq. (A7)}$$

- h = vertical web depth of the tub section.

First, compute δ_b :

$$\delta_b = \frac{2 \left(1 + \frac{120}{81} \right)}{\sqrt{1 + \left[\frac{120+81}{2(78)} \right]^2}} (0.36) = 1.10 \frac{\text{in.}^2}{\text{kip}}$$

Calculate the cross frame stiffness ratio, q . The area of one diagonal, A_b , in the internal cross frame is assumed to be equal to 5.0 in.^2 , and the length of the diagonal, L_b , is equal to 87.9 in.

$$q = \left[\frac{(29,000)(5.0)}{(87.9)(196)(0.36)} \right] (1.10)^2 = 28.3$$

From Figure 15, for $q = 28.3$ and $\beta \ell = 0.64$, C_t is approximately equal to 0.12 . Therefore, the transverse bending stress range at the top or bottom corners of the tub section is:

$$\sigma_t = (0.12)(208)(0.00327) \frac{1}{2(120)} (729(12)) = 2.98 \text{ ksi}$$

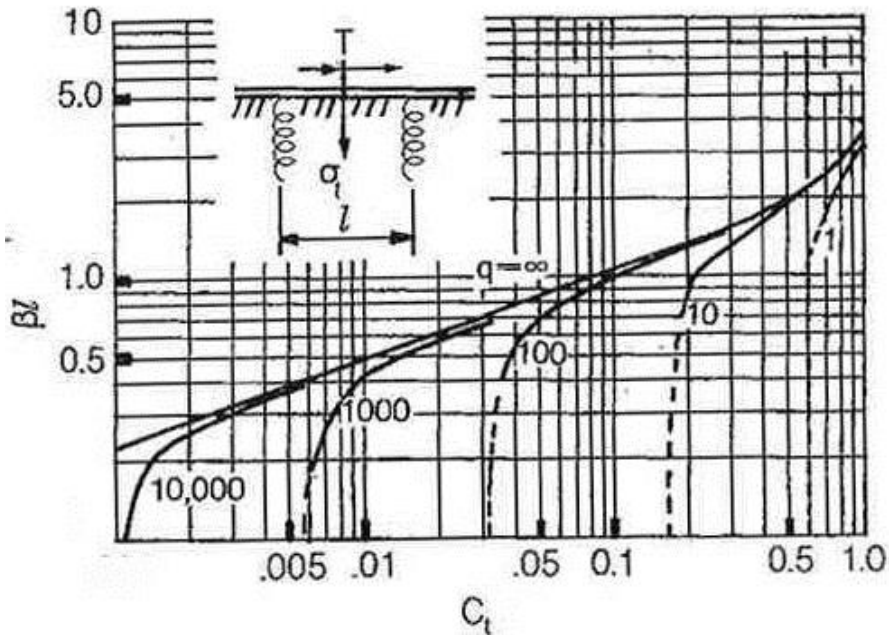


Figure 15 Concentrated Torque at Mid-panel on Continuous Beam - Distortional Bending Stress at Load (DGBGB Figure A6 [11])

As discussed previously, the base metal adjacent to the termination of fillet welds connecting transverse elements to webs and box flanges is assumed to be a Category E detail for transverse bending. Thus, the transverse bending stress range would be compared to the appropriate nominal fatigue resistance for a Category E detail computed according to the provisions of Article 6.6.1.2.5.

The fatigue longitudinal warping stress range at the top and bottom corners of the tub section due to cross section distortion can be computed as follows:

$$\sigma_{dw} = \frac{C_w y}{I \beta a} T_{\text{range}} \quad \text{DGBGB Eq. (A10)}$$

where:

C_w = BEF factor for determining the distortional longitudinal stress from DGBGB Figure A9 (see Figure 16)

y = distance along the transverse vertical axis of the tub section from the neutral axis to the point under consideration

Obtain C_w from the graph shown in Figure 16, where $q = 28.3$ and $\beta l = 0.64$. C_w is approximately 0.55. Therefore, using the short-term composite section properties with the

transformed deck at Section G2-2 (see Table 13), the factored distortional longitudinal stresses are:

$$\sigma_{dw_TOP} = \frac{(0.55)(17.23)}{(833,768)(0.00327)(120)} (729(12)) = 0.25 \text{ ksi}$$

$$\sigma_{dw_BOT} = \frac{(0.55)(60.77)}{(833,768)(0.00327)(120)} (729(12)) = 0.89 \text{ ksi}$$

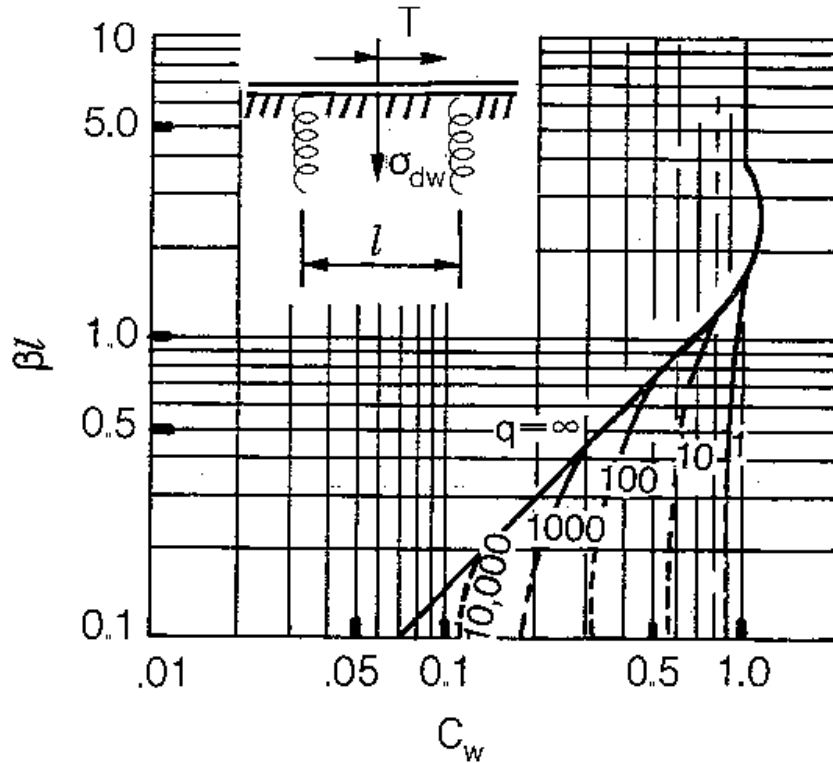


Figure 16 Concentrated Torque at Mid-panel on Continuous Beam – Normal Distortional Warping Stress at Mid-panel (DGBGB Table A9 [11])

The distortional longitudinal warping stress range at the bottom of the tub section would be considered in checking the fatigue resistance of the base metal at the connection plate welds to the bottom flange at locations where the flange is subject to a net tensile stress. The distortional longitudinal warping stress range would simply be added to the major-axis bending stress range at the detail. The distortional longitudinal warping stress at the top of the tub section may be ignored since the top flanges are continuously braced by the concrete deck.

7.10 Girder Check: Section G2-2, Strength Limit State (Article 6.11.6)

7.10.1 Flexure (Article 6.11.6.2)

For composite sections in negative flexure at the strength limit state, Article 6.11.6.2.3 directs the Engineer to Article 6.11.8. Furthermore, Article 6.11.6.2.3 states that the provisions of Appendix A6 do not apply to tub girders, nor is redistribution of negative moment in accordance with Appendix B6 permitted.

At the strength limit state, the top flanges in tension are continuously braced by the concrete deck, and are to satisfy:

$$f_{bu} \leq \phi_f F_{nt} \quad \text{Eq. (6.11.8.1.2-1)}$$

where F_{nt} is the nominal flexural resistance of the tension flanges determined as specified in Article 6.11.8.3.

At the strength limit state, tub flanges (bottom flanges) in compression are to satisfy:

$$f_{bu} \leq \phi_f F_{nc} \quad \text{Eq. (6.11.8.1.1-1)}$$

where F_{nc} is the nominal flexural resistance of the bottom flange determined as specified in Article 6.11.8.2.

The unfactored bending moments at Section G2-2 from the analysis are shown below (see Table 4). The live load moment includes the centrifugal force and dynamic load allowance effects.

Noncomposite Dead Load:	M_{DC1}	= -15,426 kip-ft
Composite Dead Load:	M_{DC2}	= -1,923 kip-ft
Future Wearing Surface Dead Load:	M_{DW}	= -2,550 kip-ft
Live Load (incl. IM and CF):	M_{LL+IM}	= -8,127 kip-ft

Compute the factored flange flexural stresses at Section G2-2 for the Strength I load combination, without consideration of flange lateral bending. For loads applied to the composite section, cracked section properties are used to compute the major-axis bending stresses at the strength limit state in accordance with Article 4.5.2.2. Shear lag need not be considered since the box flange (bottom flange) does not exceed one-fifth of the span of the bridge (Article C6.11.1.1). Therefore, the major-axis bending stress is assumed to be uniform across the flange because shear lag need not be considered. Also, the longitudinal warping stress due to cross-section distortion does not need to be considered at the strength limit state, in accordance with Article 6.11.1.1. As discussed previously, the η factor is taken equal to 1.0 in this example. Therefore:

For Strength I:

Top Flange:

$$f_{bu} = -1.0 \left[\frac{1.25(-15,426)}{10,057} + \frac{1.25(-1,9232)}{10,654} + \frac{1.5(-2,550)}{10,654} + \frac{1.75(-8,127)}{11,862} \right] 12 = 44.41 \text{ ksi}$$

Bottom Flange:

$$f_{bu} = 1.0 \left[\frac{1.25(-15,426)}{11,316} + \frac{1.25(-1,923)}{11,447} + \frac{1.5(-2,550)}{11,447} + \frac{1.75(-8,127)}{11,674} \right] 12 = -41.60 \text{ ksi}$$

In accordance with Article 6.11.1.1, the effects of both flexural and St. Venant torsional shear are to be considered for horizontally curved bridges. Therefore, compute the factored St. Venant torsional shear stress, f_v , in the bottom flange for the Strength I load combination. f_v is determined by dividing the St. Venant torsional shear flow [$f = T/(2A_o)$] by the thickness of the bottom flange:

$$f_v = \frac{T}{2 A_o t_f} \quad \text{Eq. (6.11.3.2-5)}$$

where:

- T = internal torque due to factored loads (kip-in.)
- A_o = enclosed area within the box section (in.³)
- t_f = bottom flange thickness (in.)

The unfactored torques at Section G2-2 obtained from the analysis are shown below (see Table 6). The live load torque includes the centrifugal force and dynamic load allowance effects. The positive torques are used in the calculations that follow as the total of the positive torques governs over the absolute total of the negative torques.

Noncomposite Dead Load:	$T_{DC1} = 36 \text{ kip-ft} + (-33 \text{ kip-ft}) = 3 \text{ kip-ft}$
Composite Dead Load:	$T_{DC2} = 192 \text{ kip-ft}$
Future Wearing Surface Dead Load:	$T_{DW} = 255 \text{ kip-ft}$
Live Load (incl. IM and CF):	$T_{LL+IM} = 980 \text{ kip-ft}$

Article C6.11.1.1 indicates that for torques applied to the noncomposite section, A_o is to be computed for the noncomposite section. Since the top lateral bracing in this example is attached to the top flange, the vertical depth can be calculated as the distance between the mid-thicknesses of the top and bottom flanges. Furthermore, for torques applied to the composite section, A_o is to be computed for the composite section using the depth from the mid-thickness of the bottom flange to the mid-thickness of the concrete deck. In this example, the height of the deck haunch is considered.

Compute the enclosed area of the noncomposite tub section, A_{o_NC} .

$$A_{o_NC} = \frac{[120 + (83 - 2(1))]}{2} \left(\frac{3.00}{2} + 78 + \frac{1.50}{2} \right) = 8,065 \text{ in.}^2$$

Compute the enclosed area of the composite tub section, A_{o_C} .

$$A_{o_C} = \frac{[120 + (83 - 2(1))]}{2} \left(78 + \frac{1.50}{2} + 4.00 + \frac{9.50}{2} \right) = 8,794 \text{ in.}^2$$

Compute the factored Strength I St. Venant torsional shear stress in the bottom flange of the noncomposite section:

$$f_{v_NC} = (1.0) \frac{(1.25)(3)(12)}{2(8,065)(1.50)} = 0.002 \text{ ksi}$$

Compute the factored Strength I St. Venant torsional shear stress in the bottom flange of the composite section:

$$f_{v_C} = (1.0) \frac{[(1.25)(192) + (1.50)(255) + (1.75)(980)](12)}{2(8,794)(1.50)} = 1.063 \text{ ksi}$$

Therefore the total factored Strength I St. Venant torsional shear stress is computed as:

$$f_v = 0.002 + 1.063 = 1.07 \text{ ksi}$$

According to Article 6.11.1.1, the factored St. Venant torsional shear stress in box flanges (bottom flange in this tub girder) at the strength limit state is not to exceed the factored torsional shear resistance of the flange, F_{vr} , taken as:

$$F_{vr} = 0.75\phi_v \frac{F_{yf}}{\sqrt{3}} \quad \text{Eq. (6.11.1.1-1)}$$

where:

$$\phi_v = \text{resistance factor for shear specified in Article 6.5.4.2}$$

Therefore:

$$F_{vr} = 0.75(1.0) \frac{50}{\sqrt{3}} = 21.65 \text{ ksi} > f_v = 1.07 \text{ ksi} \quad \text{OK}$$

7.10.2 Top Flange

Calculate the nominal flexural resistance of the top flanges in tension, F_{nt} , in accordance with Article 6.11.8.3.

$$F_{nt} = R_h F_{yt} \quad \text{Eq. (6.11.8.3-1)}$$

For a homogenous girder, R_h , is equal to 1.0 (Article 6.10.1.10.1). Therefore:

$$F_{nt} = (1.0)(50.0) = 50.0 \text{ ksi}$$

For Strength I:

$$f_{bu} \leq \phi_f F_{nt} \quad \text{Eq. (6.11.8.1.2-1)}$$

$$f_{bu} = 44.41 \text{ ksi} < \phi_f F_{nt} = (1.0)(50.00) = 50.00 \text{ ksi} \quad \text{OK} \quad (\text{Ratio} = 0.888)$$

7.10.3 Bottom Flange

Calculate the nominal flexural resistance of the bottom flange in compression, F_{nc} , in accordance with Article 6.11.8.2. The bottom flange is longitudinally stiffened at this location, with a single WT 8x28.5 stiffener placed at the center of the bottom flange.

$$\lambda_f = \frac{b_{fc}}{t_{fc}} \quad \text{Eq. (6.11.8.2.2-8)}$$

where, in this case:

$$b_{fc} = w = \text{larger of the width of the flange between the longitudinal flange stiffeners or the distance from a web to the nearest longitudinal flange stiffener.}$$

Since the longitudinal stiffener is at the center of the bottom flange, w is the distance from the longitudinal stiffener to the centerline of the web.

$$\lambda_f = \frac{\left(\frac{81}{2}\right)}{1.50} = 27.00$$

Calculate the first limiting slenderness ratio:

$$\lambda_p = 0.57 \sqrt{\frac{Ek}{F_{yc} \Delta}} \quad \text{Eq. (6.11.8.2.2-9)}$$

where k is computed as specified in Article 6.11.8.2.3 for longitudinally stiffened flanges, and Δ is computed in accordance with Article 6.11.8.2.2.

As specified in Article 6.11.8.2.3, since a single bottom flange stiffener is used, $n = 1$ and the plate-buckling coefficient for uniform normal stress, k , is to be taken as:

$$k = \left(\frac{8 I_s}{w t_{fc}^3} \right)^{\frac{1}{3}} \quad \text{Eq. (6.11.8.2.3-1)}$$

and:

$$\Delta = \sqrt{1 - 3 \left(\frac{f_v}{F_{yc}} \right)^2} \quad \text{Eq. (6.11.8.2.2-11)}$$

where:

- f_v = factored St. Venant torsional shear stress in the flange (ksi)
- n = number of equally spaced longitudinal flange stiffeners
- k = plate-buckling coefficient for uniform normal stress, $1.0 \leq k \leq 4.0$
- I_s = moment of inertia of a single longitudinal flange stiffener about an axis parallel to the flange and taken at the base of the stiffener (in.⁴)

Structural tees are efficient shapes for longitudinal stiffeners because they provide a high ratio of stiffness to cross-sectional area. For the WT 8x28.5 stiffener, $I_x = 48.7 \text{ in.}^4$, $A = 8.39 \text{ in.}^2$, and the elastic neutral axis (N.A.) is 6.28 in. from the tip of the stem. Therefore, I_s is computed as:

$$I_s = 48.7 + (8.39)(6.28)^2 = 379.6 \text{ in.}^4$$

Compute the plate-buckling coefficient k :

$$k = \left(\frac{8(379.6)}{\left(\frac{81}{2} \right) (1.50^3)} \right)^{\frac{1}{3}} = 2.81 \leq 4.0$$

Compute the Δ term:

$$\Delta = \sqrt{1 - 3 \left(\frac{1.07}{50.0} \right)^2} = 0.999$$

Compute λ_p :

$$\lambda_p = 0.57 \sqrt{\frac{(29,000)(2.81)}{(50.0)(0.999)}} = 23.02$$

Since λ_f is greater than 23.02 ($\lambda_f = 27.00$), it is necessary to compute the second limiting slenderness ratio:

$$\lambda_r = 0.95 \sqrt{\frac{Ek}{F_{yr}}} \quad \text{Eq. (6.11.8.2.2-10)}$$

where:

$$F_{yr} = (\Delta - 0.3)F_{yc} \leq F_{yw} \quad \text{Eq. (6.11.8.2.2-13)}$$

$$F_{yr} = (0.999 - 0.3)(50) = 35.0 \text{ ksi} \leq F_{yw} = 50 \text{ ksi}$$

Compute λ_r :

$$\lambda_r = 0.95 \sqrt{\frac{(29,000)(2.81)}{35.0}} = 45.84$$

Since $\lambda_p < \lambda_f = 27.00 \leq \lambda_r$, then the nominal axial compression buckling resistance of the flange under compression alone, F_{cb} , is calculated as follows:

$$F_{cb} = R_b R_h F_{yc} \left[\Delta - \left(\Delta - \frac{\Delta - 0.3}{R_h} \right) \left(\frac{\lambda_f - \lambda_p}{\lambda_r - \lambda_p} \right) \right] \quad \text{Eq. (6.11.8.2.2-3)}$$

The hybrid factor, R_h , is equal to 1.0, as specified in Article 6.10.1.10.1.

Determine the web load-shedding factor, R_b . First, compute the depth of the web in compression, D_c , in accordance with the provisions of Article D6.3.1. These provisions state that for composite sections in negative flexure at the strength limit state, D_c is to be computed for the section consisting of the steel girder plus the longitudinal deck reinforcement. For this example, D_c is calculated using the short-term (n) section property computations for the steel section plus the longitudinal reinforcement shown in Table 15. As indicated in Article C6.11.8.2.2, in calculating R_b for a tub section, use one-half of the effective box (bottom) flange width in conjunction with one top flange and a single web.

Therefore, compute D_c along the inclined web:

$$D_c = (41.58 - 1.50) \sqrt{\frac{4^2 + 1}{4^2}} = 41.31 \text{ in.}$$

According to the provisions of Article 6.10.1.10.2:

$$\frac{2D_c}{t_w} = \frac{2(41.31)}{0.5625} = 146.9 \quad \text{Eq. (6.10.1.10.2-2)}$$

$$\lambda_{rw} = 5.7 \sqrt{\frac{E}{F_{yc}}} = 5.7 \sqrt{\frac{29,000}{50}} = 137.3 \quad \text{Eq. (6.10.1.10.2-4)}$$

Since $\frac{2D_c}{t_w} > \lambda_{rw}$, calculate R_b as follows:

$$R_b = 1 - \left(\frac{a_{wc}}{1200 + 300a_{wc}} \right) \left(\frac{2D_c}{t_w} - \lambda_{rw} \right) \leq 1.0 \quad \text{Eq. (6.10.1.10.2-3)}$$

where,

$$a_{wc} = \frac{2D_c t_w}{b_{fc} t_{fc}} = \frac{2(41.31)(0.5625)}{(81.0/2)(1.50)} = 0.765 \quad \text{Eq. (6.10.1.10.2-5)}$$

Therefore,

$$R_b = 1 - \left(\frac{0.765}{1200 + 300(0.765)} \right) \left(\frac{2(41.31)}{0.5625} - 137.3 \right) = 0.995 \leq 1.0$$

Compute the nominal axial compression buckling resistance:

$$F_{cb} = (0.995)(1.0)(50) \left[0.999 - \left(0.999 - \frac{0.999 - 0.3}{1.0} \right) \left(\frac{27.00 - 23.02}{45.84 - 23.02} \right) \right]$$

$$F_{cb} = 47.10 \text{ ksi}$$

Compute the nominal flexural resistance of the compression flange:

$$F_{nc} = F_{cb} \sqrt{1 - \left(\frac{f_v}{\phi_v F_{cv}} \right)^2} \quad \text{Eq. (6.11.8.2.2-1)}$$

where:

F_{cv} = nominal shear buckling resistance of the flange under shear alone (ksi)

In order to compute F_{cv} , first calculate k_s , the plate-buckling coefficient for shear stress in accordance with Article 6.11.8.2.3:

$$k_s = \frac{5.34 + 2.84 \left(\frac{I_s}{w t_{fc}^3} \right)^{\frac{1}{3}}}{(n+1)^2} \leq 5.34 \quad \text{Eq. (6.11.8.2.3-3)}$$

$$k_s = \frac{5.34 + 2.84 \left(\frac{379.6}{(40.5)(1.50^3)} \right)^{\frac{1}{3}}}{(1+1)^2} = 2.33 \leq 5.34$$

As specified in Article 6.11.8.2.2, if $\lambda_f \leq 1.12 \sqrt{\frac{Ek_s}{F_{yc}}}$, then:

$$F_{cv} = 0.58 F_{yc} \quad \text{Eq. (6.11.8.2.2-5)}$$

$$\lambda_f = 27.00 \leq 1.12 \sqrt{\frac{(29,000)(2.33)}{50}} = 41.17$$

Therefore:

$$F_{cv} = 0.58(50) = 29.0 \text{ ksi}$$

Compute F_{nc} :

$$F_{nc} = 47.10 \sqrt{1 - \left(\frac{1.07}{(1.0)(29.0)} \right)^2} = 47.07 \text{ ksi}$$

Checking compliance with Eq. 6.11.8.1.1-1:

$$f_{bu} \leq \phi_f F_{nc} \quad \text{Eq. (6.11.8.1.1-1)}$$

For Strength I:

$$f_{bu} = |-41.60 \text{ ksi}| < \phi_f F_{nc} = (1.00)(47.07) = 47.07 \text{ ksi} \quad \text{OK} \quad (\text{Ratio} = 0.884)$$

Article C6.11.8.1.1 states that in general, bottom box flanges at interior pier sections are subjected to biaxial stresses due to major-axis bending of the tub section and major-axis bending

of the internal diaphragm over the bearing sole plate. The bottom flange is also subject to shear stresses due to the internal diaphragm vertical shear and, in cases where it needs to be considered, the St. Venant torsional shear. For cases where the shear stresses and/or bending of the internal diaphragm are deemed significant, Article C6.11.8.1.1 suggests that the following equation be used to check the combined stress state in the box flange at the strength limit state:

$$\sqrt{f_{bu}^2 - f_{bu}f_{by} + f_{by}^2 + 3(f_d + f_v)^2} \leq \phi_f R_b R_h F_{yc} \quad \text{Eq. (C6.11.8.1.1-1)}$$

where:

- f_{bu} = factored longitudinal stress at the section under consideration calculated without consideration of longitudinal warping (ksi)
- f_{by} = factored stress in the flange caused by major-axis bending of the internal diaphragm over the bearing sole plate (ksi)
- f_d = factored shear stress in the flange caused by the internal diaphragm vertical shear (ksi)
- f_v = factored St. Venant torsional shear stress in the flange (ksi)
- R_b = web load-shedding factor determined as specified in Article 6.10.1.10.2
- R_h = hybrid factor determined as specified in Article 6.10.1.10.1

In this example, each tub girder is supported on two bearings at each support. Therefore, the bottom flange bending stresses due to major-axis bending of the diaphragm over the bearing sole plates are relatively small and are neglected in this example ($f_{by} = 0.0$ ksi). The effect of these forces in a tub section supported on a single bearing is likely to be more significant and should be considered. As specified in Article C6.11.8.1.1 an effective flange width of 6 times the thickness of the tub girder bottom flange may be considered effective with the internal diaphragm for computing the stress in the box flange (bottom flange in this tub girder) caused by major-axis bending of the internal diaphragm over the bearing sole plate. Furthermore, if an access hole is provided within the internal diaphragm, the hole should be considered in calculating the section properties of the effective diaphragm section.

From previous calculations, the total factored St. Venant torsional shear stress in the bottom flange, f_v , is equal to 1.07 ksi.

To estimate the shear stress in the bottom flange due to the internal diaphragm shear, a 1 in. by 12 in. top flange for the diaphragm is assumed. The diaphragm web is assumed to be 78 inches deep and 1 inch thick, and for simplicity in this example, an access hole is assumed not to be provided in the web. As specified in Article C6.11.8.1.1, a box flange width equal to 6 times its thickness may be considered effective with the internal diaphragm. Therefore:

$$b_{bf_EFF} = 6(1.50) = 9.0 \text{ in.}$$

Therefore, the effective bottom flange of the internal diaphragm is 9.0 inches wide and has a thickness of 1.50 inches. The thickness of the effective bottom flange of the internal diaphragm is the same as the thickness of the tub girder bottom flange.

From separate calculations not shown here, the moment of inertia of the effective internal diaphragm is 79,565 in.⁴, and the neutral axis is located 39.89 in. above the bottom of the bottom flange. Calculations associated with the design of the internal diaphragm, shown later, indicate that the total factored vertical component of the diaphragm shear is 1,406 kips. The shear stress in the tub girder bottom flange, f_d , caused by the internal diaphragm vertical shear due to factored loads is approximated as:

$$f_d = \frac{V Q}{I t_{fc}} \quad \text{Eq. (C6.11.8.1.1-2)}$$

where:

- V = vertical shear in the internal diaphragm due to flexure plus St. Venant torsion (kip)
- Q = first moment of inertia of one-half the effective box-flange area about the neutral axis of the effective internal diaphragm (in.³)
- I = moment of inertia of the effective internal diaphragm section (in.⁴)

The first moment of inertia of one-half the effective box-flange area about the neutral axis of the effective internal diaphragm, Q, is computed as:

$$Q = \frac{1}{2}(9.0)(1.50)\left(39.89 - \frac{1.50}{2}\right) = 264.2 \text{ in.}^3$$

Therefore,

$$f_d = \frac{V Q}{I t_{fc}} = \frac{(1,406)(264.2)}{(79,565)(1.50)} = 3.11 \text{ ksi}$$

Only one-half of the effective flange area is used in computing the first moment of inertia, Q, used in this calculation since the shear stress in the flange is a maximum at the diaphragm and assumed to be zero at each edge of the effective flange (with a linear distribution assumed in-between).

The factored longitudinal stress in the tub girder bottom flange, f_{bu} , resulting from major-axis bending was computed previously as -41.60 ksi. Also, R_h is equal to 1.0, and R_b was computed in previous computations and is equal to 0.995.

Checking compliance with Eq. C6.11.8.1.1-1:

$$\sqrt{(-41.60)^2 - (-41.60)(0) + (0)^2 + 3(3.11 + 1.07)^2} = 42.23 \text{ ksi}$$

$$42.23 \text{ ksi} \leq \phi_f R_b R_h F_{yc} = (1.0)(0.995)(1.0)(50) = 49.75 \text{ ksi} \quad \text{OK} \quad (\text{Ratio} = 0.849)$$

7.10.3.1 Cross-section Distortion Stresses

In accordance with Article 6.11.1.1, transverse bending stress due to cross-section distortion are to be considered at the strength limit state. The transverse bending stresses due to factored loads are not to exceed 20.0 ksi at the strength limit state. Longitudinal warping stresses due to cross-section distortion may be ignored at the strength limit state.

As shown previously in the fatigue computations for Section G2-2, the transverse bending stress range at the top or bottom corners of the tub section may be determined as:

$$\sigma_t = C_t F_d \beta \frac{1}{2a} T \quad \text{DGBGB Eq. (A8)}$$

The same values computed under the fatigue computations may be used at the strength limit state, thus C_t is equal to 0.12, F_d is equal to 208 in.⁻¹, β is equal to 0.00327 in.⁻¹, and a is equal to 120 in. T represents the total factored concentrated torque, and is computed as follows:

For Strength I:

$$T = 1.25(3) + 1.25(192) + 1.50(255) + 1.75(980) = 2,341 \text{ kip - ft}$$

Therefore, the factored transverse bending stress due to cross-section distortion is computed as:

$$\sigma_t = (0.12)(208)(0.00327) \frac{1}{2(120)} (2,341(12)) = 9.55 \text{ ksi} < 20.0 \text{ ksi} \quad \text{OK (Ratio} = 0.478)$$

7.10.4 Shear (Article 6.11.6.3)

Article 6.11.6.3 invokes the provision of Article 6.11.9 to determine the shear resistance at the strength limit state. Article 6.11.9 further directs the Engineer to the provision of Article 6.10.9 for determining the factored shear resistance of a single web. For the case of inclined webs, D , is to be taken as the depth of the web measured along the slope. The factored shear load in the inclined web is to be taken as:

$$V_{ui} = \frac{V_u}{\cos(\theta)} \quad \text{Eq. (6.11.9-1)}$$

where, V_u is the factored shear on one inclined web, and θ is the angle of inclination of the web plate. For tub sections, especially those in horizontally curved bridges, St. Venant torsional shear must be considered in the design of the webs. The total shear in one web is greater than the shear in the other web at the same section since the torsional shear is of opposite sign in the two webs. The critical shear should be the maximum combination of factored shear due to

major-axis bending and the St. Venant torsional shear. For practicality, both webs are designed for the critical shear.

At the strength limit state, webs must satisfy the following:

$$V_u \leq \phi_v V_n \quad \text{Eq. (6.10.9.1-1)}$$

where:

- ϕ_v = resistance factor for shear = 1.0 (Article 6.5.4.2)
- V_n = nominal shear resistance determined as specified in Articles 6.10.9.2 and 6.10.9.3 for unstiffened and stiffened webs, respectively (kip)
- $V_u = V_{ui}$ = shear in a single web at the section under consideration due to factored loads (kip)

The unfactored shears at Section G2-2 obtained from the analysis are shown below (see Table 2). The unfactored shears are vertical shears and are the summation of the shears due to major-axis bending and St. Venant torsion in the critical web. The live load moment includes the centrifugal force and dynamic load allowance effects. The positive shears are used in the calculations that follow as the total of the positive shears governs over the absolute total of the negative shears.

Noncomposite Dead Load:	V_{DC1}	= 232 kip
Composite Dead Load:	V_{DC2}	= 44 kip
Future Wearing Surface Dead Load:	V_{DW}	= 58 kip
Live Load (incl. IM and CF):	V_{LL+IM}	= 160 kip

The η factor is again taken equal to 1.0 in this example at the strength limit state. The total factored shear at the interior pier in the inclined web is:

$$V_{ui} = \frac{1.0[1.25(232 + 44) + 1.5(58) + 1.75(160)]}{\cos(14.036^\circ)} = 734 \text{ kips}$$

7.10.4.1 Interior Panel (Article 6.10.9.3.2)

Article 6.10.9.1 stipulates that the transverse stiffener spacing for interior panels without a longitudinal stiffener is not to exceed $3D = 3(80.40) = 241.2$ inches. For the first panel on each side of the interior support, a transverse stiffener spacing of 62 inches is assumed for this design example, satisfying the 3D requirement.

For interior panels of girders with the section along the entire panel proportioned such that:

$$\frac{2Dt_w}{(b_{fc} t_{fc} + b_{ft} t_{ft})} \leq 2.5 \quad \text{Eq. (6.10.9.3.2-1)}$$

the nominal shear resistance is to be taken as the sum of the shear-buckling resistance and the post-buckling resistance due to tension-field action, which is to be computed according to:

$$V_n = V_p \left[C + \frac{0.87(1-C)}{\sqrt{1 + \left(\frac{d_o}{D}\right)^2}} \right] \quad \text{Eq. (6.10.9.3.2-2)}$$

in which:

$$V_p = 0.58F_{yw} D t_w \quad \text{Eq. (6.10.9.3.2-3)}$$

where:

- d_o = transverse stiffener spacing (in.)
- V_n = nominal shear resistance of the web panel (kip)
- V_p = plastic shear force (kip)
- C = ratio of the shear-buckling resistance to the shear yield strength.

According to Article 6.11.9, for box flanges, b_{fc} (in this case) is to be taken as one-half the effective flange width between webs in checking Eq. 6.10.9.3.2-1, but not to exceed 18 times the thickness of the box flange. Therefore, $(81.0/2) = 40.5$ in. $> 18(1.50) = 27.0$ in. Use $b_{fc} = 27.0$ in. to check Eq. 6.10.9.3.2-1. For the interior web panel under consideration, check Eq. 6.10.9.3.2-1 as follows:

$$\frac{2(80.40)(0.5625)}{((27.0)(1.50) + (18)(3.00))} = 0.96 < 2.5$$

Therefore, Eq. (6.10.9.3.2-2) is applicable. First, compute the shear-buckling coefficient, k :

$$k = 5 + \frac{5}{\left(\frac{d_o}{D}\right)^2} = 5 + \frac{5}{\left(\frac{62}{80.40}\right)^2} = 13.41 \quad \text{Eq. (6.10.9.3.2-7)}$$

Since:

$$\frac{D}{t_w} = \frac{80.4}{0.5625} = 142.9 > 1.40 \sqrt{\frac{Ek}{F_{yw}}} = 1.40 \sqrt{\frac{29,000(13.41)}{50}} = 123.5$$

$$C = \frac{1.57}{\left(\frac{D}{t_w}\right)^2} \left(\frac{Ek}{F_{yw}} \right) \quad \text{Eq. (6.10.9.3.2-6)}$$

$$C = \frac{1.57}{(142.9)^2} \left(\frac{29,000(13.41)}{50} \right) = 0.598$$

V_p is the plastic shear force and is calculated as follows:

$$V_p = 0.58 F_{yw} D t_w \quad \text{Eq. (6.10.9.3.3-2)}$$

$$V_p = 0.58 (50.0)(80.40)(0.5625) = 1,312 \text{ kips}$$

Therefore,

$$V_n = (1,312) \left[0.598 + \frac{0.87(1 - 0.598)}{\sqrt{1 + \left(\frac{62.0}{80.40}\right)^2}} \right] = 1,148 \text{ kips}$$

Checking compliance with Eq. (6.10.9.1-1):

$$V_u = 734 \text{ kips} < \phi_v V_n = (1.0)(1,148) = 1,148 \text{ kips} \quad \text{OK} \quad (\text{Ratio} = 0.639)$$

7.11 Bottom Flange Longitudinal Stiffener

A single longitudinal flange stiffener is used on the bottom flange of the tub girders in the negative moment regions. The longitudinal stiffeners are terminated at the bolted field splices at each end of field sections 2 and 4. By terminating the longitudinal stiffener at the bolted field splices, it is not necessary to consider fatigue at the terminus of the stiffener. The bottom flange splice plates inside the tub girder must be designed and fabricated to permit the longitudinal stiffener to extend to the free edge of the flange, where the longitudinal stress is zero.

A single WT 8x28.5 is utilized for the longitudinal stiffener with the stem welded to the bottom flange, and it is placed at the centerline of the bottom flange. As specified in Article 6.11.11.2, longitudinal compression flange stiffeners on tub girder bottom flanges (box flanges) are to be equally spaced across the width of the flange. Furthermore, the yield strength of the longitudinal stiffener must not be less than the yield strength of the flanges to which they are attached.

The projecting width, b_1 , of the longitudinal flange stiffener must satisfy Eq. (6.11.11.2-1):

$$b_{\ell} \leq 0.48 t_s \sqrt{\frac{E}{F_{yc}}} \quad \text{Eq. (6.11.11.2-1)}$$

where:

t_s = thickness of the projecting longitudinal stiffener element (in.)

In the case of a structural tee, t_s is taken as the flange thickness of the structural tee since each half-flange would buckle similarly to a single plate connected to the web. Furthermore, the projecting width, b_1 , of structural tees is to be taken as one-half the width of the tee flange. Therefore,

$$b_1 \leq 0.48 (0.715) \sqrt{\frac{29,000}{50}} = 8.27 \text{ in.}$$

$$b_1 = \frac{7.12}{2} = 3.56 \text{ in.} < 8.27 \text{ in.} \quad \text{WT 8x28.5 flange is OK}$$

The moment of inertia, I_{ℓ} , of each stiffener about an axis parallel to the flange and taken at the base of the stiffener must satisfy:

$$I_{\ell} \geq \psi w t_{fc}^3 \quad \text{Eq. (6.11.11.2-2)}$$

where:

$$\psi = 0.125k^3 \text{ for } n = 1$$

$$= 1.120k^3 \text{ for } n = 2$$

k = plate buckling coefficient for uniform stress, $1.0 \leq k \leq 4.0$

n = number of equally spaced longitudinal flange stiffeners

w = larger of the width of the flange between longitudinal flange stiffeners or the distance from a web to the nearest longitudinal flange stiffener (in.)

t_{fc} = thickness of the tub girder compression flange (in.)

Calculate the moment of inertia of the stiffener, I_{ℓ} , about the base of the stiffener:

$$I_{\ell} = I_o + Ad^2 = 48.7 + (8.39)(8.22 - 1.94)^2 = 379.6 \text{ in}^4$$

As specified in Article C6.11.11.2, the actual longitudinal flange stiffener moment of inertia, I_s , used in determining the plate-buckling coefficient for uniform normal stress, k , from either Eq. 6.11.8.2.3-1 or Eq. 6.11.8.2.3-2, as applicable, automatically satisfies Eq. 6.11.11.2-2. Alternatively, for preliminary sizing of the stiffener for example, a value of k can be assumed in lieu of Eq. 6.11.8.2.3-1 or Eq. 6.11.8.2.3-2, but a range of 2.0 to 4.0 should generally apply. For completeness, check Eq. 6.11.11.2-2, where k was previously calculated as 2.81:

$$379.6 \text{ in.}^4 \geq 0.125(2.81)^3 \left(\frac{81}{2} \right) (1.5)^3 = 379.1 \text{ in.}^4 \quad \text{OK}$$

Since Eq. 6.11.11.2-1 and Eq. 6.11.11.2-2 are satisfied, the WT 8x25 is acceptable for the bottom flange longitudinal stiffener.

7.12 Internal Pier Diaphragm Design

Article 6.11.1 directs the designer to the provision of Article 6.7.4 for general design considerations for internal and external cross-frames and diaphragms. The internal diaphragms are subject to major-axis bending over the bearing sole plates in addition to shear. Article C6.11.8.1.1 requires that the principal stresses in the internal support diaphragm at the strength limit state not exceed the compressive resistance given by Eq. C6.11.8.1.1-1, which is a yield criterion for combined stress. In this example, each tub girder is supported by two bearings, therefore, as specified in Article C6.11.8.1.1, the major-axis bending stress in the internal diaphragms, f_{by} , is typically small and can be neglected.

Example calculations are demonstrated for the Girder G2 internal diaphragms at the Pier 1 supports (Girder Section G2-2). A 1.0 inch thick Grade 50 steel plate is assumed for the internal diaphragm web at this location. Figure 17 shows a sketch of the internal diaphragm. For simplicity, the access hole in the web for inspection purposes is not considered in this example.

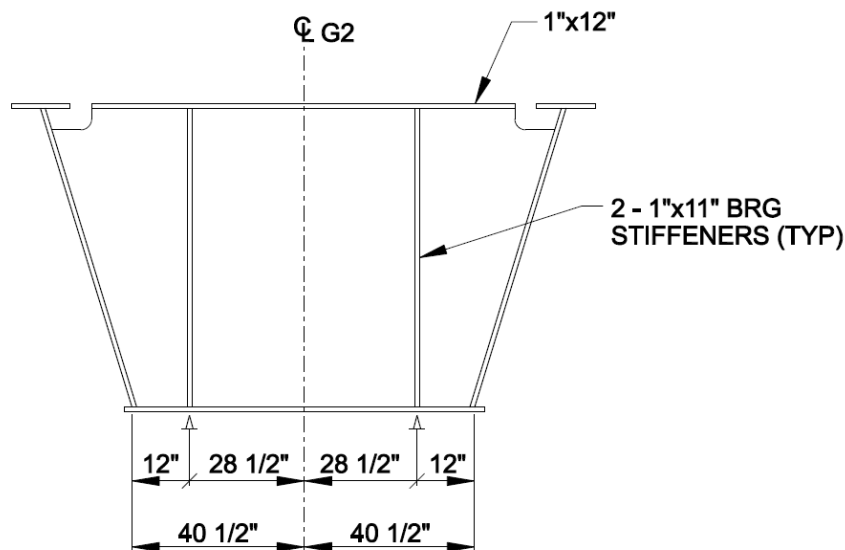


Figure 17 Sketch of the Internal Diaphragm and Bearing Locations

First, summarize the maximum vertical shears and torsional moments acting on the internal diaphragm. The unfactored shears are taken from Table 2, and most of the unfactored torques are taken from Table 6.

The maximum unfactored vertical shears acting on the internal diaphragm, using the critical tub girder web are shown below. The unfactored vertical shears are due to the combined effects of

bending and St. Venant torsion in the critical tub girder web. Therefore, it is necessary to separate out the shears due to bending and St. Venant torsion in computations that follow later in this section.

The maximum unfactored vertical shears in the critical tub girder web, due to tub girder flexure and St. Venant torsion, are:

Steel Dead Load:	$V_{DC1-STEEL} = 47 + -46 = 93$ kips
Concrete Deck Dead Load:	$V_{DC1-CONC} = 185 + -185 = 370$ kips
Composite Dead Load:	$V_{DC2} = 44 + -41 = 85$ kips
Future Wearing Surface Dead Load:	$V_{DW} = 58 + -55 = 113$ kips
Live Load (incl. IM and CF):	$V_{LL+IM} = 160 + -155 = 315$ kips

The maximum unfactored torques acting on the internal diaphragm, are:

Steel Dead Load:	$T_{DC1-STEEL} = -22 + 36 = 58$ kip-ft
Concrete Dead Load:	$T_{DC1-CONC} = 48 + -33 = 81$ kip-ft
Composite Dead Load:	$T_{DC2} = -149 + 192 = 341$ kip-ft
Future Wearing Surface Dead Load:	$T_{DW} = -197 + 255 = 452$ kip-ft
Live Load (incl. IM and CF):	$T_{LL+IM} = 980 + -425 = 1405$ kip-ft

For computing the Live Load torque above, assumed concurrent torques are used that produce the largest torsional reaction at the support, thus the largest torque acting on the internal diaphragm.

Compute the maximum factored shear stress in the diaphragm web. The vertical shear acting on the critical tub girder web is equal to the maximum shear in the internal diaphragm. First, it is necessary to separate out the shears due to tub girder flexure (bending), V_b , and the shears due to St. Venant torsion, V_T , as the maximum unfactored vertical shears above include the web shear due to torsion.

7.12.1 Web Shear Check

The calculations in this section check the combined principal stresses in the internal diaphragm web and the shear in the internal diaphragm web. To perform these checks it is necessary to separately consider the shear in the internal diaphragm for tub girder flexure (bending) and the shear due to torsion.

7.12.1.1 Noncomposite Shear Force

The sum of the total noncomposite Strength I factored shears is:

$$V_{DC1} = 1.25 (93 + 370) = 579 \text{ kips}$$

To compute the shear due to torsion, it is necessary to compute the shear flow in the noncomposite tub girder section. The enclosed area of the noncomposite tub section, A_{o_NC} , was computed previously as 8,065 in². The factored shear flow in the noncomposite section is computed as:

$$f_v = \frac{T}{2 A_o} \quad \text{Eq. (C6.11.1.1-1)}$$

where:

T = internal torque due to factored loads (kip-in.)
 A_o = enclosed area within the box section (in.³)

$$f_v = \frac{T}{2 A_o} = \frac{1.25(58 + 81)(12)}{2(8,065)} = 0.129 \text{ kip/in}$$

Note that the internal factored noncomposite dead load torque is equal to 173.8 kip-ft.

To obtain the factored noncomposite dead load St. Venant torsional shear, V_T , multiply the factored shear flow by the depth of the tub girder web along the incline:

$$V_T = 0.129 (80.40) = 10.37 \text{ kips}$$

The vertical component of V_T is computed as:

$$(V_T)_{\text{vert}} = 10.37 \left(\frac{78.0}{80.40} \right) = 10.06 \text{ kips}$$

The factored vertical shear in the diaphragm web due to tub girder flexure alone and noncomposite dead loads is then computed by subtracting the vertical component of the factored noncomposite dead load St. Venant torsional shear from the total noncomposite dead load shear:

$$V_b = 579 - 10.06 = 569 \text{ kips}$$

Figure 18 provides an illustration of the above calculation.

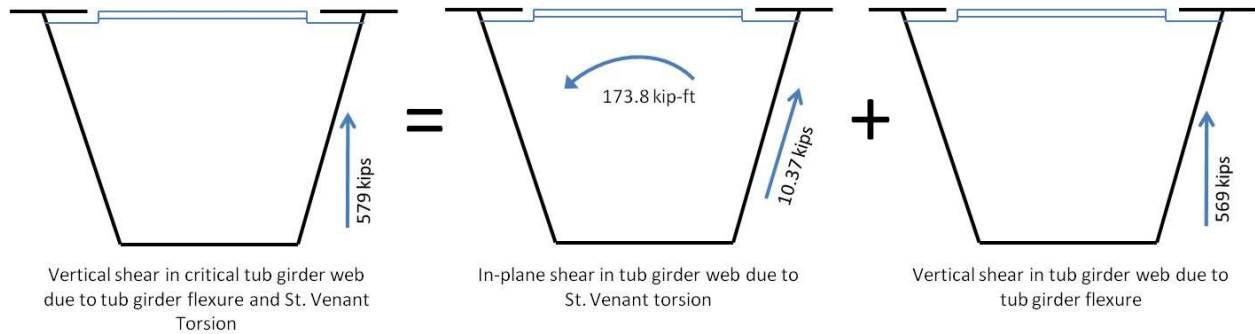


Figure 18 Illustration for the computation of the shear in the internal diaphragms due to St. Venant torsion and tub girder flexure

7.12.1.2 Composite Shear Force

The sum of the total composite Strength I factored shear is:

$$V_{DC2+DW+(LL+I)} = 1.25 (85) + 1.5 (113) + 1.75 (315) = 827 \text{ kips}$$

The enclosed area of the composite tub section, $A_{o,C}$, was computed previously as 8,794 in². The factored shear flow in the composite section is computed as:

$$f_v = \frac{T}{2 A_o} = \frac{[1.25(341) + 1.5(452) + 1.75(1,405)](12)}{2(8,794)} = 2.43 \text{ kip/in}$$

To obtain the factored composite St. Venant torsional shear, V_T , multiply the factored shear flow by the depth of the web along the incline:

$$V_T = 2.43 (80.40) = 195.4 \text{ kips}$$

The vertical component of V_T is computed as:

$$(V_T)_{\text{vert}} = 195.4 \left(\frac{78.0}{80.40} \right) = 190 \text{ kips}$$

The factored vertical shear in the diaphragm web due to tub girder flexure alone and composite loads is then computed by subtracting the vertical component of the factored composite St. Venant torsional shear from the total factored composite shear:

$$V_b = 827 - 190 = 637 \text{ kips}$$

7.12.1.3 Total Factored Shear Force

The total factored shear stress in the diaphragm web due to torsion is calculated by dividing the shear flows by the thickness of the web:

$$(f_v)_T = \frac{0.129}{1.0 \text{ in.}} + \frac{2.43}{1.0 \text{ in.}} = 2.56 \text{ ksi}$$

The average Strength I factored shear stress in the diaphragm web due to tub girder flexure (bending) is calculated by dividing the total factored shear by the area of the web:

$$(f_v)_b = \frac{569 + 637}{78(1.0)} = 15.46 \text{ ksi}$$

7.12.1.4 Check of Internal Diaphragm Web

As discussed previously, for a tub girder supported on two bearings, the bending stresses in the plane of the internal diaphragm due to vertical bending of the diaphragm over the bearing sole plates are relatively small and will be neglected in this example for simplicity. For a tub girder supported on a single bearing, the effects of the bending stresses in the plane of the diaphragm are likely to be more significant and should be considered. As specified in Article C6.11.8.1.1, a width of the bottom (box) flange equal to 6 times the thickness may be considered effective with the diaphragm in resisting in-plane bending.

Therefore, for this example, since bending in the plane of the diaphragm is ignored, the maximum principal stress is simply equal to the total factored shear stress:

$$f_v = (f_v)_T + (f_v)_b = 2.56 + 15.46 = 18.02 \text{ ksi}$$

The combined principal stresses in the diaphragm due to factored loads are checked using the general form of the Huber-von Mises-Hencky yield criterion, which is similar to Eq. C6.11.8.1.1-1. The general form of the Huber-von Mises-Hencky yield criterion is:

$$\sqrt{\sigma_1^2 - \sigma_1\sigma_2 + \sigma_2^2} \leq F_y$$

where σ_1 and σ_2 are the maximum and minimum principal stresses in the diaphragm web, and:

$$\sigma_1, \sigma_2 = \left(\frac{\sigma_y + \sigma_z}{2} \right) \pm \sqrt{\left(\frac{\sigma_y - \sigma_z}{2} \right)^2 + f_v^2}$$

There is a major-axis bending moment that must be carried by the internal diaphragm, resulting from the fact that the web is cantilevered out from the bearing (see Figure 17). Assuming that the vertical shear force acts at the mid-depth of the web, the internal diaphragm moment at the centerline of the bearing is computed as:

$$M_{ID} = (569 \text{ kips} + 637 \text{ kips}) (12.0 \text{ in.} + 9.75 \text{ in.}) = 26,231 \text{ kip-in.}$$

It was stated earlier in these calculations that the moment of inertia of the effective internal diaphragm is 79,565 in.⁴, and the neutral axis is located 39.89 in. above the bottom of the bottom

flange. The bottom flange thickness is equal to the bottom flange thickness of the tub girder, which is 1.50 inches. Therefore, the major-axis bending stress, σ_y in the internal diaphragm web is computed as:

$$\sigma_y = \frac{M_{IDc}}{I} = \frac{(26,231)(39.89 - 1.50)}{79,565} = 12.66 \text{ ksi}$$

σ_z is equal to zero because there are no loads applied that cause stress in vertical direction in the internal diaphragm web.

Therefore, the principal stresses are computed as:

$$\sigma_{1,2} = \left(\frac{12.66 + 0}{2} \right) \pm \sqrt{\left(\frac{12.66 - 0}{2} \right)^2 + 18.02^2} = \pm 25.43 \text{ ksi}$$

Check the combined principal stress using the Huber-von Mises-Hencky yield criterion:

$$\sqrt{25.43^2 - (25.43)(-25.43) + (-25.43)^2} = 44.05 \text{ ksi} < F_y = 50.0 \text{ ksi} \quad \text{OK (Ratio= 0.881)}$$

Next, check the shear resistance of the internal diaphragm and compare the computed resistance to the factored diaphragm shear force. Compute the shear resistance according to Article 6.11.9 which specifies the use of the provision of Article 6.10.9 for I-girders. Calculations not shown here indicate that $C = 1.0$.

$$V_u \leq \phi_v V_n \quad \text{Eq. (6.10.9.1-1)}$$

$$V_n = V_{cr} = CV_p \quad \text{Eq. (6.10.9.2-1)}$$

$$V_p = 0.58F_{yw} Dt_w = 0.58(50.0)(78)(1.0) = 2,262 \text{ kips} \quad \text{Eq. (6.10.9.2-2)}$$

$$V_n = (1.0)(2,262) = 2,262 \text{ kips}$$

Check Eq. 6.10.9.1-1:

$$V_u = 569 + 639 = 1,208 \text{ kips} < \phi_v V_n = (1.0)(2,262) = 2,262 \text{ kips} \quad \text{OK (Ratio 0.534)}$$

7.12.2 Bearing Stiffeners

Bearing stiffeners are placed on each side of the web of the internal diaphragm at each bearing location. The design of the Girder G2 bearing stiffeners at Pier 1 (Section G2-2) is illustrated in this section. It is assumed that the bearings at Pier 1 are fixed, thus there is no expansion causing eccentric loading on the bearing stiffeners that are attached to the internal diaphragm. According

to Article 6.11.11.1, bearing stiffeners attached to the internal diaphragms are to be designed using the provisions of Article 6.10.11.2.4b applied to the diaphragm rather than the girder web.

Bearing stiffeners must extend the full depth of the web and as closely as practical to the outer edges of the flanges. Each stiffener must be either milled to bear against the flange through which it receives its load or attached to that flange by a full penetration groove weld. Typical practice is for the bearing stiffeners to be milled to bear plus fillet welded to the appropriate flange. Full penetration groove welds are costly and often result in welding deformation of the flange.

The unfactored reactions are as shown below for the left and right bearings at Pier 1, Girder G2. These results are taken directly from the three-dimensional analysis.

Left Bearing:

Steel Dead Load:	$R_{DC1-STEEL} = 79$ kips
Concrete Deck Dead Load:	$R_{DC1-CONC} = 238$ kips
Composite Dead Load:	$R_{DC2} = 85$ kips
Future Wearing Surface Dead Load:	$R_{DW} = 113$ kips
Live Load (incl. IM and CF):	$R_{LL+IM} = 294$ kips

Right Bearing:

Steel Dead Load:	$R_{DC1-STEEL} = 93$ kips
Concrete Deck Dead Load:	$R_{DC1-CONC} = 370$ kips
Composite Dead Load:	$R_{DC2} = 11$ kips
Future Wearing Surface Dead Load:	$R_{DW} = 15$ kips
Live Load (incl. IM and CF):	$R_{LL+IM} = 287$ kips

The maximum Strength I factored reactions for each bearing are computed as:

$$R_{LEFT} = 1.25 (79 + 238 + 85) + 1.5 (113) + 1.75 (294) = 1,187 \text{ kips}$$

$$R_{RIGHT} = 1.25 (93 + 370 + 11) + 1.5 (15) + 1.75 (287) = 1,117 \text{ kips}$$

The factored reaction at the left bearing is larger, and therefore controls. The bearing stiffeners are assumed to have a yield stress of 50 ksi, and are 1 in. by 11 in. plates. As shown in Figure 17, there is one bearing stiffener on each side of the internal diaphragm web, and therefore two at each bearing location.

The width, b_t , of the projecting stiffener element must satisfy:

$$b_t \leq 0.48 t_p \sqrt{\frac{E}{F_{ys}}} \quad \text{Eq. (6.10.11.2.2-1)}$$

$$b_t = 11.0 \text{ in.} \leq 0.48 t_p \sqrt{\frac{E}{F_{ys}}} = 0.48 (1.0) \sqrt{\frac{29,000}{50}} = 11.6 \text{ in.} \quad \text{OK}$$

7.12.2.1 Bearing Resistance

According to Article 6.10.11.2.3, the factored bearing resistance for the fitted ends of bearing stiffeners is taken as:

$$(R_{sb})_r = \phi_b (R_{sb})_n \quad \text{Eq. (6.10.11.2.3-1)}$$

where:

$$\begin{aligned} \phi_b &= \text{resistance factor for bearing specified in Article 6.5.4.2 } (\phi_b = 1.0) \\ (R_{sb})_n &= \text{nominal bearing resistance for fitted ends of bearing stiffeners (kip)} \end{aligned}$$

and:

$$(R_{sb})_n = 1.4A_{pn}F_{ys} \quad \text{Eq. (6.10.11.2.3-2)}$$

where:

$$\begin{aligned} A_{pn} &= \text{area of the projecting elements of the stiffener outside of the web-to-flange fillet} \\ &\quad \text{welds but not beyond the edge of the flange (in.}^2\text{)} \\ F_{ys} &= \text{specified minimum yield strength of the stiffener (ksi)} \end{aligned}$$

Assuming a 1 inch stiffener clip, compute A_{pn} as follows:

$$A_{pn} = 2(11-1)(1.00) = 20.0 \text{ in}^2$$

The nominal bearing resistance of the stiffeners at a single bearing is computed as:

$$(R_{sb})_n = 1.4(20.0)(50) = 1,400 \text{ kips}$$

The factored bearing resistance of the stiffeners at a single bearing is computed as:

$$(R_{sb})_r = 1.0(1,400) = 1,400 \text{ kips} > R_u = 1,187 \text{ kips} \quad \text{OK}$$

7.12.2.2 Axial Resistance

Determine the axial resistance of the bearing stiffener according to Article 6.10.11.2.4. This article directs the Engineer to Article 6.9.2.1 for calculation of the factored axial resistance, P_r . The yield strength is F_{ys} , the radius of gyration is computed about the midthickness of the web, and the effective length is 0.75 times the web depth ($K\ell = 0.75D$).

$$P_r = \phi_c P_n \quad \text{Eq. (6.9.2.1-1)}$$

where: P_n = nominal compressive resistance determined using the provisions of Article 6.9.4 (kip)

ϕ_c = resistance factor for compression as specified in Article 6.5.4.2 ($\phi_c = 0.95$)

As indicated in Article 6.9.4.1.1, P_n is the smallest value of the applicable modes of buckling, and in the case of bearing stiffeners, torsional buckling and flexural-torsional buckling are not applicable. Therefore, P_n is computed for flexural buckling only.

To compute P_n , first compute P_e and P_o . P_e is the elastic critical buckling resistance determined as specified in Article 6.9.4.1.2 for flexural buckling. P_o is the equivalent nominal yield resistance equal to QF_yA_g , where Q is the slender element reduction factor taken equal to 1.0 for bearing stiffeners in accordance with Article 6.9.4.1.1:

$$P_e = \frac{\pi^2 E}{\left(\frac{K\ell}{r_s}\right)^2} A_g \quad \text{Eq. (6.9.4.1.2-1)}$$

In accordance with Article 6.10.11.2.4, the effective length, $K\ell$, is to be taken as 0.75D:

$$K\ell = 0.75D = 0.75(80.40) = 60.3 \text{ in.}$$

Compute the radius of gyration about the midthickness of the web.

$$r_s = \sqrt{\frac{I_s}{A_s}}$$

According to the provisions of Article 6.10.11.2.4b, for stiffeners welded to the web, a portion of the web is to be included as part of the effective column section. For stiffeners consisting of two plates welded to the web, the effective column section is to consist of the two stiffener elements, plus a centrally located strip of web extending $9t_w$ on each side of the outer projecting elements of the group. The area of the web that is part of the effective section is computed as follows:

$$A_w = 2(9)(1.0)(1.0) = 18.0 \text{ in.}^2$$

The total area of the effective section is therefore:

$$A_s = 18.0 + 2(1.00)(11.00) = 40.0 \text{ in.}^2$$

Next, compute the moment of inertia of the effective section about the centerline of the diaphragm of the web, conservatively using the stiffeners only:

$$I = 2 \left[\frac{1}{12} (1.0)(11.0)^3 + 11.0 \left(\frac{11.0}{2} + \frac{1.0}{2} \right)^2 \right] = 1,014 \text{ in.}^4$$

Compute the radius of gyration:

$$r_s = \sqrt{\frac{1,014}{40.0}} = 5.03 \text{ in.}$$

The elastic critical buckling resistance is computed as follows:

$$P_e = \frac{\pi^2(29,000)}{\left(\frac{60.3}{5.03}\right)^2}(40.0) = 79,663 \text{ kips}$$

The equivalent nominal yield resistance is computed as follows, with A_s used for A_g :

$$P_o = QF_y A_g = (1.0)(50)(40.0) = 2,000 \text{ kips}$$

Since

$$\frac{P_e}{P_o} = \frac{79,663}{2,000} = 39.8 > 0.44,$$

the nominal compressive resistance is computed as:

$$P_n = \left[0.658 \left(\frac{P_o}{P_e} \right) \right] P_o \quad \text{Eq. (6.9.4.1.1-1)}$$

$$P_n = \left[0.658 \left(\frac{1}{39.8} \right) \right] (2,000) = 1,979 \text{ kips}$$

The factored compressive resistance of the bearing stiffeners is computed as follows:

$$P_r = \phi_c P_n = 0.95(1,979) = 1,880 \text{ kips}$$

$$P_u = 1,187 \text{ kips} < P_r = 1,880 \text{ kips} \quad \text{OK} \quad (\text{Ratio} = 0.631)$$

The 1.0 in. by 11.0 in. bearing stiffeners selected satisfy the requirements for design.

7.13 Top Flange Lateral Bracing Design

Top flanges of tub girders should be braced so that the section acts as a pseudo-box for noncomposite loads applied before the concrete deck hardens or is made composite. Herein, calculations demonstrate the design of the top flange single diagonal bracing member in Span 1 of Girder G2 in the first bay adjacent to the abutment for constructibility. However, top flange bracing must also be designed to satisfy the strength limit state for the final condition as well as for constructibility. In many cases, the factored forces during construction will govern over the factored forces in the final condition.

Article 6.11.1 specifies that the top lateral bracing for tub girders must satisfy the provisions of Article 6.7.5. The bracing is designed according to the provision of Articles 6.8 and 6.9 for tension and compression, respectively. Wind lateral loading and the lateral force caused by deck overhang brackets are neglected in this design example.

The unfactored axial forces in the diagonal bracing member in the first bay of Span 1 of Girder G2 are obtained from the three-dimensional analysis and are as follows:

Steel Dead Load:	$P_{STEEL} = -13 \text{ kip}$
Deck Cast #1 Dead Load:	$P_{CONC} = -100 \text{ kip}$

In accordance with Article 3.4.2.1, when investigating Strength I, III, and V during construction, load factors for the weight of the structure and appurtenances, DC and DW, are not to be taken to be less than 1.25. Therefore, the factored axial load is computed as:

$$P_u = P_{axial} = 1.25 [-13 + (-100)] = -141 \text{ kips (C)}$$

Compute the unbraced length of the top flange lateral bracing member, L_b :

Tub width at the top flanges = 120 in.

Top flange width = 16 in.

Clear distance between top flanges = $120 - 16 = 104$ in.

Spacing of top flange lateral bracing = $16.3 \text{ ft} = 196$ in.

$$L_b = \sqrt{104^2 + 196^2} = 222 \text{ in.}$$

A structural tee is used for the top flange lateral bracing, with the stem down and its flange bolted to the bottom of the top flanges, which is the preferable method of connection. A WT 9x48.5 is selected for the top flange lateral bracing. From the AISC Steel Construction Manual, the section properties for a WT 9x48.5 are:

$$\text{Area} = 14.2 \text{ in.}^2; y = 1.91 \text{ in.}; S_x = 12.7 \text{ in.}^3; r_x = 2.56 \text{ in.}; r_y = 2.65 \text{ in.}; J = 2.92 \text{ in.}^4$$

Check buckling about the x-axis as this is the governing condition. The eccentricity of the connection to the center of gravity of the structural tee causes a moment on the member. The moment due to eccentricity is computed as:

$$M_{ux} = P_{axial} y = (141)(1.91) = 269 \text{ kip-in.}$$

Since the structural tee is subjected to axial compression and flexure, it is necessary to check the combined effects of axial compression and flexure, in accordance with Article 6.9.2.2.

First, check the limiting slenderness ratio for secondary members in compression, as specified in Article 6.9.3. The effective length factor, K , as specified in Article 4.6.2.5, for bolted connections at both ends is 0.75.

$$\frac{K \ell}{r_x} = \frac{(0.75)(222)}{2.56} = 65.0 < 140 \quad \text{OK}$$

Determine if the stem of the WT 9x48.5 is a nonslender member element in accordance with Article 6.9.4.2.1:

$$\frac{b}{t} < k \sqrt{\frac{E}{F_y}} \quad \text{Eq. (6.9.4.2-1)}$$

where:

- k = plate buckling coefficient as specified in Table 6.9.4.2.1-1
- b = width of plate as specified in Table 6.9.4.2.1-1 (in.)
- t = plate thickness (in.)

The plate buckling coefficient is taken as 0.75 from Table 6.9.4.2-1 for stems of rolled tees. The width, b , is taken as the full depth of the tee section and thickness, t , is for that of the stem. Check Eq. 6.9.4.2-1:

$$\frac{b}{t} = \frac{9.30}{0.535} = 17.4 < k \sqrt{\frac{E}{F_y}} = 0.75 \sqrt{\frac{29,000}{50}} = 18.1$$

Since Eq. 6.9.4.2-1 is satisfied, the slender element reduction factor, Q , specified in Article 6.9.4.1.1 is taken as 1.0. (Note: similar calculations, not shown, indicate that the flange of the tee section is also a nonslender element.)

Compute the compressive resistance in accordance with Article 6.9.2.1, where the factored compressive resistance, P_r , is taken as:

$$P_r = \phi_c P_n \quad \text{Eq. (6.9.2.1-1)}$$

where:

- ϕ_c = resistance factor for compression as specified in Article 6.5.4.2 ($\phi_c = 0.95$)
- P_n = nominal compressive resistance as specified in Article 6.9.4 or 6.9.5, as applicable (kip)

Compute the nominal compressive resistance, P_n , in accordance with Article 6.9.4.1.1. In order to determine which equation to use to compute the nominal compressive resistance, it is necessary to compute the elastic critical buckling resistance, P_e , and the equivalent nominal yield resistance, P_o .

The elastic critical buckling resistance, P_e , is specified in Article 6.9.4.1.2 for flexural buckling, and specified in Article 6.9.4.1.3 for flexural-torsional buckling. In accordance with Table 6.9.4.1.1-1, flexural buckling and flexural-torsional buckling must be considered to determine the compressive resistance of structural tees. Separate calculations, not provided here, show that flexural buckling governs in this particular case.. The computation of P_e for the flexural buckling resistance is illustrated herein.

Compute the elastic critical buckling resistance, P_e , based on flexural buckling in accordance with Article 6.9.4.1.2:

$$P_e = \frac{\pi^2 E}{\left(\frac{K \ell}{r_s}\right)^2} A_g \quad \text{Eq. (6.9.4.1.2-1)}$$

where:

- A_g = gross cross-sectional area of the member (in.²)
- K = effective length factor in the plane of buckling determined as specified in Article 4.6.2.5
- ℓ = unbraced length in the plane of buckling (in.)
- r_s = radius of gyration about the axis normal to the plane of buckling (in.)

The elastic critical buckling resistance is then computed as:

$$P_e = \frac{\pi^2 (29,000)}{(65.0)^2} (14.2) = 962 \text{ kips}$$

The equivalent nominal yield resistance, P_o , is computed in accordance with Article 6.9.4.1.1 as follows:

$$P_o = Q F_y A_g$$

where:

- Q = slender element reduction factor determined as specified in Article 6.9.4.2.

As stated previously, since Eq. 6.9.4.2-1 is satisfied for both the stem and flange of the tee section, Q can be taken as 1.0. Therefore, the nominal yield resistance, P_o , is computed as:

$$P_o = (1.0)(50)(14.2) = 710 \text{ kips}$$

As specified in Article 6.9.4.1.1, check the result of P_e / P_o :

$$\frac{P_e}{P_o} = \frac{962}{710} = 1.35$$

Since P_e / P_o is greater than 0.44, the nominal compressive resistance, P_n , is computed in accordance with Eq. 6.9.4.1.1-1.

$$P_n = \left[0.658^{\left(\frac{P_o}{P_e}\right)} \right] P_o \quad \text{Eq. (6.9.4.1.1-1)}$$

$$P_n = \left[0.658^{\left(\frac{710}{962}\right)} \right] (710) = 521 \text{ kips}$$

Compute the factored compressive resistance, P_r , in accordance with Article 6.9.2.1:

$$P_r = \phi_c P_n = (0.95)(521) = 495 \text{ kips} \quad \text{Eq. (6.9.2.1-1)}$$

Determine the factored flexural resistance about the x-axis using the provisions of Article 6.12.1.2 for miscellaneous flexural members, and specifically Article 6.12.2.2.4 for structural tees.

The factored flexural resistance, M_r , is to be taken as:

$$M_r = \phi_f M_n \quad \text{Eq. (6.12.1.2.1-1)}$$

where:

$$\begin{aligned} \phi_f &= \text{resistance factor for flexure as specified in Article 6.5.4.2 } (\phi_f = 1.0) \\ M_n &= \text{nominal flexural resistance specified in Articles 6.12.2.2 or 6.12.2.3, as applicable} \\ &\quad \text{(kip-in.)} \end{aligned}$$

In accordance with Article 6.12.2.2.4, the nominal flexural resistance is to be taken as the smallest value based on yielding, lateral torsional buckling, or local buckling of the elements, as applicable.

For yielding, the nominal flexural resistance is given as:

$$M_n = M_p = F_y Z_x \quad \text{Eq. (6.12.2.2.4-1)}$$

where:

$$\begin{aligned} M_p &= \text{plastic moment (kip-in.)} \\ F_y &= \text{specified minimum yield strength (ksi)} \\ Z_x &= \text{plastic section modulus about the x-axis (in.³)} \end{aligned}$$

Also as specified in Article 6.12.2.2.4, M_n in Eq. 6.12.2.2.4-1 is limited to $1.6M_y$ for stems in tension, and M_y for stems in compression, where M_y is the yield moment based on the distance to the tip of the stem. Determine if the tip of the stem is in compression or tension:

$$f_{\text{tip,stem}} = \frac{P_{\text{axial}}}{A_g} + \frac{M_{ux}}{S_x} = \frac{-141}{14.2} + \frac{269}{12.7} = 11.3 \text{ ksi} \quad (\text{tension})$$

Therefore, the nominal flexural resistance for yielding is limited to $1.6M_y$. The nominal flexural resistance for yielding is computed as:

$$\begin{aligned} M_n &= M_p = F_y Z_x = (50)(22.6) = 1,130 \text{ kip-in} \\ 1.6M_y &= 1.6F_y S_x = 1.6(50)(12.7) = 1,016 \text{ kip-in} \quad (\text{governs}) \\ M_n &= 1,016 \text{ kip-in} \quad (\text{for yielding}) \end{aligned}$$

For lateral torsional buckling, the nominal flexural resistance is to be taken as:

$$M_n = \frac{\pi \sqrt{E I_y G J}}{L_b} \left[B + \sqrt{1 + B^2} \right] \quad \text{Eq. (6.12.2.2.4-2)}$$

in which:

$$B = \pm 2.3 \frac{d}{L_b} \sqrt{\frac{I_y}{J}} \quad \text{Eq. (6.12.2.2.4-3)}$$

where:

$$\begin{aligned} d &= \text{total depth of the section (in.)} \\ G &= \text{shear modulus of elasticity for steel} = 0.385E \text{ (ksi)} \\ I_y &= \text{moment of inertia about the y-axis (in.⁴)} \\ J &= \text{St. Venant torsional shear constant (in.⁴)} \\ L_b &= \text{unbraced length (in.)} \end{aligned}$$

The plus sign for B in Eq. 6.12.2.2.4-3 applies when the stem is in tension, and the minus sign applies when the stem is in compression anywhere along the length of the unbraced length. Therefore, the term B is computed as:

$$B = +2.3 \left(\frac{9.30}{222} \right) \sqrt{\frac{100}{2.92}} = 0.567$$

The lateral torsional buckling resistance is then computed as:

$$M_n = \frac{\pi \sqrt{(29,000)(100)(11,200)(2.92)}}{222} \left[0.567 + \sqrt{1 + 0.567^2} \right] = 7,481 \text{ kip-in}$$

Since the flange is in compression, flange local buckling must also be considered in accordance with Article 6.12.2.2.4. First check if the flange slenderness, λ_f , exceeds the limiting slenderness for a compact flange, λ_{pf} . If λ_{pf} is not exceeded, flange local buckling does not need to be checked.

$$\lambda_f = \frac{b_f}{2t_f} = \frac{11.1}{2(0.870)} = 6.38$$

$$\lambda_{pf} = 0.38 \sqrt{\frac{E}{F_y}} = 0.38 \sqrt{\frac{29,000}{50}} = 9.15 \quad \text{Eq. (6.12.2.2.4-7)}$$

$$\lambda_f = 6.38 < \lambda_{pf} = 9.15$$

Given that $\lambda_f < \lambda_{pf}$, local flange buckling does not need to be checked. Also, because the stem is in tension, local buckling of the stem does not need to be investigated, and is not a concern even if the stem was in compression as long as Eq. 6.12.2.2.4-2 is satisfied.

Thus, the nominal flexural resistance, M_n , of the tee section is governed by yielding, and is equal to 1,016 kip-in. Compute the factored flexural resistance, M_r , as follows:

$$M_r = \phi_f M_n = (1.0)(1,016) = 1,016 \text{ kip-in.} \quad \text{Eq. (6.12.1.2.1-1)}$$

Check the combined axial compression and flexure as specified in Article 6.9.2.2. First, it is necessary to determine the value of the factored axial compressive load, P_u , divided by the factored compressive resistance, P_r .

$$\frac{P_u}{P_r} = \frac{|-141|}{495} = 0.285 > 0.2$$

Since the above ratio is greater than 0.2, Eq. 6.9.2.2-2 is to be used to check the combined axial compression and flexure, noting that there is no bending about the y-axis.

$$\frac{P_u}{P_r} + \frac{8.0}{9.0} \left(\frac{M_{ux}}{M_{rx}} \right) \leq 1.0 \quad \text{Eq. (6.9.2.2-2)}$$

where:

M_{ux} = factored flexural moment about the x-axis (kip-in.)

M_{rx} = factored flexural resistance (kip-in.)

Check Eq. 6.9.2.2-2 as follows:

$$\frac{P_u}{P_r} + \frac{8.0}{9.0} \left(\frac{M_{ux}}{M_{rx}} \right) = \frac{|-141|}{495} + \frac{8.0}{9.0} \left(\frac{269}{1,016} \right) = 0.52 \leq 1.0 \quad \text{OK}$$

The WT 9x48.5 serving as the top flange diagonal bracing member in Span 1 of Girder G2 in the first bay adjacent to the abutment satisfies the interaction ratio for combined axial compression and flexure for constructibility loading. Design checks would be performed for all top flange lateral bracing members, investigating both tension and compression constructibility forces.

7.14 Bolted Field Splice Design

This section will show the design of a bolted field splice, in accordance with the provisions of Article 6.13.6. The design computations will be illustrated for the Field Splice #1 on Girder G2 (see Figure 9). First, single bolt capacities are computed for slip resistance (Article 6.13.2.8) and shear resistance (Article 6.13.2.7), and the bearing resistance on the connected material (Article 6.13.2.9). The field splice is then checked for constructibility, the service limit state, and the strength limit state.

All bolts used in the field splice are 0.875 inch diameter ASTM A325 bolts. Table 6.13.2.4.2-1 shows that a standard hole diameter size for a 0.875 inch diameter bolt is 0.9375 inch. The connection is designed assuming a Class B surface condition is provided, which corresponds to unpainted and blast-cleaned surfaces and blast-cleaned surfaces with Class B coatings. Also, it is assumed that the bolt threads will not be permitted in the shear planes.

Article 6.13.6.1.4a requires at least two rows of bolts on each side of the connection. Oversize or slotted holes in either the member or the splice plates are not permitted. The bolt pattern for the top flange splice is shown in Figure 19, the bolt pattern for the bottom flange splice is shown in Figure 20, and the bolt pattern for the web splice is shown in Figure 21. It should be noted that a 0.5 inch gap is assumed between the edges of the field pieces at this splice location.

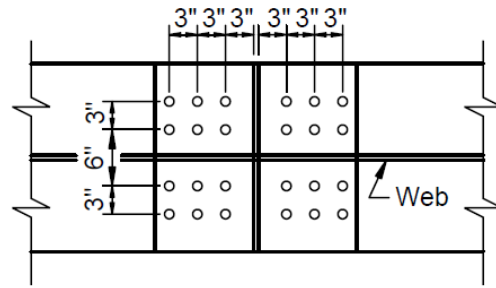


Figure 19 Bolt Pattern for the Top Flange Field Splice

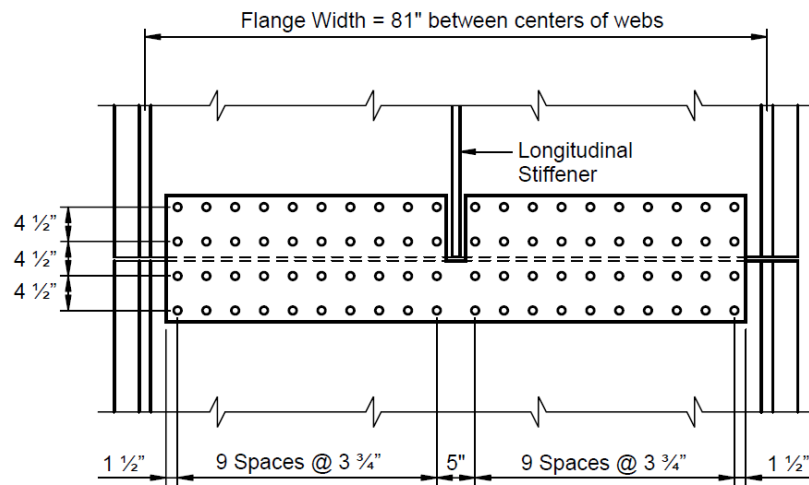


Figure 20 Bolt Pattern for the Bottom Flange Field Splice, shown inside the tub girder looking down at the bottom flange

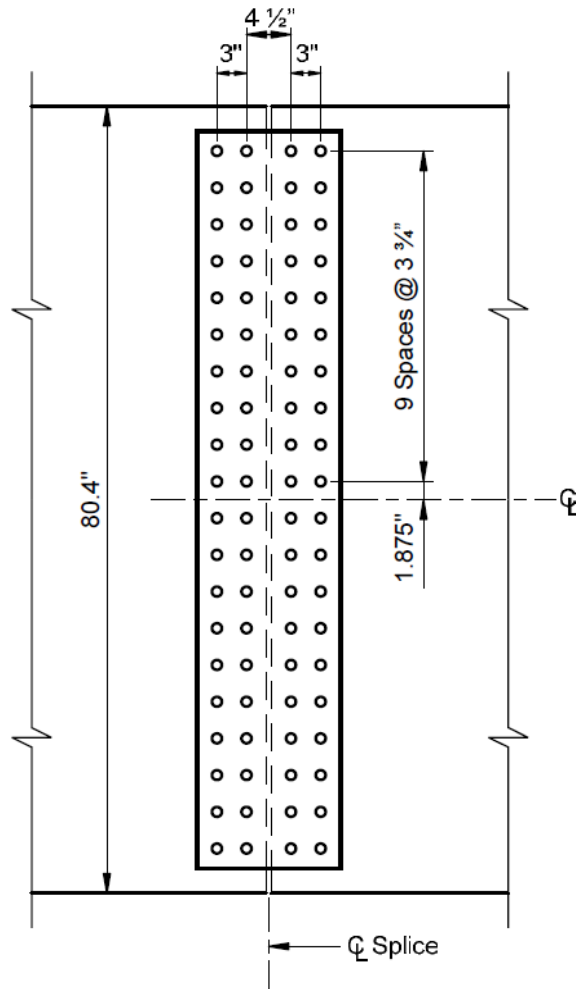


Figure 21 Bolt Pattern for the Web Field Splice, shown along the web slope

Unfactored analysis results for the girder major-axis bending moments, torques, shears, and top flange lateral bending moments at Field Splice #1 on Girder G2 are summarized in Table 16.

Table 16 Unfactored Analysis Results for the Design of Field Splice #1 on Girder G2

Unfactored Demands at G2 Field Splice 1							
Demand	Dead Load					LL+I	
	DC1 _{STEEL}	DC1 _{CONC}	DC1 _{CAST1}	DC2	DW	Pos.	Neg.
Moment (kip-ft)	462	1941	2749	326	428	5221	-3080
Torque (kip-ft)	-36	-125	-188	-58	-76	346	-517
Top Flange Lateral Moment (kip-ft)	-1	-7	-15	n/a	n/a	n/a	n/a
Shear (kips)	-17	-69	-61	-12	-16	36	-85

Note: Reported shears are the vertical shears and are for major-axis bending plus torsion in the critical tub girder web.

As specified in Article C6.13.6.1.4a, for a flexural member, it is recommended that the smaller section at the point of the splice be taken as the side of the splice that has the smaller product of the calculated moment of inertia for the noncomposite steel section and the smallest specified minimum flange yield strength on the side of the splice under consideration.. Therefore, girder section properties at Field Splice #1 on Girder G2 should be taken as those computed previously for the design Section G2-1 illustrated in this design example, as it is the smaller section at this splice location. Reference the tables and computations provided in Section 7.2 of this design example.

Furthermore, in accordance with Article 6.13.6.1.4a, the flexural stresses due to the factored loads at the strength limit state and for checking slip of bolted connections at the point of the splice are to be determined using gross section properties.

In accordance with Article C6.13.6.1.4c, for horizontally curved tub girders, the St. Venant torsional shear must be considered in the design of bottom flange splices at all limit states. The St. Venant torsional shears are typically neglected in the top flanges of tub sections once the flanges are continuously braced. St. Venant torsional shears in the top flange are not considered in the design of the top flange splice in this design example, as these shears are negligible.

7.14.1 Bolt Resistance for the Service Limit State and Constructibility

For slip-critical connections, the factored resistance, R_r , of a bolt at the Service II load combination is taken as:

$$R_r = R_n \quad \text{Eq. (6.13.2.2-1)}$$

where:

R_n = the nominal slip resistance as specified in Article 6.13.2.8 (kip)

The nominal slip resistance of a bolt in a slip-critical connection is to be taken as:

$$R_n = K_h K_s N_s P_t \quad \text{Eq. (6.13.2.8-1)}$$

where:

N_s = number of slip planes per bolt

P_t = minimum required bolt tension specified in Table 6.13.2.8-1(kip)

K_h = hole size factor specified in Table 6.13.2.8-2

K_s = surface condition factor specified in Table 6.13.2.8-3

For this design example:

- 2 slip planes are provided as there are two splice plates on each side of the girder element, thus N_s equals 2;

- As specified in Table 6.13.2.8-1, for 0.875 inch diameter A325 bolt, P_t is equal to 39 kips;
- As specified in Table 6.13.2.8-2, for a standard size hole, K_h is equal to 1.00; and
- As specified in Table 6.13.2.8-3, for Class B surface conditions, K_s is equal to 0.50.

Therefore, the factored slip resistance for service and constructibility checks is:

$$R_r = R_n = (1.0)(0.50)(2)(39) = 39 \text{ kips/bolt}$$

7.14.2 Bolt Resistance for the Strength Limit State

The factored resistance, R_r , of a bolted connection at the strength limit state is to be taken as:

$$R_r = \phi R_n \quad \text{Eq. (6.13.2.2-2)}$$

where:

$$\phi = \text{resistance factor for bolts specified in Article 6.5.4.2}$$

Article 6.13.6.1.4a states that the factored flexural resistance of the flanges at the point of the splice at the strength limit state must satisfy the applicable provisions of Article 6.10.6.2, which relates to flexure. The girder satisfies the applicable provisions of Article 6.10.6.2 at the splice location; however, the checks at this particular location are not included in this example.

7.14.2.1 Bolt Shear Resistance

The nominal shear resistance, R_n , of a high-strength bolt at the strength limit state where threads are excluded from the shear plane is computed as follows:

$$R_n = 0.48A_b F_{ub} N_s \quad \text{Eq. (6.13.2.7-1)}$$

where:

A_b = area of bolt corresponding to the nominal diameter (in.²)

F_{ub} = specified minimum tensile strength of the bolt in accordance with Article 6.4.3(ksi)

N_s = number of shear planes

In accordance with Article 6.4.3, the minimum tensile strength of a 0.875 inch diameter A325 bolt is 120 ksi. Two shear planes exist for all field splice connections. Therefore, the nominal shear resistance is computed as:

$$R_n = 0.48(0.601)(120)(2) = 69.2 \text{ kips/bolt}$$

The factored shear resistance, R_r , of a high-strength bolt at the strength limit state is computed as follows:

$$R_r = \phi_s R_n \quad \text{Eq. (6.13.2.2-2)}$$

where:

$$\phi_s = \text{shear resistance factor for bolts in shear from Article 6.5.4.2 } (\phi_s = 0.80)$$

Therefore, the factored shear resistance is:

$$R_r = (0.80)(69.2) = 55.4 \text{ kips/bolt}$$

7.14.2.2 Bearing Resistance on Connected Material

The nominal bearing resistance of interior and end bolt holes at the strength limit, R_n , is taken as one of the following two terms, depending on the bolt clear distance and the clear end distance.

- (1) With bolts spaced at a clear distance between holes not less than $2.0d$ and with a clear end distance not less than $2.0d$:

$$R_n = 2.4dtF_u \quad \text{Eq. (6.13.2.9-1)}$$

- (2) If either the clear distance between holes is less than $2.0d$ or the clear end distance is less than $2.0d$:

$$R_n = 1.2L_c tF_u \quad \text{Eq. (6.13.2.9-2)}$$

where:

- d = nominal diameter of the bolt (in.)
- t = thickness of the connected material (in.)
- F_u = tensile strength of the connected material specified in Table 6.4.1-1 (ksi)
- L_c = clear distance between holes or between the holed and the end of the member in the direction of the applied force

In the case of the web, the end distance is 2.0 inches. For simplicity, although the bolt hole diameter is actually 0.9375 in., assume for this calculation that the bolt hole diameter is 1 inch, creating a clear end distance of 1.5 inches, which is less than $2.0d$. Therefore, Eq. 6.13.2.9-2 applies. The tensile strength of the girder and splice plates in this design example is conservatively taken as 65 ksi. The nominal bearing resistance for the end row of bolts in the web is:

$$R_n = 1.2(1.5)(0.5625)(65) = 65.81 \text{ kips/bolt}$$

The factored bearing resistance, R_r , is computed as:

$$R_r = \phi_{bb}R_n \quad \text{Eq. (6.13.2.2-2)}$$

where:

$$\begin{aligned} \phi_{bb} &= \text{shear resistance factor for bolts bearing on material from Article 6.5.4.2} \\ (\phi_{bb} &= 0.80) \end{aligned}$$

Therefore, the factored bearing resistance is:

$$R_r = \phi_{bb}R_n = (0.80)(65.81) = 52.65 \text{ kips/bolt}$$

The bearing resistance above is computed for the thinnest element, the web, but it can conservatively be used for the flanges as well, as the web thickness is less than the flange thickness. Alternatively, the bearing resistance for the flange elements can be computed as well.

For interior rows of bolts, Eq. 6.13.2.9-1 applies, and the nominal bolt resistance is computed as:

$$R_n = 2.4dtF_u \quad \text{Eq. (6.13.2.9-1)}$$

$$R_n = 2.4(0.875)(0.5625)(65) = 76.78 \text{ kips/bolt}$$

Therefore, the factored bearing resistance is:

$$R_r = \phi_{bb}R_n = (0.80)(76.78) = 61.42 \text{ kips/bolt}$$

Again, the bearing resistance above is computed for the thinnest element, the web, but it can conservatively be used for the flanges as well.

7.14.3 Constructibility Checks

According to Article 6.13.6.1.4a, connections must be proportioned to prevent slip during the erection of the steel and during the casting of the concrete deck. Article 6.13.6.1.4c requires that lateral bending effects be considered in the design of curved girder splices. Therefore, flange lateral bending must be considered for the top flanges of tub girders prior to hardening of the concrete deck, as the top flanges are discretely braced in this situation. To account for the effects of flange lateral bending, the flange splice bolts will be designed for the combined effects of shear and moment using the traditional elastic vector method. The shear on the bolts is caused by the flange force calculated from the average major-axis bending stress in the flange, and the moment on the bolts is caused by the flange lateral bending.

Concrete deck Cast #1 causes a larger positive major-axis moment at the splice location than the moment caused by assuming the entire concrete deck is placed at one time. Therefore, for this field splice, perform the constructibility checks for the loading case of steel self-weight plus concrete deck Cast #1. For Strength I for constructibility, the dead load factor is 1.25 according to the provisions of Article 3.4.2.1 (Note: as mentioned previously, the special load combination

for primary steel superstructure components during construction specified in Article 3.4.2.1 is not considered in this example).

In accordance with Article C6.13.6.1.4c, longitudinal warping stresses due to cross-section distortion are to be considered when checking the slip resistance of the bolts for constructibility and at the service limit state for flange splices in horizontally curved tub-girder bridges. The internal cross frame spacing in the region of the splice is approximately 16.0 feet. An examination of the longitudinal warping stresses at the top and bottom of the tub girder for constructibility and at the bottom of the girder for the service limit state for this internal cross frame spacing (according to calculations similar to those illustrated for design Section G2-1) indicates that these longitudinal stresses are negligible in this case and will be ignored in calculations provided herein.

7.14.3.1 Constructibility Check of Top Flange Splice Bolts

To check constructibility of the top flange, first compute the polar moment of inertia of the top flange bolt pattern, shown in Figure 19. The bolt pattern consists of the 12 bolts in the flange on one side of the connection. The polar moment of inertia, I_p , is computed as:

$$I_p = [2(3)(3.0^2 + 6.0^2) + 2(4)(3.0^2)] = 342 \text{ in}^2$$

Compute the total unfactored major-axis bending moment due to vertical loads and the total unfactored flange lateral moment from the analysis results provided in Table 16 for steel plus concrete for Cast #1 ($DC1_{STEEL} + DC1_{CAST1}$):

$$\text{Major-axis bending moment} = 462 + 2,749 = 3,211 \text{ kip-ft}$$

$$\text{Top flange lateral bending moment} = -1 + (-15) = -16 \text{ kip-ft}$$

As discussed previously, the section properties of Field Section 1 of Girder 2 are used to compute the bending stresses since Field Section 1 is the smaller of the two girder sections connected by the splice. This splice location has the same section properties as those computed for design Section G2-1. The Construction Strength I factored major-axis bending stress at the mid-thickness of the top flange is computed as:

$$f_{\text{top}} = -(1.25) \left(\frac{3,211(12)(42.77 - 1.0/2)}{185,384} \right) = -10.98 \text{ ksi}$$

Compute the factored force in the top flange using the major-axis bending stress at the mid-thickness the flange. Multiply the factored flange stress by the gross section of the flange to check for slip.

$$F_{\text{top}} = (-10.98)(16.0)(1.0) = -176 \text{ kips}$$

Compute the factored longitudinal force in each bolt resulting from the major-axis bending, by dividing the factored flange force by the number of bolts on one side of the splice:

$$F_{\text{Long vert}} = \frac{|-176|}{12} = 14.67 \text{ kips/bolt}$$

Compute the factored longitudinal component of force in the critical bolt due to the flange lateral moment, noting that the transverse distance from the centroid of the bolt group to the critical bolt is 6.0 inches:

$$F_{\text{Long lat}} = (1.25) \frac{|-16|(12)(6.0)}{342} = 4.21 \text{ kips/bolt}$$

Therefore, the total factored longitudinal force in the critical bolt is computed as:

$$F_{\text{Long tot}} = 14.67 + 4.21 = 18.88 \text{ kips/bolt}$$

Compute the factored transverse component of force in the critical bolt due to the flange lateral moment, noting that the longitudinal distance from the centroid of the bolt group to the critical bolt is 3.0 inches:

$$F_{\text{Trans}} = (1.25) \frac{|-16|(12)(3.0)}{342} = 2.11 \text{ kips/bolt}$$

Compute the resultant force on the critical bolt:

$$R_u = \sum F = \sqrt{18.88^2 + 2.11^2} = 19.00 \text{ kips/bolt}$$

Check that the factored resultant force on the critical bolt, R_u is less than the factored slip resistance of one bolt, R_r , calculated previously as 39 kips/bolt:

$$R_u = 19.00 \text{ kips/bolt} < R_r = 39 \text{ kips/bolt} \quad \text{OK}$$

7.14.3.2 Constructibility Check of Bottom Flange Splice Bolts

To check constructibility of the bottom flange, first compute the polar moment of inertia of the bottom flange bolt pattern, shown in Figure 20. The bolt pattern consists of the 40 bolts in the flange on one side of the connection. The polar moment of inertia, I_p , is computed as:

$$I_p = [2(20)(2.25)^2 + 2(2)(2.5^2 + 6.25^2 + 10.0^2 + 13.75^2 + 17.5^2 + 21.25^2 + 25.0^2 + 28.75^2 + 32.5^2 + 36.25^2)] = 19,859 \text{ in.}^4$$

Compute the total unfactored major-axis bending moment due to vertical loads, and the unfactored torque from the analysis results provided in Table 16 for steel plus concrete for Cast #1 ($DC1_{STEEL} + DC1_{CAST1}$):

$$\text{Major-axis bending moment} = 462 + 2,749 = 3,211 \text{ kip-ft}$$

$$\text{Torque} = -36 + (-188) = -224 \text{ kip-ft}$$

As discussed previously, the section properties of Field Section 1 of Girder 2 are used to compute the bending stresses since Field Section 1 is the smaller of the two girder sections connected by the splice. This splice location has the same section properties as those computed for design Section G2-1. The Construction Strength I factored major-axis bending stress at the mid-thickness of the bottom flange is computed as:

$$f_{\text{bot}} = (1.25) \left(\frac{3,211(12)(36.86 - 0.625/2)}{185,384} \right) = 9.50 \text{ ksi}$$

Compute the factored force in the bottom flange using the average major-axis bending stress at the mid-thickness of the flange. Multiply the factored flange stress by the gross section of the flange to check for slip.

$$F_{\text{bot}} = (-9.50)(83.0)(0.625) = 493 \text{ kips}$$

The bottom flange splice bolts should be design for the combined effects of St. Venant torsional shear and major-axis bending moment. The enclosed area of the noncomposite tub girder, A_o , was previously computed to be $7,921 \text{ in.}^2$ in the constructibility check of the bottom flange of section G2-1. The unfactored St. Venant torsional shear in the bottom flange is computed as:

$$V_{\text{botflg}} = \frac{T}{2A_o} b_f = \frac{|-224|(12)}{2(7921)} (81) = 13.7 \text{ kips}$$

Because the St. Venant torsional shear is assumed to act at the centerline of the field splice, it produces a lateral moment on the bottom flange bolt group on each side of the splice. The factored lateral moment on the bolt group, computed at the centroid of the bolt group is:

$$M_{\text{LAT}} = (13.7) \left(\frac{4.5}{2} + \frac{4.5}{2} \right) = 61.7 \text{ kip - in.}$$

Compute the factored longitudinal component of force in the critical bolt due to the lateral moment in the bottom flange, noting that the transverse distance from the centroid of the bolt group to the critical bolt is 36.25 inches:

$$F_{\text{Long lat}} = (1.25) \frac{|61.7|(36.25)}{19,859} = 0.14 \text{ kips/bolt}$$

Compute the factored longitudinal force in each bolt resulting from the major-axis bending, by dividing the factored flange force by the number of bolts on one side of the splice:

$$F_{\text{Long vert}} = \frac{493}{40} = 12.33 \text{ kips/bolt}$$

Therefore, the total factored longitudinal force in the critical bolt is computed as:

$$F_{\text{Long tot}} = 0.14 + 12.33 = 12.47 \text{ kips/bolt}$$

Compute the factored transverse component of force in the critical bolt due to the lateral moment in the bottom flange, noting that the longitudinal distance from the centroid of the bolt group to the critical bolt is 2.25 inches:

$$F_{\text{Trans lat}} = (1.25) \frac{61.7(2.25)}{19,859} = 0.01 \text{ kips/bolt}$$

Compute the factored transverse force in each bolt resulting from the St. Venant torsional shear force by dividing the shear force by the number of bolts on one side of the splice, and multiplying by the 1.25 load factor:

$$F_{\text{Trans Shear}} = (1.25) \frac{13.7}{40} = 0.43 \text{ kips/bolt}$$

Therefore, the total factored transverse force in the critical bolt is computed as:

$$F_{\text{Trans tot}} = 0.01 + 0.43 = 0.44 \text{ kips/bolt}$$

Compute the resultant force on the critical bolt:

$$R_u = \sum F = \sqrt{12.47^2 + 0.44^2} = 12.48 \text{ kips/bolt}$$

Check that the factored resultant force on the critical bolt, R_u is less than the factored slip resistance of one bolt, R_r , calculated previously as 39 kips/bolt:

$$R_u = 12.48 \text{ kips/bolt} < R_r = 39 \text{ kips/bolt} \quad \text{OK}$$

7.14.3.3 Constructibility Check of Web Splice Bolts

A pattern of two rows of 7/8 inch diameter bolts spaced vertically at 3.75 inches is designed for the web splice. There are 40 bolts on each side of the connection, and the pattern is previously shown in Figure 21. In this example, the web splice is designed conservatively, assuming that

the maximum major-axis bending moment and maximum vertical shear at the splice occur under the same loading condition.

First, compute the polar moment of inertia of the web bolt group about the centroid of the bolt group on one side of the splice using Eq. C6.13.6.1.4b-3:

$$I_p = \frac{n m}{12} [s^2(n^2 - 1) + g^2(m^2 - 1)] \quad \text{Eq. (C6.13.6.1.4b-3)}$$

where:

- n = number of bolts in one vertical row
- m = number of vertical rows of bolts
- s = vertical pitch (in.)
- g = horizontal pitch (in.)

Therefore the web bolt group polar moment is computed as:

$$I_p = \frac{(20)(2)}{12} [3.75^2(20^2 - 1) + 3.00^2(2^2 - 1)] = 18,793 \text{ in.}^4$$

Compute the total unfactored shear at the splice (flexure plus torsional shear in the critical web) from the analysis results provided in Table 16 for steel plus concrete for Cast #1 (DC1_{STEEL} + DC1_{CAST1}):

$$\text{Shear} = -17 + (-61) = -78 \text{ kips}$$

Therefore, using the Construction Strength I load factor for dead load of 1.25, the factored shear is:

$$V = (1.25) (-78) = 97.5 \text{ kips}$$

Compute the moment, M_v , due to the eccentricity of the factored shear about the centroid of the connection (refer to the web bolt pattern in Figure 21).

$$M_v = V \times e = 97.5 \left(\frac{3}{2} + \frac{4.5}{2} \right) \left(\frac{1}{12} \right) = 30.5 \text{ kip} \cdot \text{ft}$$

Determine the portion of the major-axis bending moment resisted by the web, M_{uw} , and the horizontal force resultant in the web, H_{uw} , using the equations provided in Article C6.13.6.1.4b. M_{uw} and H_{uw} are assumed to be applied at the mid-depth of the web. The factored bending stresses at the mid-thickness of the top and bottom flanges for Steel plus Cast #1 were previously computed as follows:

$$\text{Top flange: } f_s = f_{top} = -10.98 \text{ ksi (C)}$$

Bottom flange: $f_{os} = f_{bot} = 9.50$ ksi (T)

where:

f_s = maximum factored major-axis bending stress for constructibility loading at the mid-thickness of the flange under consideration for the smaller section at the point of the splice; positive for tension, negative for compression (ksi) (see Article C6.13.6.1.4b)

f_{os} = factored major-axis bending stress for constructibility loading at the mid-thickness of the other flange at the point of the splice with f_s in the flange under consideration; positive for tension, negative for compression (ksi) (see Article C6.13.6.1.4b)

Using the factored flexural stresses, use the following equations to compute a suggested design moment, M_{uw} , and a design horizontal resultant, H_{uw} that will be applied at the mid-depth of the web for designing the web splice plates and their connections:

$$M_{uw} = \frac{t_w D^2}{12} |R_h F_{cf} - R_{cf} f_{ncf}| \quad \text{Eq. (C6.13.6.1.4b-1)}$$

$$H_{uw} = \frac{t_w D}{2} (R_h F_{cf} + R_{cf} f_{ncf}) \quad \text{Eq. (C6.13.6.1.4b-2)}$$

where:

t_w = web thickness of the smaller section at the point of the splice (in.)

D = web depth of the smaller section at the point of the splice (in.)

R_h = hybrid factor specified in Article 6.10.1.10.1, and is equal to 1.0 in this example

R_{cf} = for checking slip resistance, this ratio is taken as 1.0 as specified in Article C6.13.6.1.4b.

F_{cf} = f_s , as specified in Article C6.13.6.1.4b

f_{ncf} = f_{os} , as specified in Article C6.13.6.1.4b

Therefore, using the vertical web depth of 78 inches, M_{uw} and H_{uw} are computed as:

$$M_{uw} = \frac{t_w D^2}{12} |R_h f_s - R_{cf} f_{os}| = \frac{(0.5625)(78)^2}{12} |1.0(-10.98) - 1.0(9.50)| \left(\frac{1}{12} \right) = 487 \text{ kip-ft}$$

$$H_{uw} = \frac{t_w D}{2} (R_h f_s + R_{cf} f_{os}) = \frac{(0.5625)(78)}{2} (1.0(-10.98) + 1.0(9.50)) = -32.5 \text{ kips}$$

The total factored moment applied to the web splice is the sum of the moment caused by the vertical shear, M_v , and the moment computed by Eq. C6.13.6.1.4b-1, M_{uw} :

$$M_{\text{tot}} = M_v + M_{\text{uw}} = 30.5 + 487 = 518 \text{ kip-ft}$$

Compute the factored force in each bolt resulting from the vertical shear by dividing the factored shear by the number of bolts on one side of the splice:

$$F_{\text{Shear vert}} = \frac{97.5}{40} = 2.44 \text{ kips/bolt}$$

However, the above bolt force, $F_{\text{Shear vert}}$, is in the vertical plane, and must be resolved to the inclined plane of the web. Therefore, the in-plane bolt force is computed as:

$$F_s = \frac{F_{\text{Shear vert}}}{\cos(\theta)} = \frac{2.44}{\cos(14.04^\circ)} = 2.52 \text{ kips/bolt}$$

Compute the in-plane factored force in each bolt resulting from the horizontal force resultant, by dividing the factored resultant by the number of bolts on one side of the splice:

$$F_H = \frac{|-32.5|}{40} = 0.81 \text{ kips/bolt}$$

Compute the in-plane factored vertical component of force in the critical bolt due to the total factored moment on the splice, noting that the horizontal distance from the centroid of the bolt group to the critical bolt is 1.5 inches:

$$F_{M_v} = \frac{M_{\text{tot}x}}{I_p} \left(\frac{1}{\cos(\theta)} \right) = \frac{(518)(12)(1.5)}{18,793} \left(\frac{1}{\cos(14.04^\circ)} \right) = 0.51 \text{ kips/bolt}$$

Compute the in-plane factored horizontal component of force in the critical bolt due to the total factored moment on the splice, noting that the vertical distance from the centroid of the bolt group to the critical bolt is 35.625 inches:

$$F_{M_h} = \frac{M_{\text{tot}y}}{I_p} = \frac{(518)(12)(35.625)}{18,793} = 11.78 \text{ kips/bolt}$$

Compute the resultant in-plane force on the critical bolt:

$$R_u = F_r = \sqrt{(F_s + F_{M_v})^2 + (F_H + F_{M_h})^2}$$

$$R_u = \sqrt{(2.52 + 0.51)^2 + (0.81 + 11.78)^2} = 12.95 \text{ kips/bolt}$$

Check that the factored resultant force on the critical bolt, R_u is less than the factored slip resistance of one bolt, R_r , calculated previously as 39 kips/bolt:

$$R_u = 12.95 \text{ kips/bolt} < R_r = 39 \text{ kips/bolt} \text{ OK}$$

7.14.4 Service Limit State

According to the provisions of Article 6.13.6.1.4c, bolted connections for flange splices are to be designed as slip-critical connections for the flange design force. As a minimum, for checking slip of the flange splice bolts, the design force for the flange under consideration must be taken as the Service II design stress, F_s , times the gross flange area of the flange in the smaller section. F_s is calculated as follows:

$$F_s = \frac{f_s}{R_h} \quad \text{Eq. (6.13.6.1.4c-6)}$$

where:

f_s = maximum flexural stress due to Load Combination Service II at the mid-thickness of the flange under consideration in the smaller section at the point of the splice (ksi)

R_h = hybrid factor specified in Article 6.10.1.10.1, and is equal to 1.0 in this example

Compute the flexural stresses for the top and bottom flanges at the mid-thickness of the flange, for both the negative and positive live load bending cases and using the load factors for the Service II load combination from Table 3.4.1-1.

Positive live load bending case

$$f_{s,\text{topflg}} = - \left[\frac{1.0(462 + 1,941)(42.27)}{185,384} + \frac{1.0(326 + 428)(24.10)}{352,505} + \frac{1.30(5,221)(10.57)}{478,009} \right] (12) = -8.99 \text{ ksi (C)}$$

$$f_{s,\text{botflg}} = \left[\frac{1.0(462 + 1,941)(36.55)}{185,384} + \frac{1.0(326 + 428)(54.72)}{352,505} + \frac{1.30(5,221)(68.25)}{478,009} \right] (12) = 18.73 \text{ ksi (T)}$$

Negative live load bending case

Note that the flange stresses for the negative live load bending cases are computed conservatively, assuming that the negative live load bending moments act on the steel section only, and contribution from the longitudinal reinforcement, or concrete deck if applicable, is ignored. Furthermore, to maximize the flange stress for negative live load bending, the bending moment due to DW is ignored as well, since it is the opposite sign of the negative live load moment and DW is a future loading.

$$f_{s,topflg} = -\left[\frac{1.0(462 + 1,941)(42.27)}{185,384} + \frac{1.0(326)(24.10)}{352,505} + \frac{1.30(-3,080)(42.27)}{185,384} \right] (12) = 4.11 \text{ ksi (T)}$$

$$f_{s,botflg} = \left[\frac{1.0(462 + 1,941)(36.55)}{185,384} + \frac{1.0(326)(54.72)}{352,505} + \frac{1.30(-3,080)(36.55)}{185,384} \right] (12) = -3.18 \text{ ksi (C)}$$

The above calculations of factored flange stress show that the positive live load bending case governs at this field splice for the Service Limit State. The positive live load bending will be the only case considered in the Service Limit State check of the flange field splice bolts.

7.14.4.1 Service Limit State Check of Top Flange Splice Bolts

Flange lateral bending does not need to be considered in checking slip of the top flange bolts at the Service Limit State because the flange is continuously braced.

Compute the factored force in the top flange using the major-axis bending stress at the mid-thickness of the flange. Multiply the factored flange stress by the gross area of the flange to check for slip.

$$F_{top} = (-8.99)(16.0)(1.0) = -144 \text{ kips}$$

Compute the factored longitudinal force in each bolt resulting from the major-axis bending, by dividing the factored flange force by the number of bolts on one side of the splice:

$$F_{Long} = \frac{|-144|}{12} = 12.00 \text{ kips/bolt}$$

Check that the factored longitudinal force on each bolt is less than the factored slip resistance of one bolt, R_r , calculated previously as 39 kips/bolt:

$$F_{Long} = 12.00 \text{ kips/bolt} < R_r = 39 \text{ kips/bolt} \text{ OK}$$

7.14.4.2 Service Limit State Check of Bottom Flange Splice Bolts

Compute the Service II factored torques acting on the noncomposite and composite sections from the analysis results provided in Table 16. The negative live load torque is used, as it controls over the positive live load torque.

$$\text{Factored Noncomposite Torque} = 1.0[-36 + (-125)] = -161 \text{ kip-ft}$$

$$\text{Factored Composite Torque} = 1.0[-58 + (-76)] + 1.30[-517] = -806 \text{ kip-ft}$$

The bottom flange splice bolts should be designed for the combined effects of St. Venant torsional shear and major-axis bending moment. The enclosed area of the noncomposite tub girder, A_o , was previously computed to be 7,921 in.² The factored St. Venant torsional shear in the bottom flange due to noncomposite loads is computed as:

$$V_{NCbotflg} = \frac{T}{2A_o} b_f = \frac{|-161|(12)}{2(7,921)} (81) = 9.9 \text{ kips}$$

The enclosed area of the composite tub girder, A_o , was previously computed to be 8,750 in.² The factored St. Venant torsional shear in the bottom flange due to composite loads is computed as:

$$V_{Cbotflg} = \frac{T}{2A_o} b_f = \frac{|-806|(12)}{2(8,750)} (81) = 44.8 \text{ kips}$$

Because the St. Venant torsional shear is assumed to act at the centerline of the field splice, it produces a lateral moment on the bottom flange bolt group on each side of the splice. The factored lateral moment on the bolt group, computed at the centroid of the bolt group is:

$$M_{LAT} = (9.9 + 44.8) \left(\frac{4.5}{2} + \frac{4.5}{2} \right) = 246.2 \text{ kip} \cdot \text{in.}$$

Compute the factored longitudinal component of force in the critical bolt due to the factored lateral moment in the bottom flange, noting that the transverse distance from the centroid of the bolt group to the critical bolt is 36.25 inches:

$$F_{Long \text{ lat}} = \frac{|246.2|(36.25)}{19,859} = 0.45 \text{ kips/bolt}$$

Compute the factored transverse component of force in the critical bolt due to the factored lateral moment in the bottom flange, noting that the longitudinal distance from the centroid of the bolt group to the critical bolt is 2.25 inches:

$$F_{Trans \text{ lat}} = \frac{|246.2|(2.25)}{19,859} = 0.03 \text{ kips/bolt}$$

Compute the factored force in the bottom flange using the average major-axis bending stress at the mid-thickness of the flange. Multiply the factored flange stress by the gross area of the flange to check for slip.

$$F_{bot} = (18.73)(83.0)(0.625) = 972 \text{ kips}$$

Compute the factored longitudinal force in each bolt resulting from the major-axis bending by dividing the factored flange force by the number of bolts on one side of the splice:

$$F_{\text{Long vert}} = \frac{972}{40} = 24.30 \text{ kips/bolt}$$

Therefore, the total factored longitudinal force in the critical bolt is computed as:

$$F_{\text{Long tot}} = 0.45 + 24.30 = 24.75 \text{ kips/bolt}$$

Compute the factored transverse force in each bolt resulting from the factored St. Venant torsional shear force by dividing the shear force by the number of bolts on one side of the splice:

$$F_{\text{Trans Shear}} = \frac{(9.9 + 44.8)}{40} = 1.37 \text{ kips/bolt}$$

Therefore, the total factored transverse force in the critical bolt is computed as:

$$F_{\text{Trans tot}} = 1.37 + 0.03 = 1.40 \text{ kips/bolt}$$

Compute the resultant force on the critical bolt:

$$R_u = \sum F = \sqrt{24.75^2 + 1.40^2} = 24.79 \text{ kips/bolt}$$

Check that the factored resultant force on the critical bolt, R_u is less than the factored slip resistance of one bolt, R_r , calculated previously as 39 kips/bolt:

$$R_u = 24.79 \text{ kips/bolt} < R_r = 39 \text{ kips/bolt} \text{ OK}$$

7.14.4.3 Service Limit State Check of Web Splice Bolts

According to the provisions of Article 6.13.6.1.4b, bolted connections for web splices are to be designed as slip-critical connections for the maximum resultant bolt design force. As a minimum, for checking slip of the web splice bolts, the design shear is to be taken as the shear at the point of splice under Load Combination Service II, as specified in Table 3.4.1-1. Calculations for the Service Limit State check of the web bolts are not provided herein, but would be similar to those carried out for the Constructibility check and would use loads combined for the Service II load combination. Calculations not provided herein show that the web splice bolts are satisfactory for the Service Limit State.

7.14.5 Strength Limit State

Bolted splices are designed at the strength limit state to satisfy the requirements specified in Article 6.13.1. In basic terms, Article 6.13.1 indicates that a splice is to be designed for the larger of: (a) the average of the factored applied stresses and the factored resistance of the member, or (b) 75 percent of the factored resistance of the member.

At the strength limit state, splice plates and their connections on the controlling flange are to be proportioned to provide a minimum resistance taken as the design stress, F_{cf} , times the effective flange area, A_e , of the controlling flange, where F_{cf} is defined as:

$$F_{cf} = \frac{\left| \frac{f_{cf}}{R_h} \right| + \alpha \phi_f F_{yf} R_g}{2} \geq 0.75 \alpha \phi_f F_{yf} R_g \quad \text{Eq. (6.13.6.1.4c-1)}$$

in which:

A_e = effective area of the flange (in.²). For compression flanges, A_e is to be taken as the gross area of the flange A_g . For tension flanges, A_e is to be taken as:

$$A_e = \left(\frac{\phi_u F_u}{\phi_y F_{yt}} \right) A_n \leq A_g \quad \text{Eq. (6.13.6.1.4c-2)}$$

R_g = flange resistance modification factor taken as:

$$R_g = \frac{\left[\alpha A_e F_{yf} \right]_{LS}}{\left[\alpha A_e F_{yf} \right]_{SS}} \leq 1.0 \quad \text{Eq. (6.13.6.1.4c-3)}$$

$\left[\alpha A_e F_{yf} \right]_{LS}$ = product of the effective area times αF_{yf} for the flange under consideration in the larger section at the point of the splice

$\left[\alpha A_e F_{yf} \right]_{SS}$ = product of the effective area times αF_{yf} for the flange under consideration in the smaller section at the point of the splice

where:

f_{cf} = maximum flexural stress due to factored loads at the mid-thickness of the controlling flange at the point of the splice (ksi)

R_h = hybrid factor specified in Article 6.10.1.10.1; for this example is equal to 1.0.

α = 1.0, except a lower value equal to (F_n/F_{yf}) may be used for flanges where F_n is less than F_{yf} .

ϕ_f = resistance factor for flexure specified in Article 6.5.4.2 ($\phi_f = 1.0$)

F_n = nominal flexural resistance of the flange (ksi)

F_{yf} = specified minimum yield strength of the flange (ksi)

ϕ_u = resistance factor for fracture of tension members specified in Article 6.5.4.2 ($\phi_u = 0.80$)

ϕ_y = resistance factor for yielding of tension members specified in Article 6.5.4.2 ($\phi_y = 0.95$)

A_n = net area of the tension flange determined as specified in Article 6.8.3 (in.²)

- F_u = specified minimum tensile strength of the tension flange determined as specified in Table 6.4.1-1 (ksi)
 F_{yt} = specified minimum yield strength of the tension flange (ksi)

The controlling flange is defined as either the top or bottom flange in the smaller section at the point of the splice, whichever flange has the maximum ratio of the elastic flexural stress at its mid-thickness due to factored loads for the loading condition under investigation to its factored flexural resistance. The other flange is termed the noncontrolling flange. In areas of stress reversal, the splice must be checked independently for both positive and negative flexure.

Splice plates and their connections on the noncontrolling flange at the strength limit state are to be proportioned to provide a minimum resistance taken as the design stress, F_{ncf} , times the effective flange area, A_e , of the noncontrolling flange, where F_{ncf} is defined as:

$$F_{ncf} = R_{cf} \left| \frac{f_{ncf}}{R_h} \right| \geq 0.75 \alpha_f F_{yf} R_g \quad \text{Eq. (6.13.6.1.4c-4)}$$

where:

- R_{cf} = the absolute value of the ratio of F_{cf} to f_{cf} for the controlling flange
 f_{ncf} = flexural stress due to factored loads at the mid-thickness of the noncontrolling flange at the point of the splice concurrent with f_{cf} (ksi)
 R_h = hybrid factor specified in Article 6.10.1.10.1; for this example is equal to 1.0.
 R_g = flange resistance modification factor determined from Eq. 6.13.6.1.4c-3

First, compute the flexural stresses for the top and bottom flanges at the mid-thickness of the flange, for both the negative and positive live load bending cases and using the load factors for the Strength I load combination from Table 3.4.1-1.

Positive live load bending case

$$f_{s,topflg} = - \left[\frac{1.25(2,403)(42.27)}{185,384} + \frac{[1.25(326)+1.5(428)](24.10)}{352,505} + \frac{1.75(5,221)(10.57)}{478,009} \right] (12)$$

$$f_{s,topflg} = -11.50 \text{ ksi (C)}$$

$$f_{s,botflg} = \left[\frac{1.25(2,403)(36.55)}{185,384} + \frac{[1.25(326)+1.5(428)](54.72)}{352,505} + \frac{1.75(5,221)(68.25)}{478,009} \right] (12)$$

$$f_{s,botflg} = 24.72 \text{ ksi (T)}$$

Negative live load bending case

Note that the flange stresses for the negative live load bending cases are computed conservatively, assuming that the negative live load bending moments act on the steel section only, and contribution from the longitudinal reinforcement is ignored. Furthermore, to maximize the flange stress for negative live load bending, the bending moment due to DW is ignored as well, since it is the opposite sign of the negative live load moment and DW is a future loading. The minimum load factor for component dead load, 0.9, as specified in Table 3.4.1-2 is used as well, in order to maximize the negative live load effects.

$$f_{s,topflg} = - \left[\frac{0.90(2,403)(42.27)}{185,384} + \frac{0.90(326)(24.10)}{352,505} + \frac{1.75(-3,080)(42.27)}{185,384} \right] (12)$$

$$f_{s,topflg} = 8.59 \text{ ksi (T)}$$

$$f_{s,botflg} = \left[\frac{0.90(2,403)(36.55)}{185,384} + \frac{0.90(326)(54.72)}{352,505} + \frac{1.75(-3,080)(36.55)}{185,384} \right] (12)$$

$$f_{s,botflg} = -7.09 \text{ ksi (C)}$$

As specified in Article C6.13.6.1.4c, in areas of stress reversal, which is the case for this field splice, the splice must be independently checked for both positive and negative flexure.

In accordance with Article C6.13.6.1.4c, longitudinal warping stresses due to cross-section distortion in horizontally curved tub girders may be ignored when checking the splices in the top and bottom flanges at the strength limit state.

7.14.5.1 Positive Flexure Strength Limit State Design Forces

Compute the effective flange areas, A_e , of the top and bottom flanges, as these areas will be used in subsequent computations. Since the top flange is in compression for positive flexure, in accordance with Article 6.13.6.1.4c, the effective top flange area is equal to the gross area of the flange, A_g :

$$A_{e,top\ flg} = A_g = (16.0)(1.0) = 16.0 \text{ in.}^2$$

The bottom flange is in tension for positive flexure, therefore the effective area of the flange must consider the net area of the flange, A_n , and be computed in accordance with Eq. 6.13.6.1.4c-2:

$$A_e = \left(\frac{\phi_u F_u}{\phi_y F_{yt}} \right) A_n \leq A_g \quad \text{Eq. (6.13.6.1.4c-2)}$$

The net area of the bottom flange is computed in accordance with Article 6.8.3, which states that the net area, A_n , of an element is the product of the thickness of the element and its smallest net

width. The width of each standard bolt hole shall be taken as the nominal diameter of the hole. Therefore, the net area of the bottom flange at the location of the splice is computed as:

$$A_{n, \text{bot flg}} = [83.0 - 20(0.875 + 0.0625)](0.625) = 40.1 \text{ in.}^2$$

The effective area of the bottom flange is then computed as:

$$A_{e, \text{bot flg}} = \left(\frac{\phi_u F_u}{\phi_y F_{yt}} \right) A_n = \left(\frac{(0.8)(65)}{(0.95)(50)} \right) (40.1) = 43.9 \text{ in.}^2 \leq A_g = (83.0)(0.625) = 51.9 \text{ in.}^2$$

$$A_{e, \text{bot flg}} = 43.9 \text{ in.}^2$$

For the positive live load bending case, the controlling flange is the bottom flange since it has the largest ratio of the flexural stress to the corresponding critical flange stress. Therefore, the design stress, F_{cf} , is computed in accordance with Eq. 6.13.6.1.4c-1. However, first compute the flange resistance modification factor, R_g , for the bottom flange, noting that $\alpha = 1.0$ for flanges in tension. Since the effective areas of the adjoining flanges are equal and the yield strengths are equal, $[\alpha A_e F_{yf}]_{LS} = [\alpha A_e F_{yf}]_{SS}$ and $R_g = 1.0$

$$F_{cf} = \frac{\left(\frac{f_{cf}}{R_h} \right) + \alpha \phi_f F_{yf} R_g}{2} = \frac{\left(\frac{24.72}{1.0} \right) + (1.0)(1.0)(50)(1.0)}{2} = 37.36 \text{ ksi}$$

$$F_{cf} = 0.75 \alpha \phi_f F_{yf} R_g = 0.75(1.0)(1.0)(50)(1.0) = 37.50 \text{ ksi}$$

Therefore, F_{cf} is taken as 37.50 ksi.

For the positive live load bending case, the minimum design force for the controlling flange (bottom flange), P_{cf} , is taken equal to F_{cf} times the effective area, A_e , of the controlling flange. The minimum design force, P_{cf} , is computed as:

$$P_{cf} = F_{cf} A_{e, \text{bot flg}} = (37.50)(43.9) = 1,646 \text{ kips (T)}$$

For the positive live load bending case, the minimum design stress for the noncontrolling flange (top flange), F_{ncf} , is computed in accordance with Eq. (6.13.6.1.4c-4). First, it is necessary to compute R_{cf} , the absolute value of the ratio of F_{cf} to f_{cf} for the controlling flange:

$$R_{cf} = \left| \frac{F_{cf}}{f_{cf}} \right| = \left| \frac{37.50}{24.72} \right| = 1.52$$

Compute F_{ncf} , in accordance with Eq. (6.13.6.1.4c-4):

$$F_{ncf} = R_{cf} \left| \frac{f_{ncf}}{R_h} \right| = (1.52) \left| \frac{-11.50}{1.0} \right| = 17.48 \text{ ksi}$$

$$F_{ncf} = 0.75\alpha\phi_f F_{yf} R_g = 0.75(1.0)(1.0)(50)(1.0) = 37.50 \text{ ksi}$$

Therefore, F_{ncf} is taken as 37.50 ksi.

For the positive live load bending case, the minimum design force for the noncontrolling flange (top flange), P_{ncf} , is taken equal to F_{ncf} times the effective area, A_e , of the noncontrolling flange. The minimum design force, P_{ncf} , is computed as:

$$P_{ncf} = F_{ncf} A_{e,top \text{ flg}} = (37.50)(16.0) = 600 \text{ kips (C)}$$

7.14.5.2 Negative Flexure Strength Limit State Design Forces

Compute the effective flange areas, A_e , of the top and bottom flanges, as these will be used in subsequent computations. Since the bottom flange is in compression for negative flexure, as specified in Article 6.13.6.1.4c, the effective bottom flange area is equal to the gross area of the flange, A_g :

$$A_{e,bot \text{ flg}} = A_g = (83.0)(0.625) = 51.88 \text{ in.}^2$$

The top flange is in tension for negative flexure, therefore the effective area of the flange must consider the net area of the flange, A_n , and be computed in accordance with Eq. 6.13.6.1.4c-2:

$$A_e = \left(\frac{\phi_u F_u}{\phi_y F_{yt}} \right) A_n \leq A_g \quad \text{Eq. (6.13.6.1.4c-2)}$$

The net area of the top flange is computed in accordance with Article 6.8.3. The width of each standard bolt hole is to be taken as the nominal diameter of the hole. Therefore, the net area of the top flange at the location of the splice is computed as:

$$A_{n,top \text{ flg}} = [16 - 4(0.875 + 0.0625)](1.0) = 12.25 \text{ in.}^2$$

The effective area of the top flange is then computed as:

$$A_{e,top \text{ flg}} = \left(\frac{\phi_u F_u}{\phi_y F_{yt}} \right) A_n = \left(\frac{(0.8)(65)}{(0.95)(50)} \right) (12.25) = 13.41 \text{ in.}^2 \leq A_g = (16.0)(1.00) = 16.0 \text{ in.}^2$$

$$A_{e,top \text{ flg}} = 13.41 \text{ in.}^2$$

For the negative live load bending case, the controlling flange is top flange since it has the largest ratio of the flexural stress to the corresponding critical flange stress. Therefore, the

design stress, F_{cf} , is computed in accordance with Eq. 6.13.6.1.4c-1. However, first compute the flange resistance modification factor, R_g , for the bottom flange, noting that $\alpha = 1.0$ for tension flanges. Since the effective areas of the adjoining flanges are equal and the yield strengths are equal, $[\alpha A_e F_{yf}]_{LS} = [\alpha A_e F_{yf}]_{SS}$ and $R_g = 1.0$

$$F_{cf} = \frac{\left(\frac{f_{cf}}{R_h}\right) + \alpha \phi_f F_{yf} R_g}{2} = \frac{\left(\frac{8.59}{1.0}\right) + (1.0)(1.0)(50)(1.0)}{2} = 29.30 \text{ ksi}$$

$$F_{cf} = 0.75 \alpha \phi_f F_{yf} R_g = 0.75(1.0)(1.0)(50)(1.0) = 37.50 \text{ ksi}$$

Therefore, F_{cf} is taken as 37.50 ksi.

For the negative live load bending case, the minimum design force for the controlling flange (top flange), P_{cf} , is taken equal to F_{cf} times the effective area, A_e , of the controlling flange. The minimum design force, P_{cf} , is computed as:

$$P_{cf} = F_{cf} A_{e, \text{top flg}} = (37.50)(13.41) = 503 \text{ kips (T)}$$

For the negative live load bending case, the minimum design stress for the noncontrolling flange (bottom flange), F_{ncf} , is computed in accordance with Eq. 6.13.6.1.4c-4. First, it is necessary to compute R_{cf} , the absolute value of the ratio of F_{cf} to f_{cf} for the controlling flange:

$$R_{cf} = \left| \frac{F_{cf}}{f_{cf}} \right| = \left| \frac{37.50}{8.59} \right| = 4.37$$

Compute F_{ncf} , in accordance with Eq. (6.13.6.1.4c-4):

$$F_{ncf} = R_{cf} \left| \frac{f_{ncf}}{R_h} \right| = (4.37) \left| \frac{-7.09}{1.0} \right| = 30.98 \text{ ksi}$$

$$F_{ncf} = 0.75 \alpha \phi_f F_{yf} R_g = 0.75(1.0)(1.0)(50)(1.0) = 37.50 \text{ ksi}$$

Therefore, F_{ncf} is taken as 37.50 ksi.

For the negative live load bending case, the minimum design force for the noncontrolling flange (bottom flange), P_{ncf} , is taken equal to F_{ncf} times the effective area, A_e , of the noncontrolling flange. The minimum design force, P_{ncf} , is computed as:

$$P_{ncf} = F_{ncf} A_{e, \text{bot flg}} = (37.50)(51.88) = 1,946 \text{ kips (C)}$$

7.14.5.3 Summary of Flexure Strength Limit State Design Forces

A summary of the factored design forces for the bottom and top flange splices at the strength limit state is as follows:

$$\begin{aligned}\text{Top Flange: } P_{ncf} &= 600 \text{ kips (C)} \\ P_{cf} &= 503 \text{ kips (T)}\end{aligned}$$

$$\begin{aligned}\text{Bottom Flange: } P_{cf} &= 1,646 \text{ kips (T)} \\ P_{ncf} &= 1,946 \text{ kips (C)}\end{aligned}$$

7.14.5.4 Strength Limit State Check of Top Flange Splice Bolts

St. Venant torsional shear is not considered in the top flanges of tub girders. The composite deck is assumed to resist the majority of the torsional shear acting on the top of the tub girder once the section is closed. Flange lateral bending in the top flange is also not considered after the deck has hardened and the flange is continuously braced.

Therefore, compute the factored longitudinal force in each bolt resulting from the major-axis bending by dividing the governing flange design force by the number of bolts on one side of the splice:

$$R_u = F_{\text{top flg bolt}} = \frac{P_{ncf}}{12} = \frac{600}{12} = 50.00 \text{ kips/bolt}$$

Check that the factored bolt force, R_u is less than the factored shear resistance of one bolt, R_r , calculated previously as 55.4 kips/bolt:

$$R_u = 50.00 \text{ kips/bolt} < R_r = 55.4 \text{ kips/bolt} \quad \text{OK}$$

Since a fill plate is not required for the top flange splice, no reduction in the bolt design shear resistance is required as specified in Article 6.13.6.1.5.

7.14.5.5 Strength Limit State Check of Bottom Flange Splice Bolts

Determine the St. Venant torsional shear in the bottom flange of the tub girder at the strength limit state. As discussed previously, the longitudinal warping stresses do not need to be considered in the design of bolted box flange splices (bottom flange of tub) at the strength limit state. Compute the Strength I factored torques acting on the noncomposite and composite sections from the analysis results provided in Table 16. The negative live load torque is used, as it controls over the positive live load torque.

$$\text{Factored Noncomposite Torque} = 1.25[-36 + (-125)] = -201 \text{ kip-ft}$$

$$\text{Factored Composite Torque} = 1.25(-58) + 1.5(-76) + 1.75(-517) = -1,091 \text{ kip-ft}$$

The enclosed area of the noncomposite tub girder, A_o , was previously computed to be 7,921 in.² The factored St. Venant torsional shear in the bottom flange due to the noncomposite loads is computed as:

$$V_{NC\ botflg} = \frac{T}{2A_o} b_f = \frac{|-201|(12)}{2(7,921)} (81) = 12.3 \text{ kips}$$

The enclosed area of the composite tub girder, A_o , was previously computed to be 8,750 in.² The factored St. Venant torsional shear in the bottom flange due to the composite loads is computed as:

$$V_{C\ botflg} = \frac{T}{2A_o} b_f = \frac{|-1,091|(12)}{2(8,750)} (81) = 60.6 \text{ kips}$$

Therefore, the total factored St. Venant torsional shear force at the centerline of the splice is computed as:

$$V_{tot} = 12.3 + 60.6 = 72.9 \text{ kips}$$

Because the St. Venant torsional shear is assumed to act at the centerline of the field splice, it produces a lateral moment on the bottom flange bolt group on each side of the splice. The factored lateral moment on the bolt group, computed at the centroid of the bolt group is:

$$M_{LAT} = (72.9) \left(\frac{4.5}{2} + \frac{4.5}{2} \right) = 328.1 \text{ kip} \cdot \text{in.}$$

It should be noted that in accordance with Article C6.13.6.1.4c, at the strength limit state, the factored torsional shear does not need to be multiplied by the factor, R_{cf} , when computing the moment in the splice due to the torsional shear.

Compute the factored longitudinal component of force in the critical bolt due to the factored lateral moment in the bottom flange, noting that the transverse distance from the centroid of the bolt group to the critical bolt is 36.25 inches, and the polar moment of inertia of the bolt group, I_p , was previously computed as 19,859 in.²:

$$F_{Long\ lat} = \frac{|328.1|(36.25)}{19,859} = 0.60 \text{ kips/bolt}$$

Compute the factored transverse component of force in the critical bolt due to the factored lateral moment in the bottom flange, noting that the longitudinal distance from the centroid of the bolt group to the critical bolt is 2.25 inches:

$$F_{Trans\ lat} = \frac{|328.1|(2.25)}{19,859} = 0.04 \text{ kips/bolt}$$

Compute the factored longitudinal force in each bolt resulting from the major-axis bending by dividing the governing design flange force by the number of bolts on one side of the splice:

$$F_{\text{botflg bolt}} = \frac{P_{\text{cf}}}{40} = \frac{1,946}{40} = 48.65 \text{ kips/bolt}$$

Therefore, the total factored longitudinal force in the critical bolt is computed as:

$$F_{\text{Long tot}} = 0.60 + 48.65 = 49.25 \text{ kips/bolt}$$

Compute the factored transverse force in each bolt resulting from the factored St. Venant torsional shear force by dividing the shear force by the number of bolts on one side of the splice:

$$F_{\text{Trans Shear}} = \frac{(72.9)}{40} = 1.82 \text{ kips/bolt}$$

Therefore, the total factored transverse force in the critical bolt is computed as:

$$F_{\text{Trans tot}} = 1.82 + 0.04 = 1.86 \text{ kips/bolt}$$

Compute the resultant force on the critical bolt:

$$R_u = \sum F = \sqrt{49.25^2 + 1.86^2} = 49.29 \text{ kips/bolt}$$

Check that the factored bolt force, R_u is less than the factored shear resistance of one bolt, R_r , calculated previously as 55.4 kips/bolt:

$$R_u = 49.29 \text{ kips/bolt} < R_r = 55.4 \text{ kips/bolt} \quad \text{OK}$$

Since a fill plate is not required for the bottom flange splice, no reduction in the bolt design shear resistance is required as specified in Article 6.13.6.1.5.

7.14.5.6 Strength Limit State Check of Web Splice Bolts

In accordance with Article 6.13.6.1.4b, web splice plates and their connections are to be designed for shear, the moment due to the eccentricity of the shear at the point of the splice, and the portion of the flexural moment assumed to be resisted by the web at the point of the splice. Additionally, for horizontally curved tub girders, the shear is to be taken as the sum of the flexural and St. Venant torsional shears in the web. Also, for inclined webs, the web splice and connections are to be designed for the component of shear in the plane of the web.

For this design example, only the positive live load bending case will be used to illustrate the check of the web splice for the strength limit state.

As a minimum, at the strength limit state, the design shear, V_{uw} , is to be taken as follows:

If $V_u < 0.5 \phi_v V_n$, then:

$$V_{uw} = 1.5V_u \quad \text{Eq. (6.13.6.1.4b-1)}$$

Otherwise:

$$V_{uw} = \frac{(V_u + \phi_v V_n)}{2} \quad \text{Eq. (6.13.6.1.4b-2)}$$

where:

ϕ_v = resistance factor for shear specified in Article 6.5.4.2 ($\phi_v = 1.0$)

V_u = factored shear at the point of the splice (kip)

V_n = nominal shear resistance determined as specified in Articles 6.10.9.2 and 6.10.9.3 for unstiffened and stiffened webs, respectively (kip)

Determine the vertical design shear, V_{uw} , for the web splice design according to the provisions of Article 6.13.6.1.4b.

First, compute the Strength I factored girder shear, V_u , from the analysis results provided in Table 16. The girder shear provided in Table 16 is the summation of the flexural shear and St. Venant torsional shear in the critical web, therefore additional calculations for the torsional shear in the web are not required. By inspection, the negative live load shear case governs.

$$V_u = |1.25 [-17 + (-69) + (-12)] + 1.5 (-16) + 1.75 (-85)| = 295 \text{ kips}$$

Compute the shear in the plane of the web.

$$V_{ui} = \frac{295}{\cos(14.04^\circ)} = 304 \text{ kips}$$

Compute the nominal shear resistance of the 0.5625-inch-thick web at the splice according to the provisions of Articles 6.10.9.2 and 6.10.9.3 for unstiffened and stiffened webs, respectively. For this design example, separate calculations indicate that transverse stiffeners are required at the splice, therefore Article 6.10.9.3 is employed. A stiffener spacing equal to the internal cross frame spacing used on Girder G2 is assumed, where $d_o = 196$ inches.

It is necessary to compute the nominal shear resistance, V_n , in order to determine the appropriate design shear, V_{uw} . The nominal shear resistance of an interior web panel is computed in accordance with Article 6.10.9.3.2. First, determine if Eq. 6.10.9.3.2-1 is satisfied.

According to Article 6.11.9, for box flanges, b_{fc} (in this case) is to be taken as one-half the effective flange width between webs in checking Eq. 6.10.9.3.2-1, but not to exceed 18 times the

thickness of the box flange. Therefore, $(81.0/2) = 40.5 \text{ in.} > 18(0.625) = 11.25 \text{ in.}$ Use $b_{fc} = 11.25 \text{ in.}$ to check Eq. 6.10.9.3.2-1 as follows:

$$\frac{2Dt_w}{(b_{fc} t_{fc} + b_{ft} t_{ft})} \leq 2.5 \quad \text{Eq. (6.10.9.3.2-1)}$$

$$\frac{2Dt_w}{(b_{fc} t_{fc} + b_{ft} t_{ft})} = \frac{2(80.40)(0.5625)}{((11.25)(0.625) + (16)(1.0))} = 3.93 > 2.5$$

Since Eq. 6.10.9.3.2-1 is not satisfied, the nominal shear resistance, V_n , is computed in accordance with Eq. (6.10.9.3.2-8).

$$V_n = V_p \left[C + \frac{0.87(1-C)}{\left(\sqrt{1 + \left(\frac{d_o}{D} \right)^2} + \frac{d_o}{D} \right)} \right] \quad \text{Eq. (6.10.9.3.2-8)}$$

where:

- V_n = nominal shear resistance of the web panel (kip)
- V_p = plastic shear force (kip)
- C = ratio of shear-buckling resistance to the shear yield strength
- d_o = transverse stiffener spacing (in.)

The plastic shear force, V_p , is computed according to Eq. 6.10.9.3.2-3 as follows:

$$V_p = 0.58 F_{yw} D t_w \quad \text{Eq. (6.10.9.3.2-3)}$$

Determine which equation is to be used to compute the ratio of shear-buckling resistance to the shear yield strength, C .

$$k = 5 + \frac{5}{\left(\frac{d_o}{D} \right)^2} = 5 + \frac{5}{\left(\frac{196}{80.40} \right)^2} = 5.84 \quad \text{Eq. (6.10.9.3.2-7)}$$

Since:

$$\frac{D}{t_w} = \frac{80.4}{0.5625} = 142.9 > 1.40 \sqrt{\frac{Ek}{F_{yw}}} = 1.40 \sqrt{\frac{29,000(5.84)}{50}} = 81$$

$$C = \frac{1.57}{\left(\frac{D}{t_w}\right)^2} \left(\frac{Ek}{F_{yw}} \right) \quad \text{Eq. (6.10.9.3.2-6)}$$

$$C = \frac{1.57}{(142.9)^2} \left(\frac{29,000(5.84)}{50} \right) = 0.260$$

V_p is the plastic shear force and is calculated as follows:

$$V_p = 0.58 F_{yw} D t_w \quad \text{Eq. (6.10.9.3.2-3)}$$

$$V_p = 0.58 (50.0)(80.40)(0.5625) = 1,312 \text{ kips}$$

Therefore,

$$V_n = (1,312) \left[0.260 + \frac{0.87(1 - 0.260)}{\sqrt{1 + \left(\frac{196.0}{80.40}\right)^2 + \frac{196}{80.40}}} \right] = 508 \text{ kips}$$

Checking compliance with Eq. 6.10.9.1-1:

$$V_{ui} = 304 \text{ kips} < \phi_v V_n = (1.0)(508) = 508 \text{ kips} \quad \text{OK}$$

Since $V_{ui} = 304 \text{ kips} > 0.5\phi_v V_n = 254 \text{ kips}$, the design shear, V_{uw} , is computed in accordance with Eq. 6.13.6.1.4b-2:

$$V_{uw} = \frac{(V_{ui} + \phi_v V_n)}{2} = \frac{(304 + (1.0)(508))}{2} = 406 \text{ kips} \quad \text{Eq. (6.13.6.1.4b-2)}$$

The moment, M_{uv} , due to the eccentricity of the design shear, V_{uw} , from the centerline of the splice to the centroid of the web splice bolt group is computed as follows:

$$M_{uv} = V_{uw} e$$

$$M_{uv} = (406) \left(\frac{3}{2} + \frac{4.5}{2} \right) \left(\frac{1}{12} \right) = 127 \text{ kip-ft}$$

Determine the portion of the design moment resisted by the web, M_{uw} , and the design horizontal force resultant in the web, H_{uw} , according to the recommended provisions of Article

C6.13.6.1.4b. M_{uw} and H_{uw} are applied at the mid-depth of the web. Separate calculations, not shown, indicate that the positive live load bending case controls the design of the web splice.

As computed previously for the positive live load bending case:

$$\begin{aligned} f_{cf} &= 24.72 \text{ ksi} \\ F_{cf} &= 37.50 \text{ ksi} \\ f_{ncf} &= -11.50 \text{ ksi} \\ R_{cf} &= 1.52 \end{aligned}$$

Using the above values, use the following equations to compute a suggested design moment, M_{uw} , and a design horizontal resultant, H_{uw} that will be applied at the mid-depth of the web for designing the connections:

$$M_{uw} = \frac{t_w D^2}{12} |R_h F_{cf} - R_{cf} f_{ncf}| \quad \text{Eq. (C6.13.6.1.4b-1)}$$

$$M_{uw} = \frac{(0.5625)(78.0)^2}{12} |(1.0)(37.50) - (1.52)(-11.50)| \left(\frac{1}{12}\right) = 1,307 \text{ kip-ft}$$

$$H_{uw} = \frac{t_w D}{2} (R_h F_{cf} + R_{cf} f_{ncf}) \quad \text{Eq. (C6.13.6.1.4b-2)}$$

$$H_{uw} = \frac{(0.5625)(78.0)}{2} [(1.0)(37.50) + (1.52)(-11.50)] = 439 \text{ kips}$$

The total factored moment applied to the web splice is the sum of the moment caused by the vertical shear, M_v , and the moment computed by Eq. C6.13.6.1.4b-1, M_{uw} :

$$M_{tot} = M_{uv} + M_{uw} = 127 + 1,307 = 1,434 \text{ kip-ft}$$

Compute the factored force in each bolt resulting from the vertical shear, by dividing the factored shear by the number of bolts on one side of the splice:

$$F_{\text{Shear vert}} = \frac{V_{uw}}{N_b} = \frac{406}{40} = 10.15 \text{ kips/bolt}$$

However, the above bolt force, $F_{\text{Shear vert}}$, is in the vertical plane, and must be resolved to the inclined plane of the web. Therefore, the in-plane bolt force is computed as:

$$F_S = \frac{F_{\text{Shear vert}}}{\cos(\theta)} = \frac{10.15}{\cos(14.04^\circ)} = 10.46 \text{ kips/bolt}$$

Compute the in-plane factored force in each bolt resulting from the horizontal force resultant, H_{uw} , by dividing the factored resultant by the number of bolts on one side of the splice:

$$F_H = \frac{H_{uw}}{N_b} = \frac{439}{40} = 10.98 \text{ kips/bolt}$$

Compute the in-plane factored vertical component of force in the critical bolt due to the total factored moment on the splice, noting that the horizontal distance from the centroid of the bolt group to the critical bolt is 1.5 inches:

$$F_{Mv} = \frac{M_{totx}}{I_p} \left(\frac{1}{\cos(\theta)} \right) = \frac{(1,434)(12)(1.5)}{18,793} \left(\frac{1}{\cos(14.04^\circ)} \right) = 1.42 \text{ kips/bolt}$$

Compute the in-plane factored horizontal component of force in the critical bolt due to the total factored moment on the splice, noting that the vertical distance from the centroid of the bolt group to the critical bolt is 35.625 inches:

$$F_{Mh} = \frac{M_{toty}}{I_p} = \frac{(1,434)(12)(35.625)}{18,793} = 32.62 \text{ kips/bolt}$$

Compute the resultant in-plane force on the critical bolt:

$$R_u = F_r = \sqrt{(F_s + F_{Mv})^2 + (F_H + F_{Mh})^2}$$

$$R_u = \sqrt{(10.46 + 1.42)^2 + (10.98 + 32.62)^2} = 45.2 \text{ kips/bolt}$$

Check that the factored resultant force on the critical bolt, R_u is less than the factored slip resistance of one bolt, R_r , calculated previously as 55.4 kips/bolt:

$$R_u = 45.2 \text{ kips/bolt} < R_r = 55.4 \text{ kips/bolt} \quad \text{OK}$$

7.14.5.7 Strength Limit State Check of Top Flange Splice Plates

The width of the outside splice plate should be at least as wide as the width of the narrowest flange at the splice. In the case of this design example, the width of the top flange is the same on either side of the splice. Therefore, the following top flange splice plates are used:

Outer plate: 0.5 in. by 16.0 in. plate, Grade 50 Steel

Inner plates: Two 0.625 in. by 6 in. plates, Grade 50 Steel

As discussed in Article C6.13.6.1.4c, if the combined area of the inner splice plates is within 10 percent of the area of the outside plate, then both the inner and outer plates may be designed for one-half of the flange design force. Such is the case for this top flange splice. Also, since this

10 percent provision is satisfied, double shear can be assumed in designing the connections. If the areas differ by more than 10 percent, the design force in each splice plate and its connection at the strength limit state should be determined by multiplying the flange design force by the ratio of the area of the splice plate under consideration to the total area of the inner and outer splice plates. In this case, the shear resistance of the connection would be checked for the maximum calculated splice plate force acting on a single shear plane.

Article 6.13.5.2 specifies that splice plates in tension at the strength limit state are to be investigated for yielding on the gross section, fracture on the net section, and block shear rupture. Article 6.13.6.1.4c specifies that the design force for splice plates subjected to compression is not to exceed the factored resistance, R_r , in compression taken as:

$$R_r = \phi_c F_y A_s \quad \text{Eq. (C6.13.6.1.4c-5)}$$

where:

$$\begin{aligned} \phi_c &= \text{resistance factor for compression specific in Article 6.5.4.2 } (\phi_c = 0.95) \\ F_y &= \text{specified minimum yield strength of the splice plate (ksi)} \\ A_s &= \text{gross area of the splice plate (in.}^2\text{)} \end{aligned}$$

Flange lateral bending is ignored for the top flange splice plates at the strength limit state because the flange is continuously braced by the hardened concrete deck. St. Venant torsional shears are also typically ignored in the design of the top flanges of tub girders once the flange is continuously braced by the hardened concrete deck, as the deck is assumed to resist the majority of torsional shear acting on the top of the tub girder. Therefore, St Venant torsional shear is not considered in the design of the top flange splice plates. Lastly, as discussed previously, longitudinal warping stresses due to cross-section distortion may be ignored at the strength limit state for the design of the top and bottom flange splices.

For the positive live load bending case, the top flange is the noncontrolling flange and is subjected to compression. The total design force was previously computed as 600 kips. The factored compressive resistance, R_r , is computed in accordance with Eq. C6.13.6.1.4c-5:

$$R_r = \phi_c F_y A_s \quad \text{Eq. (C6.13.6.1.4c-5)}$$

For the outer top flange splice plate:

$$R_r = (0.95)(50)(0.5)(16.0) = 380 \text{ kips} > \frac{600}{2} = 300 \text{ kips} \quad \text{OK}$$

For the two inner top flange splice plates:

$$R_r = (0.95)(50)(2)(0.625)(6.0) = 356 \text{ kips} > \frac{600}{2} = 300 \text{ kips} \quad \text{OK}$$

For the negative live load bending case, the top flange is the controlling flange and is subjected to tension. The total design force was previously computed as 503 kips. As specified in Article 6.8.2.1, the factored tensile resistance of the splice plates, P_r , is taken as the lesser of the resistances given by following two equations:

$$P_r = \phi_y P_{ny} = \phi_y F_y A_g \quad \text{Eq. (6.8.2.1-1)}$$

$$P_r = \phi_u P_{nu} = \phi_u F_u A_n R_p U \quad \text{Eq. (6.8.2.1-2)}$$

where:

P_{ny} = nominal tensile resistance for yielding in the gross section (kip)

F_y = specified minimum yield strength (ksi)

A_g = gross cross-sectional area of the member (in.^2)

F_u = tensile strength (ksi)

A_n = net area of the member as specified in Article 6.8.3 (in.^2), but not to be taken greater than 85 percent of the gross area of the splice plate as specified in Article 6.13.5.2

R_p = reduction factor for holes taken equal to 0.90 for bolt holes punched full size and 1.0 for bolt holes drilled full size or subpunched and reamed to size; 1.0 is assumed for this design example

U = reduction factor for shear lag to be taken as 1.0 for splice plates as specified in Article 6.13.5.2

ϕ_y = resistance factor for yielding of tension members as specified in Article 6.5.4.2 ($\phi_y = 0.95$)

ϕ_u = resistance factor for fracture of tension members as specified in Article 6.5.4.2 ($\phi_u = 1.0$)

Compute the net area, A_n , for the outer and inner splice plates.

Outer splice plate:

$$A_n = [16.0 - 4(0.875 + 0.0625)](0.50) = 6.13 \text{ in.}^2 < 0.85A_g = 0.85(16.0)(0.50) = 6.8 \text{ in.}^2$$

Inner splice plates:

$$A_n = 2[6.0 - 2(0.875 + 0.0625)](0.625) = 5.16 \text{ in.}^2 < 0.85A_g = 0.85(2)(6.0)(0.625) = 6.4 \text{ in.}^2$$

Compute the factored tensile resistance of the outer splice plate:

$$P_r = \phi_y P_{ny} = \phi_y F_y A_g = 0.95 (50) (16.0) (0.50) = 380 \text{ kips}$$

$$P_r = \phi_u P_{nu} = \phi_u F_u A_n R_p U = 0.80 (65) (6.13) (1.0) (1.0) = 319 \text{ kips}$$

Compute the factored tensile resistance of the inner splice plates:

$$P_r = \phi_y P_{ny} = \phi_y F_y A_g = 0.95 (50) (2) (6.0) (0.625) = 356 \text{ kips}$$

$$P_r = \phi_u P_{nu} = \phi_u F_u A_n R_p U = 0.80 (65) (5.16) (1.0) (1.0) = 268 \text{ kips}$$

Check that the minimum resistance provided by the splice plates, 268 kips, is more than one-half the design force:

$$P_r = 268 \text{ kips} > \frac{503}{2} = 252 \text{ kips} \quad \text{OK}$$

7.14.5.8 Strength Limit State Check of Top Flange Splice Plates - Bearing

Check the bearing of the bolts on the connected material at the strength limit state for the design force of 600 kips in the top flange. The design bearing resistance, R_n , is computed in accordance with Article 6.13.2.9. Check the outer splice plate as it is thinner than the inner plates, and check the top flange of the girder itself.

For the outer plate, calculate the clear distance between holes and the clear end distance and compare to $2.0d$ (d = bolt diameter) to determine the equation to be used to compute the bearing resistance.

The center-to-center distance between the bolts in the direction of the force is 3.0 in. Therefore:

$$\text{Clear distance between holes} = 3.0 - 0.9375 = 2.06 \text{ in.}$$

For the four bolts adjacent to the end of the splice plate, the end distance is assumed to be 1.5 in. Therefore, the clear distance between the edge of the holes and the end of the splice plate is:

$$\text{Clear end distance} = 1.5 - 0.9375 / 2 = 1.03 \text{ in.}$$

The value of $2d$ is equal to 1.75 in. for a 7/8 inch diameter bolt. Since the clear end distance is less than $2.0d$, Eq. 6.13.2.9-2 is to be used to compute the nominal bearing resistance, R_n :

$$R_n = 1.2 L_c t F_u = 1.2(1.03)(0.50)(65) = 40.2 \text{ kips/bolt}$$

The factored bearing resistance, R_r , is computed as:

$$R_r = \phi_{bb} R_n \quad \text{Eq. (6.13.2.2-2)}$$

where:

$$\phi_{bb} = \text{resistance factor for bolts bearing on material specified in Article 6.5.4.2 } (\phi_{bb} = 0.80)$$

Therefore, for the outer splice plate, the factored bearing resistance at a single bolt hole is:

$$R_r = \phi_{bb} R_n = (0.80)(40.2) = 32.2 \text{ kips/bolt}$$

For the outer plate, the factored bearing resistance for the connection is computed by multiplying the single bolt hole resistance by the number of bolts in the connection. Check this total resistance against the force in the outer plate, which is one-half of the design force of 600 kips:

$$P_r = (12 \text{ bolts})(32.2 \text{ kips/bolt}) = 386 \text{ kips} > \frac{600}{2} = 300 \text{ kips} \quad \text{OK}$$

For the girder top flange itself, calculate the clear distance between holes and the clear end distance and compare to $2.0d$ to determine the equation to be used to compute the bearing resistance.

The center-to-center distance between the bolts in the direction of the force is 3.0 in. Therefore:

$$\text{Clear distance between holes} = 3.0 - 0.9375 = 2.06 \text{ in.}$$

For the four bolts adjacent to the end of the girder at the splice, the end distance is conservatively assumed to be 1.5 in. (actual end distance is 3.0 in. per Figure 19). Therefore, the clear distance between the edge of the holes and the edge of the girder is:

$$\text{Clear end distance} = 1.5 - 0.9375 / 2 = 1.03 \text{ in.}$$

The value of $2d$ is equal to 1.75 in. for a 7/8 inch diameter bolt. Since the clear end distance is less than $2.0d$, Eq. 6.13.2.9-2 is to be used to compute the nominal bearing resistance, R_n :

$$R_n = 1.2 L_c t F_u = 1.2(1.03)(1.0)(65) = 80.3 \text{ kips/bolt}$$

Therefore, for the girder top flange, the factored bearing resistance at a single bolt hole is:

$$R_r = \phi_{bb} R_n = (0.8)(80.3) = 64.2 \text{ kips/bolt}$$

For the top flange, the factored bearing resistance for the connection is computed by multiplying the single bolt hole resistance by the number of bolts in the connection. Check this total resistance against the force in the top flange, which is equal to 600 kips:

$$P_r = (12 \text{ bolts})(64.2 \text{ kips/bolt}) = 770 \text{ kips} > 600 \text{ kips} \quad \text{OK}$$

7.14.5.9 Strength Limit State Check of Bottom Flange Splice Plates

The following bottom flange splice plates are used:

Outer plate: 0.375 in. by 75.5 in. plate, Grade 50 Steel

Inner plates: Two 0.375 in. by 36.75 in. plates, Grade 50 Steel

Since the inner splice plate must be partially split to accommodate the longitudinal stiffener on the Field Section 2 side of the splice, as shown in Figure 20, the plate is conservatively treated as

two separate plates in the subsequent calculations although this is physically not the case. The combined area of the inner splice plates is within 10 percent of the area of the outside plate, therefore the inner and outer plates may be designed for one-half of the flange design force.

For the positive live load bending case, the bottom flange is the controlling flange with a design force of 1,646 kips in tension. For the negative live load bending case, the bottom flange is the noncontrolling flange with a design force of 1,946 kips in compression. The St. Venant torsional shear was computed previously for the bottom flange bolt design at the strength limit state. The factored moment resulting from the eccentricity of the torsional shear on the bolt group was computed as 328.1 kip-in.

Flange splice plates subject to compression at the strength limit state are checked for yielding on the gross section at the strength limit state, in accordance with Eq. C6.13.6.1.4c-5. In the case of the bottom flange, the flange should be checked for the combined applied stress due to the flange design compression force and lateral bending caused by eccentricity of the torsional shear. For yielding of the bottom flange splice plates, the total combined stress on the splice plates can be computed as:

$$f_{\text{botflg(C)}} = \frac{P_{\text{DesignForce}}}{A_{\text{SPL,g}}} + \frac{M_{\text{LAT}}}{S_{\text{SPL,g}}}$$

where:

$A_{\text{SPL,g}}$ = gross cross-sectional area of the splice plates (in.²)

M_{LAT} = moment resulting from eccentricity of the torsional shear (kip-in.)

$S_{\text{SPL,g}}$ = gross lateral section modulus of the splice plates (in.³)

The gross area of the bottom flange splice plates is computed as:

$$A_{\text{SPL,g}} = (0.375)(75.5) + 2(0.375)(36.75) = 55.9 \text{ in.}^2$$

The gross lateral section modulus of the outer and inner splice plates is computed as:

$$S_{\text{SPL,g}} = \frac{\left(\frac{1}{12}\right)(0.375)(75.5)^3 + 2\left(\frac{1}{12}\right)(0.375)(36.75)^3 + 2(0.375)(36.75)(19.375)^2}{\frac{75.5}{2}} = 713 \text{ in.}^3$$

Compute the total combined stress acting on the outer and inner bottom flange splice plates:

$$f_{\text{botflg(C)}} = \frac{1,946}{55.9} + \frac{328.1}{713} = 35.3 \text{ ksi}$$

Check that the total combined stress is less than the factored compressive resistance in terms of stress, as specified in Eq. C6.13.6.1.4c-5:

$$f_{\text{bot flg (C)}} = 35.3 \text{ ksi} < \phi_c F_y = (0.95)(50) = 47.5 \text{ ksi} \quad \text{OK}$$

Flange splice plates subject to tension at the strength limit state are investigated for yielding on the gross section and fracture on the net section. First, check yielding on the gross section for the tension design force. Compute the total combined stress on the splice plates as:

$$f_{\text{botflg (T), yield}} = \frac{P_{\text{DesignForce}}}{A_{\text{SPL,g}}} + \frac{M_{\text{LAT}}}{S_{\text{SPL}}} = \frac{1,646}{55.9} + \frac{328.1}{713} = 29.9 \text{ ksi}$$

Check that the total combined stress is less than the factored tension resistance in terms of stress, as specified in Eq. 6.8.2.1-1:

$$f_{\text{botflg (T), yield}} = 29.9 \text{ ksi} < \phi_y F_y = (0.95)(50) = 47.5 \text{ ksi} \quad \text{OK}$$

For fracture on the net section, the combined stress in the bottom flange splice plates can be computed as:

$$f_{\text{botflg (T), frac}} = \frac{P_{\text{DesignForce}}}{A_{\text{SPL,n}}} + \frac{M_{\text{LAT}}}{S_{\text{SPL,n}}}$$

where:

$$A_{\text{SPL,n}} = \text{net cross-sectional area of the splice plates (in.}^2\text{)}$$

$$S_{\text{SPL,n}} = \text{net lateral section modulus of the splice plates (in.}^4\text{)}$$

The net cross section areas of the outer and inner splice plates are computed as:

$$\text{Outer plate: } A_{\text{SPL,n}} = [75.5 - 20(0.875 + 0.0625)](0.375) = 21.28 \text{ in.}^2$$

$$\text{Inner plates: } A_{\text{SPL,n}} = 2[36.75 - 10(0.875 + 0.0625)](0.375) = 20.53 \text{ in.}^2$$

$$\text{Total: } A_{\text{SPL,n}} = 21.28 + 20.53 = 41.81 \text{ in.}^2$$

According to Article 6.13.5.2, for splice plates subjected to tension, A_n must not exceed $0.85A_g$. Verify that is provision is satisfied:

$$\text{Outer plate: } A_{\text{SPL,n}} = 21.28 \text{ in.}^2 < 0.85(75.5)(0.375) = 24.07 \text{ in.}^2 \quad \text{OK}$$

$$\text{Inner plates: } A_{\text{SPL,n}} = 20.53 \text{ in.}^2 < 0.85(2)(36.75)(0.375) = 23.43 \text{ in.}^2 \quad \text{OK}$$

$$\text{Total: } A_{\text{SPL},n} = 41.81 \text{ in.}^2 < 24.07 + 23.43 = 47.5 \text{ in.}^2 \quad \text{OK}$$

The net lateral section modulus of the outer and inner splice plates, $S_{\text{SPL},n}$, can be computed as follows:

$$S_{\text{SPL},n} = \frac{I_{\text{SPL},g} - \sum_{i=1}^{N_b} A_h d_i^2}{c}$$

where:

- $I_{\text{SPL},g}$ = gross lateral moment of inertia of the splice plates (in.²)
- A_h = area of a single bolt hole (in.²)
- d_i = distance from center of bolt hole to lateral neutral axis (in.)
- c = distance from lateral neutral axis to edge of splice plates (in.)

$$I_{\text{SPL},g} = \left(\frac{1}{12}\right)(0.375)(75.5)^3 + 2 \left[\left(\frac{1}{12}\right)(0.375)(36.75)^3 + (0.375)(36.75)(19.375)^2 \right] = 26,898 \text{ in.}^4$$

$$\sum_{i=1}^{N_b} A_h d_i^2 = 2(0.375)(0.9375)[2.5^2 + 6.25^2 + 10.0^2 + 13.75^2 + 17.5^2 + 21.25^2 + 25^2 + 28.75^2 + 32.5^2 + 36.25^2]$$

$$\sum_{i=1}^{N_b} A_h d_i^2 = 3,455 \text{ in.}^3$$

Therefore, $S_{\text{SPL},n}$, is computed as:

$$S_{\text{SPL},n} = \frac{26,898 - 3,455}{\frac{75.5}{2}} = 621 \text{ in.}^4$$

The combined stress in the bottom flange, for checking fracture, is then computed as:

$$f_{\text{botflg (T), frac}} = \frac{P_{\text{Design Force}}}{A_{\text{SPL},n}} + \frac{M_{\text{LAT}}}{S_{\text{SPL},n}} = \frac{1,646}{41.81} + \frac{328.1}{621} = 39.9 \text{ ksi}$$

Check that the total combined stress is less than the factored tension resistance for fracture, in terms of stress as specified in Eq. 6.8.2.1-2:

$$f_{\text{botflg (T), frac}} = 39.9 \text{ ksi} < \phi_u F_u R_p U = (0.80)(65)(1.0)(1.0) = 52.0 \text{ ksi} \quad \text{OK}$$

7.14.5.10 Strength Limit State Check of Bottom Flange Splice Plates - Bearing

Check the bearing of the bolts on the connected material at the strength limit state for the design force of 1,946 kips in the bottom flange. The design bearing resistance, R_n , is computed in accordance with Article 6.13.2.9. Check the outer splice plate as it is the same thickness as the inner plates, and check the bottom flange of the girder itself.

For the outer plate, calculate the clear distance between holes and the clear end distance and compare to $2.0d$ (d = bolt diameter) to determine the equation to be used to compute the bearing resistance.

The center-to-center distance between the bolts in the direction of the force is 4.5 in. Therefore:

$$\text{Clear distance between holes} = 4.5 - 0.9375 = 3.56 \text{ in.}$$

For the 20 bolts adjacent to the end of the splice plate, the end distance is assumed to be 1.5 in. Therefore, the clear distance between the edge of the holes and the end of the splice plate is:

$$\text{Clear end distance} = 1.5 - 0.9375 / 2 = 1.03 \text{ in.}$$

The value of $2d$ is equal to 1.75 in. for a 7/8 inch diameter bolt. Since the clear end distance is less than $2.0d$, Eq. 6.13.2.9-2 is to be used to compute the nominal bearing resistance, R_n :

$$R_n = 1.2 L_c t F_u = 1.2(1.03)(0.375)(65) = 30.1 \text{ kips/bolt}$$

The factored bearing resistance, R_r , is computed as:

$$R_r = \phi_{bb} R_n \quad \text{Eq. (6.13.2.2-2)}$$

where:

$$\phi_{bb} = \text{resistance factor for bolts bearing on material specified in Article 6.5.4.2 } (\phi_{bb} = 0.80)$$

Therefore, for the outer splice plate, the factored bearing resistance at a single bolt hole is:

$$R_r = \phi_{bb} R_n = (0.80)(30.1) = 24.1 \text{ kips/bolt}$$

For the outer plate, the factored bearing resistance for the connection is computed by multiplying the single bolt hole resistance by the number of bolts on one side of the connection. Check this total resistance against the force in the outer plate, which is one-half of the design force of 1,946 kips:

$$P_r = (40 \text{ bolts})(24.1 \text{ kips/bolt}) = 964 \text{ kips} \cong \frac{1,946}{2} = 973 \text{ kips} \quad \text{Say OK}$$

The factored bearing resistance of the outer and inner plates can be increased by slightly increasing the clear end distance of the bolts adjacent to the end of the splice plate. For example, if the end distance is increased from 1.5 in. to 1.75 in., the clear end distance (L_c) is 1.28 in., and R_r is 30.0 kips/bolt, resulting in a total connection factored bearing resistance of 1,200 kips.

For the girder bottom flange itself, calculate the clear distance between holes and the clear end distance and compare to $2.0d$ to determine the equation to be used to compute the bearing resistance.

The center-to-center distance between the bolts in the direction of the force is 4.5 in. Therefore:

$$\text{Clear distance between holes} = 4.5 - 0.9375 = 3.56 \text{ in.}$$

For the 20 bolts adjacent to the end of the girder at the splice, the end distance is 2.0 in. (see Figure 20). Therefore, the clear distance between the edge of the holes and the edge of the girder is:

$$\text{Clear end distance} = 2.0 - 0.9375 / 2 = 1.53 \text{ in.}$$

The value of $2d$ is equal to 1.75 in. for a 7/8 inch diameter bolt. Since the clear end distance is less than $2.0d$, Eq. 6.13.2.9-2 is to be used to compute the nominal bearing resistance, R_n :

$$R_n = 1.2 L_c t F_u = 1.2(1.53)(0.625)(65) = 74.6 \text{ kips/bolt}$$

Therefore, for the girder bottom flange, the factored bearing resistance at a single bolt hole is:

$$R_r = \phi_{bb} R_n = (0.8)(74.6) = 59.7 \text{ kips/bolt}$$

For the bottom flange, the factored bearing resistance for the connection is computed by multiplying the single bolt hole resistance by the number of bolts on one side of the connection. Check this total resistance against the design force in the bottom flange, which is equal to 1,945 kips:

$$P_r = (40 \text{ bolts})(59.7 \text{ kips/bolt}) = 2388 \text{ kips} > 1,946 \text{ kips} \quad \text{OK}$$

7.14.5.11 Strength Limit State Check of Web Splice Plates

The web splice is conservatively designed assuming that the maximum moment and maximum shear at the splice occur under the same loading condition. Article 6.13.6.1.4b states that the design shear is not to exceed the lesser of the factored shear resistance of the web splice plates specified in Article 6.13.4 (block shear rupture), or the factored shear resistance of the web splice plates specified in Article 6.13.5.3 (shear yielding and shear rupture). Also, at the strength limit state, the combined flexural and axial stress in the web splice plates is not to exceed the specified minimum yield strength of the splice plates times the resistance factor, ϕ_f , specified in Article 6.5.4.2.

Article 6.13.6.1.4b also specifies that for all limit states for tub sections in horizontally curved bridges, the shear due to factored loads is to be taken as the sum of the flexural and St. Venant torsional shears in the web subjected to additive shears. For tub girders with inclined webs, the web splice is to be designed for the component of vertical shear in the plane of the web.

Furthermore, webs are to be spliced symmetrically by plates on each side of the web, and the splice plates are to extend as near as practical to the full depth of the web between the flanges.

Therefore, the following web splice plates are used:

Web plates: Two - 0.375 in. by 75.25 in. deep plates, Grade 50 steel

For this design example, only the positive live load bending case will be used to illustrate the check of the web splice for the strength limit state.

First, check the flexural yielding on the gross section of the web splice plates. The design moments and design horizontal force were previously computed as:

$$\begin{aligned} M_{uv} &= 127 \text{ kip-ft [moment resulting from eccentricity of flexural shear]} \\ M_{uw} &= 1,307 \text{ kip-ft [design moment in accordance with Eq. C6.13.6.1.4b-1]} \\ H_{uw} &= 439 \text{ kips [design horizontal force in accordance with Eq. C6.13.6.1.4b-2]} \end{aligned}$$

The maximum combined flexural and axial stress in the web splice plates is computed as:

$$f_{web} = \frac{M_{uv} + M_{uw}}{S_{SPL,g}} + \frac{H_{uw}}{A_{SPL,g}}$$

where:

$$\begin{aligned} S_{SPL,g} &= \text{gross section modulus of the web splice plates in the vertical plane (in.}^2\text{)} \\ A_{SPL,g} &= \text{gross cross-sectional area of the web splice plates (in.}^2\text{)} \end{aligned}$$

$$S_{SPL,g} = \frac{I_x}{c} \cos^2 \theta = 2 \frac{\left[\frac{(0.375)(75.25)^3}{12} \right]}{\left(\frac{75.25}{2} \right)} (\cos(14.04^\circ))^2 = 666.2 \text{ in.}^3$$

$$A_{SPL,g} = 2(0.375)(75.25) = 56.4 \text{ in.}^2$$

The combined maximum stress in the web splice plates for the positive live load bending case is computed as:

$$f_{web} = \frac{M_{uv} + M_{uw}}{S_{SPL,g}} + \frac{H_{uw}}{A_{SPL,g}} = \frac{(127 + 1,307)(12)}{666.2} + \frac{439}{56.4} = 33.61 \text{ ksi}$$

Check that the combined flexural and axial stress in the web splice plates does not exceed the specified minimum yield strength of the splice plates times the resistance factor, ϕ_f , specified in Article 6.5.4.2:

$$f_{web} = 33.61 \text{ ksi} < \phi_f F_y = (1.0)(50) = 50 \text{ ksi} \quad \text{OK}$$

Check for shear yielding on the gross section of the web splice plates due to the in-plane design shear. The in-plane design shear, V_{uw} , was previously computed as 406 kips. In accordance with Article 6.13.5.3, the factored shear yielding resistance of the connection element is to be taken as:

$$R_r = \phi_v 0.58 F_y A_{vg} \quad \text{Eq. (6.13.5.3-1)}$$

where:

- ϕ_v = resistance factor for shear as specified in Article 6.5.4.2
- F_y = specified minimum yield strength of the connection element (ksi)
- A_{vg} = gross area of the connection element subject to shear (in.²)

Therefore, the factored shear yielding resistance is computed as:

$$R_r = \phi_v 0.58 F_y A_{vg} = (1.0)(0.58)(50)(56.4) = 1,636 \text{ kips}$$

The in-plane design shear is checked against the factored shear yielding resistance as follows:

$$V_{uw} = 406 \text{ kips} < R_r = 1,636 \text{ kips} \quad \text{OK}$$

Check for shear rupture on the net section of the web splice plates due to the in-plane design shear. In accordance with Article 6.13.5.3, the factored shear rupture resistance of the connection elements is to be taken as:

$$R_r = \phi_{vu} 0.58 R_p F_u A_{vn} \quad \text{Eq. (6.13.5.3-2)}$$

where:

- ϕ_{vu} = resistance factor for shear rupture of connection elements as specified in Article 6.5.4.2 ($\phi_{vu} = 0.80$)
- R_p = reduction factor for holes taken equal to 0.90 for bolt holes punched full size and 1.0 for bolt holes drilled full size or subpunched and reamed to size. 1.0 is used in this example.

F_u = ultimate tensile strength of the connection elements (ksi)
 A_{vn} = net area of the connection element subject to shear (in.²)

Therefore, the factored shear rupture resistance is computed as:

$$R_r = \phi_{vu} 0.58 R_p F_u A_{vn} = (0.80)(0.58)(1.0)(65)[56.4 - 2(20)(0.375)(0.9375)] = 1,277 \text{ kips}$$

Check that the in-plane design shear is less than the factored shear rupture resistance:

$$V_{uw} = 406 \text{ kips} < R_r = 1,277 \text{ kips} \quad \text{OK}$$

7.14.5.12 Strength Limit State Check of Web Splice – Bearing on Girder Web

Similar to the flange splices, it is necessary to check the bearing resistance of the web splice plate bolt holes at the strength limit state. The calculation herein will simply use bolt forces and factored resistance computed previously within this design example.

The maximum resultant in-plane force on the extreme bolt, R_u , was computed earlier to be 45.2 kips. The factored resistance for bearing on the girder web in the end column of bolts was previously computed as 52.65 kips. Therefore:

$$R_u = 45.2 \text{ kips} < \phi_{bb} R_n = 52.65 \text{ kips/bolt} \quad \text{OK}$$

Note that the web thickness is 0.5625 in., which is less than the total thickness of the two web splice plates (2 times 0.375 in. = 0.75 in.). Therefore, bearing on the girder web governs as it has the smaller thickness.

7.14.5.13 Strength Limit State Check of Web Splice Plates – Block Shear Rupture

In accordance with Article 6.13.4, splice plates subjected to tension are to be investigated to ensure adequate connection material is provided to develop the factored block shear rupture resistance of the connection. The connection is to be investigated by considering all possible failure planes in the member and connection plates. Such planes are to include those that are parallel and perpendicular to the applied forces. The planes parallel to the applied force are considered to resist only shear stresses. The planes perpendicular to the applied force are considered to resist only tension stresses.

Block shear rupture resistance normally does not govern for typical web splice plates, but the check is illustrated here for completeness.

The factored resistance of the combination of parallel and perpendicular planes is computed in accordance with Eq. 6.13.4-1:

$$R_r = \phi_{bs} R_p (0.58 F_u A_{vn} + U_{bs} F_u A_{tn}) \leq \phi_{bs} R_p (0.58 F_y A_{vg} + U_{bs} F_u A_{tn}) \quad \text{Eq. (6.13.4-1)}$$

where:

- ϕ_{bs} = resistance for block shear rupture specified in Article 6.5.4.2 ($\phi_{bs} = 0.80$)
 R_p = reduction factor for holes taken equal to 0.90 for bolt holes punched full size and 1.0 for bolt holes drilled full size or subpunched and reamed to size. 1.0 is used in this example.
 F_u = specified minimum tensile strength of the connected material (ksi)
 A_{vn} = net area along the plane resisting shear stress (in.²)
 A_{vg} = gross area along the plane resisting shear stress (in.²)
 U_{bs} = reduction factor for block shear rupture resistance taken equal to 0.50 when tension stress is non-uniform and 1.0 when the tension stress is uniform. 1.0 is used in this example since the tension stress is uniform.
 A_{tn} = net area along the plane resisting tension stress (in.²)

First, compute the area terms, based on the block shear failure planes:

$$A_{vg} = 2(75.25)(0.375) = 56.44 \text{ in.}^2$$

$$A_{vn} = 2[71.25 + 2 - 20.5(0.875 + 0.0625)](0.375) = 40.52 \text{ in.}^2$$

$$A_{tn} = 2[3 + 1.5 - 1.5(0.875 + 0.0625)](0.375) = 2.32 \text{ in.}^2$$

Compute the factored resistance as follows:

$$R_{r1} = 0.80(1.0)[0.58(65)(40.52) + (1.0)(65)(2.32)] = 1,343 \text{ kips (controls)}$$

$$R_{r2} = 0.80(1.0)[0.58(50)(56.44) + 1.0(65)(2.32)] = 1,430 \text{ kips}$$

$$V_{uw} = 406 \text{ kips} < R_r = 1,343 \text{ kips} \quad \text{OK}$$

Similar calculations to those illustrated here for the web splice plates show that the factored block shear rupture resistance for the top and bottom flange splice plates is not exceeded by the flange design forces. Calculations demonstrating the block shear rupture check of the top and bottom flange splice plates are not provided in this example.

8.0 SUMMARY OF DESIGN CHECKS AND PERFORMANCE RATIOS

The results for this design example at each limit state are summarized below for the maximum positive moment and maximum negative moment locations. The results for each limit state are expressed in terms of a performance ratio, defined as the ratio of a calculated value due to applied loads to the corresponding resistance.

Maximum Positive Moment Region, Span 1 (Section G2-1)

Constructibility

Flexure (Strength I)

Eq. (6.10.3.2.1-1) – Top Flange Yielding	0.424
Eq. (6.10.3.2.1-2) – Top Flange Local Buckling	0.332
Eq. (6.10.3.2.1-2) – Top Flange Lateral Torsional Buck.	0.348
Eq. (6.10.3.2.1-3) – Top Flange Web Bend Buckling	0.356
Eq. (6.11.3.2-3) – Bottom Flange Yielding	0.246

Service Limit State

No checks required in this design example

Fatigue Limit State

Flexure (Fatigue I)

Eq. (6.6.1.2.2-1) – Bottom Flange	0.426
-----------------------------------	-------

Strength Limit State

Ductility Requirement – Eq. (6.10.7.3-1)	0.330
Flexure (Strength I)	
Eq. (6.11.7.2.1-1) – Top Flange	0.507
Eq. (6.11.7.2.2-5) – Bottom Flange	0.802
Article 6.11.7.2.1 – Concrete Deck Stresses	0.417

Interior Support, Maximum Negative Moment (Section G2-2)

Constructibility

Flexure (Strength I)

Eq. (6.10.3.2.2-1) – Top Flange Yielding	0.547
Eq. (6.11.3.2-1) – Bottom Flange Local Buckling	0.432

Shear (Strength I)

Eq. (6.10.3.3-1)	0.348
------------------	-------

Service Limit State (Service II)

Web Bend-Buckling - Eq. (6.10.4.2.2-4)	0.841
--	-------

Fatigue Limit State

Flexure (Fatigue I)

Eq. (6.6.1.2.2-1) – Top Flange	0.034
--------------------------------	-------

Strength Limit State

Flexure (Strength I)

Eq. (6.11.8.1.2-1) – Top Flange Yielding	0.888
Eq. (6.11.8.1.1-1) – Bottom Flange Local Buckling	0.884
Eq. (C6.11.8.1.1-1) – Bottom Flange	0.849
Article 6.11.1.1	
Bottom Flange cross-section distortional stresses	0.478
Shear (Strength I) – Eq. (6.10.9.1-1)	0.639

9.0 REFERENCES

1. AASHTO (2014). *AASHTO LRFD Bridge Design Specifications*, 7th Edition, American Association of State Highway and Transportation Officials, Washington, DC.
2. Kulicki, J., Wassef, W., Smith, C, and Johns, K., (2005). “AASHTO-LRFD Design Example: Horizontally Curved Steel Box Girder Bridge, Final Report,” National Cooperative Highway Research Project 12-52, Transportation Research Board, Washington, D.C.
3. Wright, R.N. and Abdel-Samad, S.R., (1968). “BEF Analogy for Analysis of Box Girders,” *Journal of the Structural Division, ASCE*, Vol. 94, No. ST7.
4. Coletti, D.A., Fan, Z., Holt, J., Vogel, J., Gatti, W., (2005). *Practical Steel Tub Girder Design*, National Steel Bridge Alliance (NSBA).
5. AASHTO/NSBA, (2006). *G1.4-2006: Guidelines for Design Details*, AASHTO/NSBA Steel Bridge Collaboration.
6. Texas Department of Transportation (TxDOT), (2009). *Preferred Practices for Steel Bridge Design, Fabrication, and Erection*, Texas Steel Quality Council.
7. AASHTO/NSBA, (2003). *G12.1-2003: Guidelines for Design for Constructibility*, AASHTO/NSBA Steel Bridge Collaboration.
8. Fan, Z. and Helwig, T., (1999). “Behavior of Steel Box Girders with Top Flange Bracing,” *Journal of Structural Engineering, ASCE*, Vol. 125, No. 8, pp. 829-837.
9. Helwig, T., Yura, J., Herman, R., Williamson, E., and Li, D., (2007). “Design Guidelines for Trapezoidal Box Girder Systems,” Report No. FHWA/TX-07/0-4307-1, Center for Transportation Research, University of Texas at Austin.
10. AASHTO (2003). *AASHTO Guide Specification for Horizontally Curved Steel Girder Highway Bridges*. American Association of State Highway and Transportation Officials, Washington, DC.
11. Heins, C.P. and Hall, D.H., (1981). *Designers Guide to Steel Box Girder Bridges*, Booklet No. 3500, Bethlehem Steel Corporation.